



# Durham E-Theses

---

## *Rare Decays of Heavy Baryons using Soft Collinear Effective Theory*

YIP, MATTHEW WING YU

### How to cite:

---

YIP, MATTHEW WING YU (2013) *Rare Decays of Heavy Baryons using Soft Collinear Effective Theory*, Durham theses, Durham University. Available at Durham E-Theses Online: <http://etheses.dur.ac.uk/7758/>

### Use policy

---

The full-text may be used and/or reproduced, and given to third parties in any format or medium, without prior permission or charge, for personal research or study, educational, or not-for-profit purposes provided that:

- a full bibliographic reference is made to the original source
- a [link](#) is made to the metadata record in Durham E-Theses
- the full-text is not changed in any way

The full-text must not be sold in any format or medium without the formal permission of the copyright holders.

Please consult the [full Durham E-Theses policy](#) for further details.

# RARE DECAYS OF HEAVY BARYONS USING SOFT COLLINEAR EFFECTIVE THEORY

**Matthew Wing Yu Yip**

A thesis presented for the degree of Doctor of Philosophy



Institute for Particle Physics Phenomenology  
Department of Physics  
Durham University  
U.K.  
July 2013



*To*  
*my parents*

致  
丈公丈婆

# Rare Decays of Heavy Baryons using Soft Collinear Effective Theory

Matthew Wing Yu Yip

Submitted for the degree of Doctor of Philosophy  
July 2013

## Abstract

In the era of high-luminosity hadronic colliders, the rare heavy-to-light decay  $\Lambda_b \rightarrow \Lambda \ell^+ \ell^-$  receives increasing research attention in both experimental and theoretical particle phenomenology. This flavour-changing neutral-current decay is a potential window for the discovery of new Physics beyond the Standard Model through its helicity-sensitive nature, complementing past and ongoing searches and calculations related to the  $B$  meson.

In this work the universal soft form factor in the heavy-quark and large-recoil limits is calculated using light-cone sum rules in the framework of soft-collinear effective theory, as is the  $\mathcal{O}(\alpha_s)$  correction from hard-collinear gluon exchange. Numerical estimates on form-factor ratios and experimental observables are presented. Related issues, including baryonic transition form factors and in particular light-cone distribution amplitudes for the heavy baryon  $\Lambda_b$ , are also discussed.

# Declaration

I declare that no material presented in this thesis has previously been submitted by myself for a degree at this or any other university. This dissertation does not exceed the word limit for the respective Degree Committee. The research described in this thesis has been carried out in collaboration with Thorsten Feldmann, Yu Ming Wang and Guido Bell, and has been or will be published as follows:

- [1] Thorsten Feldmann and Matthew Wing Yu Yip  
***Form Factors for  $\Lambda_b \rightarrow \Lambda$  Transitions in SCET***  
Phys. Rev. D 85, 014035 (2012) [erratum-ibid. D 86, 079901 (2012)]  
[arXiv:hep-ph/1111.1844]
  
- [2] Guido Bell, Thorsten Feldmann, Yu-Ming Wang and Matthew Wing Yu Yip  
***Light-Cone Distribution Amplitudes for Heavy-Quark Hadrons***  
To be submitted to JHEP (2013)

The copyright of this thesis rests with the author. No quotations from it should be published without the author's prior written consent and information derived from it should be acknowledged.

Matthew Wing Yu Yip

# Acknowledgements

I should like to express my sincere gratitude to Prof. Dr. Thorsten Feldmann, my supervisor, for his patient guidance, helpfulness and personal kindness. Without him and his commitment to supporting me, this work, and the course of my doctoral studies, would doubtless have turned out very differently.

I am also grateful to my parents, for their unwavering support and concern for my general well-being; and to my fellow Ogdenites, in particular Steve, Doris, Herr Busb and Herr Hall, for their understanding. Tod. (Ich weiß nicht über dich wissen)

I am thankful for the generous financial support from the TP1 group at Universität Siegen, and the hospitality afforded me during my sojourns there. I was supported by a Durham University Doctoral Fellowship from October 2009 to March 2013.

Matthew Yip

# Contents

<b>Abstract</b>	<b>iv</b>
<b>1 Introduction</b>	<b>1</b>
<b>2 Flavour Physics, CP Violation and Experiments</b>	<b>5</b>
2.1 Quark Flavour Physics . . . . .	5
2.2 The CKM Matrix and the Unitary Triangle . . . . .	7
2.3 CP Violation . . . . .	9
2.4 B-Physics and Experiments . . . . .	11
<b>3 Effective Theories and Light-Cone Sum Rules</b>	<b>15</b>
3.1 Effective Field Theories . . . . .	15
3.1.1 In Heavy Flavour Physics . . . . .	18
3.2 Heavy-Quark Effective Theory (HQET) . . . . .	19
3.3 Soft-Collinear Effective Theory (SCET) . . . . .	22
3.4 Factorisation . . . . .	29
3.5 QCD Sum Rules (on the Light Cone) . . . . .	32
3.5.1 SCET LCSRs . . . . .	37
<b>4 Light-Cone Distribution Amplitudes and Decay Form Factors for Heavy Baryons</b>	<b>40</b>
4.1 Baryon versus Meson . . . . .	40
4.2 $\Lambda_b$ Light-Cone Distribution Amplitudes . . . . .	43
4.2.1 Introduction . . . . .	43



4.2.2	LCDAs for Heavy Baryons: A New Study . . . . .	46
4.2.3	Construction in Momentum Space . . . . .	51
4.2.4	Renormalisation-Group Behaviour . . . . .	57
4.3	Helicity-based Parametrisation for $\Lambda_b \rightarrow \Lambda$ Form Factors . . . . .	59
4.3.1	HQET Limit . . . . .	61
4.3.2	SCET Limit . . . . .	62
4.3.3	Hard-Scattering Corrections . . . . .	63
<b>5</b>	<b><math>\Lambda_b \rightarrow \Lambda \ell^+ \ell^-</math> Soft Form Factor and Correction from Hard-Collinear Gluon Exchange</b>	<b>65</b>
5.1	$\xi_\Lambda$ : Soft Form Factor . . . . .	67
5.2	$\Delta\xi_\Lambda$ : Hard-Collinear Gluon-Exchange Correction . . . . .	73
5.3	Numerical Results . . . . .	77
5.3.1	Soft Form Factor . . . . .	77
5.3.2	Form-Factor Ratios . . . . .	83
5.3.3	$\Lambda_b \rightarrow \Lambda \mu^+ \mu^-$ Observables . . . . .	86
<b>6</b>	<b>Outlook and Conclusions</b>	<b>92</b>
6.1	“Non-Factorisable” Corrections to $\Lambda_b \rightarrow \Lambda \ell^+ \ell^-$ . . . . .	92
6.2	Other Calculations on $\Lambda_b \rightarrow \Lambda \ell^+ \ell^-$ . . . . .	96
6.3	Conclusion . . . . .	98
	<b>Appendix A Differential Decay Widths for <math>\Lambda_b \rightarrow \Lambda \mu^+ \mu^-</math></b>	<b>102</b>
	<b>Appendix B Form-Factor Parametrisations</b>	<b>104</b>
B.1	Connection to Convention by Chen and Geng . . . . .	104
B.2	Symmetry-based Form-Factor Parametrisation . . . . .	105
	<b>Appendix C Corrections to Symmetry Relations</b>	<b>107</b>
C.1	HQET Symmetry Relations . . . . .	107
C.2	Hard-Vertex Corrections to SCET Symmetry Relations . . . . .	108
C.3	Hard-Collinear Gluon Exchange . . . . .	109

# List of Figures

2.1	Latest constraints on the unitarity triangle . . . . .	10
3.1	Contour on the complex $q^2$ -plane used to get the dispersion relation . . . .	35
3.2	Mesonic correlation-function diagrams using traditional and SCET LCSRs .	37
3.3	A factorisable exclusive heavy-to-light process in QCDF/SCET . . . . .	39
4.1	Shapes of the functions $f_2(\omega)$ and $g_2(u)$ in 3 different models for the LCDA $\phi_2(\omega_1, \omega_2)$ . . . . .	55
5.1	SCET correlation function relevant to the soft form factor $\xi_\Lambda$ . . . . .	67
5.2	SCET correlation functions relevant to the form factor $\Delta\xi_\Lambda$ . . . . .	68
5.3	Functional form of the partially integrated LCDA $\psi_4(\omega)$ for the exponential model . . . . .	79
5.4	Dependence of $\xi_\Lambda(n_+p' = M_{\Lambda_b})$ on $\omega_0$ . . . . .	79
5.5	Dependence of the soft form factor on $n_+p'$ , using the leading-order sum rule	80
5.6	Results for the soft form factor using the leading-order sum rule and the approximate formula . . . . .	80
5.7	Dependence of the soft form factor on the Borel parameter at maximal recoil	81
5.8	Dependence of the soft form factor on the threshold parameter at maximal recoil . . . . .	81
5.9	Energy dependence of the form-factor correction $\Delta\xi_\Lambda/\xi_\Lambda$ estimated from leading-order SCET sum rules . . . . .	84
5.10	Dependence of $\Delta\xi_\Lambda/\xi_\Lambda$ on $\omega_0$ which characterises the $\Lambda_b$ LCDA . . . . .	84
5.11	Dependence of $\Delta\xi_\Lambda$ on $\omega_M$ and $\omega_s$ at maximal recoil . . . . .	85
5.12	Energy dependence of form-factor ratios $h_\perp/f_\perp$ and $\tilde{h}_\perp/g_\perp$ including $\mathcal{O}(\alpha_s)$ corrections from hard and hard plus hard-collinear gluon exchange . . . . .	87

5.13	Differential branching ratio for $\Lambda_b \rightarrow \Lambda \mu^+ \mu^-$ as a function of $q^2$ in the large-recoil region . . . . .	88
5.14	Ratios of observables $H_L/H_T$ and $H_A/H_T$ as a function of $q^2$ . . . . .	90
6.1	Vertex corrections for $O_8$ and $O_{1-6}$ . . . . .	93
6.2	Non-factorisable corrections involving the light quark . . . . .	95
6.3	The leading annihilation diagram . . . . .	96

## List of Tables

4.1	Currently available experimental data on the decay $\Lambda_b \rightarrow \Lambda \mu^+ \mu^-$ . . . . .	42
5.1	Summary of hadronic input parameters . . . . .	77

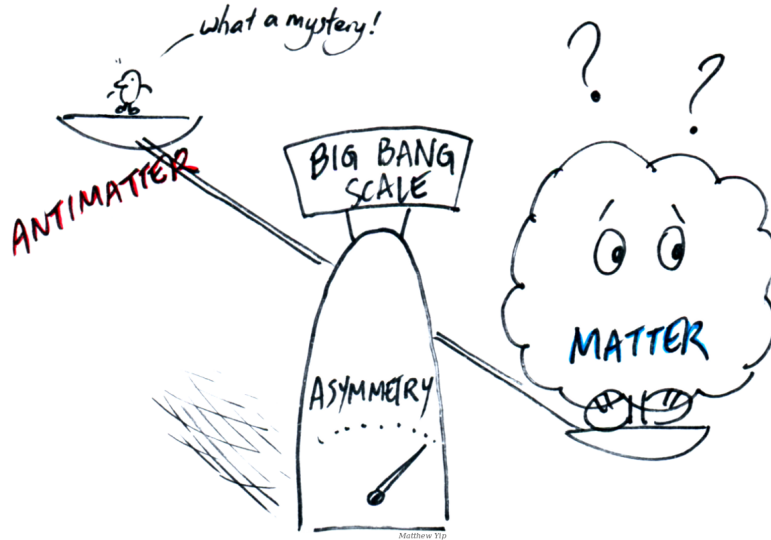
# Chapter 1

## Introduction

For all its impressive accuracy, the Standard Model, initiated in the 1960s as an integral picture of how the universe works at a fundamental level, is not complete. Various mysteries remain unsolved: there are many experimental observations, or lack thereof, for which generations of scientists have so far failed to find satisfactory explanations. The true status of neutrinos, which have been known for some time to have non-zero mass, is still elusive; the strong CP problem, for which the axion has been proposed, remains a problem; light has yet to be shed on dark matter, and there exist many an observation for which fine-tuning is simply not an elegant or likely solution. Pieces of the jigsaw puzzle that is the true nature of fundamental physics are still missing; theorists make a guess of their shapes and sizes and the locations at which they can be found, while experimentalists build ever more powerful and sophisticated machines to track the missing pieces. New physics beyond the Standard Model is widely expected.

Of these open problems, **CP violation** is a phenomenon that is of particular interest. Related to deep, unanswered questions concerning the observed matter-antimatter asymmetry in our universe, and the origin of baryogenesis, it is fully deserving of the experimental attention and theoretical scrutiny it has received for decades. Unexpected results that have shown up in recent times, for instance a surprisingly large charm-sector CP-violating effect, only highlight the inadequacies

(and sheer difficulty) of theoretical work, and the room for technical improvement in collider experiments.



The Large Hadron Collider (LHC) has been in operation, if slightly sporadically, since 2008. It is a proton-antiproton collider of never-before-achieved power, bringing the Particle Physics community alive and kicking into a “high-statistics” era. Precise measurements of decay rates, particle masses and myriad other interaction parameters have been achieved, reaching a feverish high point in July 2012, when a particle widely expected to be the elusive Standard Model Higgs boson was observed at  $5\sigma$  statistical level. Much of what had previously been considered statistically unrealistic is now possible at the LHC: Producing particles with small production rates, and observing potential new particles generated through decays with tiny cross-sections.

**Flavour physics** is the arena in which much of the investigation into CP violation is done. In the Standard Model, the interactions of different types (flavours) of quarks with one another are governed by the **Cabibbo-Kobayashi-Maskawa (CKM) matrix**, which involves a complex phase as one of its independent parameters. This is one of the few places in the Standard Model through which CP violation can occur. By studying flavour-changing weak interactions, we hope to achieve better understanding of the current framework of the Standard Model, and identify the

cracks where it begins to fail.

Within flavour physics, **B-physics** is key. The bottom quark is the heaviest of all six known flavours of quarks which form bound states. Its heavy nature – its mass is much higher than the typical scale of non-perturbative QCD,  $\Lambda_{\text{QCD}}$ , yet still much lower than the  $W$  mass – allows theorists to invoke symmetries to simplify calculations, making them often much more tractable than those involving other quarks. Studying decays of hadrons containing the  $b$  quark to a high precision, with the help of B-physics programmes at LHC, especially those at the dedicated B-physics experiment **LHCb**, B-factories such as BaBar and Belle, and beyond, we accumulate and analyse data about the CKM matrix which will either show clear inconsistencies with Standard Model predictions, or provide more stringent constraints to narrow the space in which we search for new effects, as long as we achieve, on the theoretical side, numerical predictions to an adequate level of precision.

\* \* \*

This thesis will focus on rare semi-leptonic heavy-to-light decays of  $\Lambda_b$ , one of the simplest baryons containing a  $b$  quark. Baryonic B-physics research has been a bit thin on the ground compared to its mesonic counterpart, due both to experimental challenges and theoretical complications; with ever more sophisticated machines, however, the former are no longer an insurmountable hurdle. Indeed, both Tevatron and the LHC have recently announced the first measurements of the semi-leptonic decay  $\Lambda_b \rightarrow \Lambda \mu^+ \mu^-$ . Theoretically, heavy baryons are also gradually garnering more attention.  $\Lambda_b \rightarrow \Lambda \ell^+ \ell^-$  offers the possibility to study rare semi-leptonic and radiative  $b \rightarrow s$  transitions, and involves observables which will provide complementary phenomenological information to mesonic decays. A systematic analysis and discussion of this decay will form the heart of this thesis. The technology of **light-cone sum rules (LCSRs)** within the framework of **soft-collinear effective theory (SCET)**, which has proved fruitful in analogous heavy mesonic decays, will be our weapon of choice. With it we calculate the so-called universal soft form factor which enters the

symmetry relations in the heavy-quark and large-recoil-energy limits. Similarly we obtain the leading-order factorisable correction in the strong-coupling constant  $\alpha_s$ , involving the exchange of a hard-collinear gluon.

Before then, an introduction to the calculational techniques and effective theoretical framework needed – SCET, LCSRs, QCD factorisation – will be presented in Chapter 3, following a quick but necessary overview of flavour physics, CP violation and recent experimental developments in relevant areas in Chapter 2.

Theoretical predictions for exclusive decay matrix elements require various non-perturbative hadronic inputs, and one of the most important and challenging of these is an accurate theoretical description of the heavy baryons, which enter our calculations as **light-cone distribution amplitudes (LCDAs)**. We shall discuss an updated formulation of these heavy baryonic LCDAs in detail in Chapter 4. There we also put forward an alternative parametrisation of the baryonic transition form factors which feature distinct advantages. Both of these are new developments which play crucial parts in subsequent parts of this thesis.

Chapter 5 is the aforementioned calculation and discussion of  $\xi_\Lambda$ , the soft form factor, and  $\Delta\xi_\Lambda$ , the factorisable correction due to hard-collinear gluon exchange, for the decay  $\Lambda_b \rightarrow \Lambda \ell^+ \ell^-$ , using SCET LCSRs. Results will be presented analytically and numerically and juxtaposed with the latest experimental data.

Chapter 6 offers an outlook for related calculations before concluding this work. The appendices collate extra material which are helpful but not essential to the main text.

## Chapter 2

# Flavour Physics, CP Violation and Experiments

### 2.1 Quark Flavour Physics

In the beginning (the 1960s) was the quark model: 3 particles called quarks were theoretically proposed to explain the pattern of observed mesons and baryons at the time, fitting into an (approximate) flavour  $SU(3)$  symmetry. Since then the existence of these fundamental building blocks of nature have been established and better understood, and 3 heavier quarks have been postulated and confirmed, with Quantum Chromodynamics (QCD), the non-Abelian theory of the strong force, formulated to explain the strong interactions between colour-charged quarks and gluons. Along with the electroweak sector, which contains the weak and electromagnetic interactions, QCD is part of the Standard Model (SM), which has an overall gauge structure of  $SU(3)_C \times SU(2)_L \times U(1)_Y$ , a summation of our (incomplete) knowledge of how physics work in terms of its fundamental matter and gauge fields. Fermions like quarks and leptons gain mass through the Higgs mechanism, while the gauge bosons  $W^\pm$  and  $Z$  do so via spontaneous symmetry breaking; the photon remains massless. The final missing, scalar member of the SM particle zoo, the Higgs boson (or a particle strongly expected to be it), was at long last declared discovered at the LHC in 2012, by the Atlas and CMS collaborations [4].



Quark flavour physics is concerned with flavour-violating processes of all types of quarks that are not the top quark. The study of these weak decays are vastly complicated by the presence of QCD and its confining nature, meaning what we observe are hadronic bound states, whose analytical connection to free quarks are not trivial. Calculations of hadronic quantities required for decay amplitudes of quark processes necessarily involve low-energy QCD, whose running strong coupling constant  $g_s$  results in asymptotic freedom; study of decays where flavour dynamics are the real focus becomes challenging or in some cases technically impossible due to the exchange of soft gluons, whose presence negates the use of perturbation theory and requires non-perturbative techniques. Thus all sorts of ingenious solutions are sought to alleviate the problems, to find ways around the theoretical stumbling blocks, for instance manipulating variables to make use of cancellations due to symmetries, or neglecting heavy degrees of freedom by using appropriately constructed effective theories. Of course, brute force is also often invoked, whether in Monte Carlo-type calculations or lattice gauge field theory, via intensive computing-based methods.

Despite its challenges quark flavour physics is of great research interest in the era of high-luminosity colliders, as it serves as a good arena for indirect searches of new physics (NP). Experimentally, one can focus on measuring ever more accurately SM parameters by identifying the cleanest and most promising decay channels, and one can design and measure observables of processes which are highly suppressed in the SM but not in NP scenarios. The challenges for experimentalists and engineers of collider experiments are well known; for theoretical phenomenologists, it is to make predictions of what would be observed experimentally if the SM (or an extension thereof) is correct, to a level of accuracy that would match the ever-shrinking statistical uncertainties and systematics in experimental data; by making the comparison with reality we have a handle of understanding the truth better.

## 2.2 The CKM Matrix and the Unitary Triangle

Quarks gain mass through Yukawa interactions with the scalar doublet Higgs field. After spontaneous symmetry breaking, we have in the Lagrangian the Yukawa terms

$$\mathcal{L}_{\text{Yukawa}} \supset \bar{d}'_{Li} Y_{ij}^{(d)} d'_{Rj} + \bar{u}'_{Li} Y_{ij}^{(u)} u'_{Rj} + \text{h.c.}$$

The primes denote states in the weak flavour basis, and the Yukawa matrices  $Y^{(u,d)}$  are unconstrained and completely arbitrary. By defining physical (mass) eigenstates for both left-handed ( $L$ ) and right-handed ( $R$ ) quarks:

$$D_L = U_d D'_L, \quad U_L = U_u U'_L, \quad D_R = V_d D'_R, \quad U_R = V_u U'_R,$$

where  $D_{L,R}, U_{L,R}$  are now  $3 \times 1$  vectors of 3 generations of quark states, the Yukawa matrix is diagonalised through a bi-unitary transformation, and the mass eigenvalues are attained. This in turn affects the structure of the charged-current (CC) terms:

$$\mathcal{L}_{\text{CC}} \supset \bar{U}'_L D'_L \rightarrow \bar{U}_L U_u^\dagger U_d D_L \equiv \bar{U}_L V_{\text{CKM}} D_L,$$

where  $V_{\text{CKM}}$  is the complex unitary Cabibbo-Kobayashi-Maskawa (CKM) matrix [5], resulting in fascinating phenomenology in weak quark decays.

$$\begin{pmatrix} d' \\ s' \\ b' \end{pmatrix} = V_{\text{CKM}} \begin{pmatrix} d \\ s \\ b \end{pmatrix} = \begin{pmatrix} V_{ud} & V_{us} & V_{ub} \\ V_{cd} & V_{cs} & V_{cb} \\ V_{td} & V_{ts} & V_{tb} \end{pmatrix} \begin{pmatrix} d \\ s \\ b \end{pmatrix}. \quad (2.1)$$

Neutral currents are not affected by the above: this is one way of looking at why flavour-changing neutral currents (FCNC) are not allowed at tree-level in the SM. The Glashow-Iliopoulos-Maiani (GIM) mechanism [6] provides another look at the same principle: In a loop-mediated process, where all 3 quarks of the same type (up/down) contribute, the resultant amplitude depends on their (squared) mass differences only, and in the limit of equal quark masses, the amplitude vanishes. For example, for a process like  $B_s \rightarrow \mu\mu$ ,

$$A = \sum_{q=u,c,t} V_{qs} V_{qb}^* f(m_q^2/m_W^2) = V_{ts} V_{tb}^* (f(m_t^2) - f(m_c^2)) + V_{us} V_{ub}^* (f(m_u^2) - f(m_c^2)). \quad (2.2)$$

This has made use of the unitarity of the CKM matrix:

$$\sum_q V_{qi}^* V_{qj} = \delta_{ij} \ , \quad i \neq j \ . \quad (2.3)$$

An early version of this mechanism actually anticipated the discovery of the charm quark in 1974, as a way to explain the smallness of the branching ratio of  $K_0 \rightarrow \mu\mu$ . In any case, this phenomenon (of tree-level FCNC being forbidden and loop-generated FCNC being possibly GIM-suppressed) is not necessarily a feature in extensions of the SM, providing one of the reasons why rare flavour decays are considered suitable for NP searches.

Looking at the form of the CKM matrix (2.1) again, a  $3 \times 3$  unitary matrix has 9 real parameters. Unphysical quark-field phases can be rotated away by field redefinitions, leaving just 4 independent physical CKM matrix parameters: 3 angles, and 1 complex phase. This last phase is of great significance and research interest; it is the only place in the Standard Model (with massless neutrinos) in which CP violation can occur, apart from the  $\theta$  parameter of the  $F_{\mu\nu}\tilde{F}^{\mu\nu}$  term in the QCD Lagrangian which experimentally is extremely suppressed, (a mystery known as the Strong CP Problem, see e.g. Chapter 27 of [7]). In fact it was an attempt to explain quark CP violation that led to the proposal of a third generation of quarks (a  $2 \times 2$  matrix does not allow a complex phase). The bottom and top quarks were discovered in 1977 and 1995 respectively. The numerical values [8] for the CKM matrix reveals a hierarchy, which has engendered a number of parametrisations including the commonly used Wolfenstein [9], a power expansion in a small parameter  $\lambda \sim 0.2$ :

$$V_{\text{CKM}} = \begin{pmatrix} 1 - \frac{\lambda^2}{2} & \lambda & A\lambda^3(\rho - i\eta) \\ -\lambda & 1 - \frac{\lambda^2}{2} & A\lambda^2 \\ A\lambda^3(1 - \rho - i\eta) & -A\lambda^2 & 1 \end{pmatrix} + \mathcal{O}(\lambda^4) \ . \quad (2.4)$$

To understand quark flavour-breaking interactions is to investigate the values of these CKM elements and the four physical parameters. To facilitate this, noting the unitarity condition (2.3) forms a triangle on the complex plane, the Unitarity Triangle (UT) was invented by common convention with  $i = b$  and  $j = d$ , whose sides are

the 3 terms in (2.3) divided by  $V_{cb}^*V_{cd}$ . This results in a triangle with one side of unity length on the real axis; this choice of  $i$  and  $j$  leads to a triangle which is not squashed (a result of the observed hierarchy of  $V_{CKM}$ ), and the  $V^*V$  normalisation is required for a reparametrisation-invariant observable. If the CKM formulation of the weak interactions of the Standard Model is correct, this triangle would close due to unitarity. Hence, the side lengths

$$R_t = \left| \frac{V_{tb}^*V_{td}}{V_{cb}^*V_{cd}} \right| \quad \text{and} \quad R_u = \left| \frac{V_{ub}^*V_{ud}}{V_{cb}^*V_{cd}} \right|$$

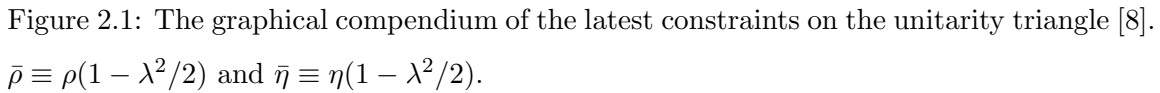
and the angles

$$\beta = \arg\left(-\frac{V_{cb}^*V_{cd}}{V_{tb}^*V_{td}}\right), \quad \alpha = \arg\left(-\frac{V_{tb}^*V_{td}}{V_{ub}^*V_{ud}}\right) \quad \text{and} \quad \gamma = \arg\left(-\frac{V_{ub}^*V_{ud}}{V_{cb}^*V_{cd}}\right)$$

are to be measured, using the best channel(s) to give the cleanest signal for each; if the resulting experimental values are all consistent to a high statistical accuracy, i.e. the triangle closes perfectly, then one might say our understanding of quarks in the weak sector can be considered accurate. Tensions between the parameters, or even within the same parameter from different channels, however, hint at missing pieces in the SM. Therefore, ideally, as many processes as realistically possible should be investigated in order to achieve an over-determination. Figure 2.1 (taken from the CKMfitter group [8]) is a summary of the experimental constraints so far attained in relation to the UT parameters.

## 2.3 CP Violation

Three discrete symmetries, charge conjugation ( $C$ ) (the relation between a particle and its antiparticle), parity ( $P$ ) and time reversal ( $T$ ), are possible in quantum field theory, and  $CPT$  together as a symmetry must be upheld as an automatic consequence of a local Lorentz-invariant field theory. Even before the time of quarks,  $C$  and  $P$  were known to be broken, for instance in weak interactions involving the neutrino; the combined  $CP$  symmetry was assumed to hold, until its non-conservation was first experimentally identified in  $K_0$  decays in 1964 [10]. It has since been found



CP violation can happen in a number of ways in quark flavour physics: when the decay amplitude of a process differs from its CP counterpart (“direct”):  $|\bar{A}_{\bar{f}}/A_f| \neq 1$  (a relative phase is unobservable); when it originates from the mixing of a flavoured (non-onium) meson (“indirect”):  $|q/p| \neq 1$  where  $q$  and  $p$  are mixing parameters characterising the physical mesonic states in terms of the flavour states; and when it arises from interference between mixing and decay.

The phenomenon of CP violation is itself utilised in the measurement of UT parameters, as in the example of the extraction of the angle  $\beta$  from the decay

$B^0, \bar{B}^0 \rightarrow J/\Psi K_S^0$ . where the consideration of time-dependent CP asymmetry results in an observable that is free of hadronic factors (for details see e.g. [7]) – a “golden channel” used as the standard for the best data on  $\beta$ . This is actually where the first non-kaon CP violation was observed at Belle and BaBar, which were built to measure this decay in particular. Latest values of this  $\beta$  (and others) can be found at [8]. Interestingly, this method cannot be straightforwardly applied to the angle  $\alpha$  with the similar decay  $B^0 \rightarrow \pi^+\pi^-$ , as an alternative diagram induced by a FCNC loop (the penguin diagram) makes a non-negligible contribution in addition to the tree-level process; careful analyses or different channels have to be used. The last angle  $\gamma$  currently suffers from sizable uncertainties; although by definition  $\gamma = \pi - \alpha - \beta$ , an independent measurement would be beneficial for the desired over-constraining of the UT. The side  $R_t$  involves  $V_{td}$  which enter  $B_0$  mixing – a box loop diagram where the top quark dominates due to the GIM mechanism; the side  $R_u$  can be measured from tree-level semi-leptonic  $B$  decays for instance, and state-of-the-art results currently reveal a tension between inclusive and exclusive measurements [12] which is not yet understood and hence interesting.

## 2.4 B-Physics and Experiments

In recent years B-physics data have been dominated by output from the 2 B-factories, Belle [13] and BaBar [14], and the 2 hadron ( $p\bar{p}$ ) colliders, Tevatron and the LHC. B-factories are  $e^+e^-$  asymmetric colliders tuned to produce as many  $B$  mesons as possible (asymmetric to allow measurements of lifetimes and time-dependent CP quantities), and as such have made many important discoveries, including the first observation of non-kaon CP violation in bottom hadrons in 2001 [15]. The advantage with such B-dedicated machines, which utilise  $e^+e^- \rightarrow \Upsilon(4s)$  to generate coherent pairs of  $B^0$ , is their hadronic environment for identifying the final states is much cleaner than at the hadronic colliders, which use  $p\bar{p} \rightarrow b\bar{b}X$ . As a result the latter, despite boasting a much higher production rate of  $bs$ , have a lower selection efficiency,

and they study a more limited range of  $B^0$  decay modes where reconstruction is easier. However, they do allow observation of states above the  $B^0$  – good for spectroscopy and interesting decays like  $B_s \rightarrow \mu^+ \mu^-$ .

The only dedicated flavour experiment at the hadronic colliders is the LHCb [16]; CMS and Atlas, despite being general-purpose detectors, also have their own flavour programmes [17]. The Tevatron collider at Fermilab, along with collaborations CDF and D0, unfortunately shut down in 2011 due to lack of funding; BaBar, the experiment at PEP-II, SLAC also ended in 2008, but some data are still coming through. In the near-term future, however, in terms of sheer volume of data, all eyes are on the LHC.

Since the beginning of the era of these major B-factories and in particular the LHCb, those large, unambiguous effects beyond the SM that have been the hope of many flavour physicists have failed to materialise, to the great disappointment of advocates of flavour-sector NP searches and the fundamental physics community at large. The alignment of predictions from the CKM theory to experimental data is impressive, establishing it to be the dominant source of flavour violation of quarks beyond doubt. The influx of data on suppressed channels only seems to reinforce the apparent unimpeachability of the Standard Model. This is not to say there are no promising hints of something important yet to come; big recent experimental news stories in flavour physics include the like-sign dimuon charge asymmetry observed in  $B^0$  mixing announced by the D0 in 2010 [18], and the discovery of unexpectedly large direct CP violation in the charm sector (in  $D^0 \rightarrow K^+ K^-, \pi^+ \pi^-$ ) in 2011 by LHCb and subsequent (sometimes contradictory) measurements elsewhere [19].

The achievements at the B-factories and hadronic colliders are too numerous to list in the last decade or two, but let us now highlight a number of channels for  $b \rightarrow s$  decays that would serve as a backdrop to  $\Lambda_b \rightarrow \Lambda \ell^+ \ell^-$  which shall be discussed in Chapters 4 to 6.

Exclusive  $B \rightarrow K^{(*)} \ell^+ \ell^-$  transitions have obvious similarities to the baryonic  $\Lambda_b \rightarrow \Lambda \ell^+ \ell^-$ , at least as far as the mediating effective operators ( $O_{7\gamma}$ ,  $O_9$  and  $O_{10}$ ), and how their hadronic form factors simplify in certain kinematic limits are concerned. The decay already offers rich opportunities for angular analyses [20] – with the subsequent  $K^* \rightarrow K\pi$  there are a total of 3 kinematic angles, and for  $\ell = \mu$  experimental searches are especially convenient. Theoretical calculations are not straightforward as they involve hadronic matrix elements, but effective theories have been shown to apply in certain situations and lead to simplified observables like differential cross-sections and forward-backward asymmetries, experimental data of which are available from both hadronic colliders and B-factories [21].

Attention should also be paid to the inclusive  $B \rightarrow X_s \gamma$  (and  $B \rightarrow X_s \ell^+ \ell^-$ ), whose latest combined branching ratio [22] is consistent with SM predictions. Inclusive decays are often less complex theoretically through the use of heavy-quark operator product expansion, but experimentally harder to discern than exclusive ones. Meanwhile the exclusive leptonic  $B_s \rightarrow \mu^+ \mu^-$  decay is a great channel for potential NP signals to spot, as not only is it highly helicity-suppressed, it is a CKM-suppressed FCNC process, with an estimated theoretical branching ratio of  $\mathcal{O}(10^{-9})$ . Various hadronic colliders have searched for this decay thanks to its clean signature, but it was not until 2012 that it was first observed, with a branching ratio that again agrees well with the SM prediction [23], putting good constraints on NP models.

\* \* \*

To sum up this chapter, despite the lack of “low-hanging fruits” in recent experiments, flavour physics is still one of the biggest potential sites for the unearthing of solutions to our various non-understandings. It might be an good time to focus on taking full advantage of the powerful weapon we now have: an abundance of data. On one hand, this simply allows us to delve into precision effects, deriving more stringent constraints on CKM parameters using high-precision data. The gauntlet



is thrown to the theorists who must now come up with better techniques – be it a better understanding of symmetries, or definition of clean observables and channels – that are sufficiently good at controlling systematic uncertainties to confront the data.

On the other hand, it is an increasingly trendy idea to use a Bayesian approach in the handling of experimental data in the view of discovering new physics (see e.g. [24]). This involves building specific, NP-encompassing models which will be pitted against data using Bayesian statistics, with a pre-defined set of priors. This kind of top-down approach enables modellers to make consistent, inter-related predictions for all processes. However, it suffers from an obviously strong model dependence and requires a huge number of observables (apart from a huge volume of data) as the new models commonly involve more free parameters than observables experiments can practically supply. For instance, the Minimal Supersymmetric Standard Model (MSSM) [25] has more than 100 parameters. With more judicious simplification, like the Minimal Flavour Violation (MFV) hypothesis [26] which assumes all flavour- and CP-breaking new phenomena have the same source as in the SM, nevertheless, this is a trail with a future in the high-statistics era, when physics comes equipped with machines like the LHC that make possible many previously infeasible independent channels of observation.

## Chapter 3

# Effective Theories and Light-Cone Sum Rules

The central calculations of this work are performed using the technique of light-cone sum rules (LCSRs) within the framework of soft-collinear effective theory (SCET). Both of these are built on years of theoretical work, and this chapter attempts to provide an introduction to these as a backdrop to the exclusive heavy-to-light baryonic decay calculations presented afterwards. Along with light-cone distribution amplitudes (Chapter 4), the topics presented here were invented, have developed and now stand alone as separate theories and technical innovations in their own right, and are put to use in multifarious contexts and to varying levels of depth in particle physics; as demonstrated here, they can also complement each other in an essential way, providing a useful and much-appreciated route to tackle challenging hadronic calculations both perturbative and non-perturbative.

### 3.1 Effective Field Theories

Quantum processes often involve different energy scales, but not every one of them is directly relevant to the particular problem at hand. This is not to say the desired final amplitudes are not sensitive to all scales; in an ideal world, all real and virtual

field effects and corrections would be taken into account. In reality, with finite computing power and knowledge of what goes on at all energy scales, approximations are indispensable. Effective field theories provide a general theoretical framework to separate different energy scales and simplify the physical problem into a manageable one, in which heavy fields (irrelevant to the problem), like the  $W$  boson, are “integrated out” as dynamical degrees of freedom. The terminology “integrating out” refers to the procedure in the path-integral formalism, in which the quantum fluctuations of heavy fields above a mass scale  $\Lambda$  are removed via functional integration from the generating functionals for the Green functions, leaving a modified, “effective” theory only valid at an energy scale below  $\Lambda$ . Technical details of the path-integral formalism can be found in textbooks and reviews, e.g. [27, 28].

As our knowledge of physics is limited at energy scales higher than those our current experimental prowess can manage to probe, the Standard Model (SM) is but an effective theory itself, encoding only what we already know of a more fundamental theory.

We can write out the effective Hamiltonian for a certain type of process using operator-product expansion (OPE) [29]: To a given order, it can be expressed as the sum of matrix elements of effective local operators  $O_i$ , each weighted by a process-independent Wilson coefficient,  $C_i$ , which encodes high-energy-scale effects down to  $M_W$ :

$$\mathcal{H}^{\text{eff}} = \sum_i C_i(\mu) O_i(\mu) + \mathcal{O}(1/M_W^2).$$

The sum has to include all gauge-invariant operators allowed by the symmetries of the theory with dimensions above 4. The OPE series is equivalent to the full theory if all orders of  $1/M_W^2$  are considered; truncation provides a systematic scheme for an approximate theory.

The beauty and power of this framework come through in its ability to drastically simplify many strong-interaction calculations, which are challenging due to the confin-

ing nature of QCD. Wilson coefficients, which are responsible for the high-frequency modes (having absorbed the effects of integrated-out heavy fields), are calculated perturbatively at a high scale (say  $M_W$ ), by equating calculations using both the effective and full theories to a given order, in a process called “matching”. They are then evolved down to the characteristic scale  $\mu$  relevant for the (low-energy) process under consideration. Large logarithms of  $(M_W/\mu)^2$  arising from this are resummed using renormalisation-group (RG) methods. (The details of RG-related technology – anomalous dimensions and beta functions etc. – are available in a wide range of didactic literature e.g. [27, 30].) Calculations of the local hadronic matrix elements remain relatively complex, to be unravelled by non-perturbative methods like sum rules or lattice calculations, and it is their systematic uncertainties that tend to dominate the final outcome.

As only the high-energy portion of any effective theory is meddled with, its infrared (IR) behaviour should directly replicate that of the full theory. It makes sense to some cases to perform the integrating-out of heavy degrees of freedom more than once, as in SCET-I and -II (see later sections); in such a scenario, the IR limit of an effective theory should give the effective theory below.

It is important to note that experimentally sought-after New-Physics effects can reveal themselves either through an alteration (from SM-predicted values) in the Wilson coefficients, or through new effective operators which are absent in the SM framework. Beyond the above introduction, we shall take the internal gears of effective theories in general as a given; now we delve more deeply into the specific effective theories, including their principles and notations, which form the backbone of form-factor calculations in Chapter 5.

### 3.1.1 In Heavy Flavour Physics

In heavy flavour physics, the characteristic energy scale can be identified as the mass of the heavy quark in question. Here we specify this to be  $m_b \sim 5 \text{ GeV}$ , the mass of the bottom quark whose FCNC decays into the light strange quark are of interest in this work. After matching (at a scale of around  $M_W$ ), the Wilson coefficients have to be evolved to this hadronic scale. The set of leading (dimension-6) effective operators for  $b \rightarrow s$  and  $\Delta B = 1$  are (following mostly the conventions of [28, 31]):

Current-current operators:

$$O_1^{(U)} = (\bar{s}_i U_j)_{V-A} (\bar{U}_j b_i)_{V-A}, \quad O_2^{(U)} = (\bar{s}_i U_i)_{V-A} (\bar{U}_j b_j)_{V-A}, \quad (3.1)$$

QCD penguins:

$$\begin{aligned} O_3 &= (\bar{s}_i b_i)_{V-A} \sum_q (\bar{q}_j q_j)_{V-A}, & O_4 &= (\bar{s}_i b_j)_{V-A} \sum_q (\bar{q}_j q_i)_{V-A}, \\ O_5 &= (\bar{s}_i b_i)_{V-A} \sum_q (\bar{q} q)_{V+A}, & O_6 &= (\bar{s}_i b_j)_{V-A} \sum_q (\bar{q}_j q_i)_{V+A}, \end{aligned} \quad (3.2)$$

Electroweak penguins:

$$\begin{aligned} O_7 &= \frac{3}{2} (\bar{s}_i b_i)_{V-A} \sum_q e_q (\bar{q}_j q_j)_{V+A}, & O_8 &= \frac{3}{2} (\bar{s}_i b_j)_{V-A} \sum_q e_q (\bar{q}_j q_i)_{V+A}, \\ O_9 &= \frac{3}{2} (\bar{s}_i b_i)_{V-A} \sum_q e_q (\bar{q}_j q_j)_{V-A}, & O_{10} &= \frac{3}{2} (\bar{s}_i b_j)_{V-A} \sum_q e_q (\bar{q}_j q_i)_{V-A}, \end{aligned} \quad (3.3)$$

Magnetic dipole penguins:

$$O_{7\gamma} = \frac{e m_b}{8\pi^2} \bar{s}_i \sigma^{\mu\nu} (1 + \gamma_5) b_i F_{\mu\nu}, \quad O_{8g} = \frac{g_s m_b}{8\pi^2} \bar{s}_i \sigma^{\mu\nu} (1 + \gamma_5) T_{ij}^a b_j G_{\mu\nu}^a, \quad (3.4)$$

Semi-leptonic operators:

$$O_{9\ell} = (\bar{s}_i b_i)_{V-A} (\bar{\ell}\ell)_V, \quad O_{10\ell} = (\bar{s}_i b_i)_{V-A} (\bar{\ell}\ell)_A, \quad (3.5)$$

where  $e_q$  is the electric charge of the relevant quark in units of  $e$ , and the sums over  $q$  include all quarks but  $t$ , except for  $O_{1,2}$  where  $U = u, c$  only. Operators for other

FCNC decays like  $b \rightarrow d$  and  $s \rightarrow d$  take analogous forms. The basic purely QCD effective Hamiltonian for the process  $b \rightarrow s\bar{q}q$  using these operators become:

$$H_{\text{eff}}^{b \rightarrow s\bar{q}q} = \frac{G_F}{\sqrt{2}} \left\{ \sum_{i=1,2} C_i(\mu) \left( \lambda_u O_i^{(u)} + \lambda_c O_i^{(c)} \right) + (\lambda_u + \lambda_c) \sum_{i=3-6,8g} C_i(\mu) O_i \right\} + \text{h.c.}, \quad (3.6)$$

where we have used the GIM mechanism to remove reference to dependences on the top quark which is no longer a dynamical degree of freedom in the effective theory.  $O_{7-10}$  and  $O_{7\gamma}$  come into the expression once electroweak corrections are included.

The two semi-leptonic operators  $O_{9\ell}$  and  $O_{10\ell}$  enter in addition for  $\Lambda_b \rightarrow \Lambda \ell^+ \ell^-$ , which this work mainly concerns. Along with the electromagnetic penguin  $O_{7\gamma}$ , these operators will be the most important and interesting especially in the numerical analysis of our results in Section 5.3; these will be re-notated as  $O_{7,9,10}$  from now on whenever necessary (it should be clear from the context). Other operators like  $O_{8g}$  and  $O_{3-6}$  only enter in sub-leading radiative corrections. The values of corresponding Wilson coefficients to the above operators and their anomalous dimensions can be found in [32].

$$H_{\text{eff}}^{b \rightarrow s\ell\ell} = \frac{G_F}{\sqrt{2}} \left\{ \sum_{i=1,2} C_i(\mu) \left( \lambda_u O_i^{(u)} + \lambda_c O_i^{(c)} \right) + (\lambda_u + \lambda_c) \sum_{\substack{i=3-10, \\ 7\gamma, 8g, 9\ell, 10\ell}} C_i(\mu) O_i \right\} + \text{h.c.}, \quad (3.7)$$

Beyond the Standard Model,  $b \rightarrow s$  transitions need no longer be left-handed in nature, and extra (primed) operators with the wrong chirality may enter the Hamiltonian with no mass suppression (also, scalar and pseudoscalar operators) – a fertile ground for exploration in NP modelling.

## 3.2 Heavy-Quark Effective Theory (HQET)

As its name suggests, heavy-quark effective theory (HQET) [33–35] describes the physics and symmetries that result when the limit  $m_Q \rightarrow \infty$  is taken, for processes

involving a heavy quark (large energy scale  $m_Q$ ) and soft interactions (typical QCD confining scale  $\Lambda_{\text{QCD}}$ ). From now on, we shall fix the identity of the heavy quark  $Q$  to be  $b$ , though the same principle, less fittingly, could also apply to the charm quark ( $m_c \simeq 1.3 \text{ GeV}$ ).

Within a hadronic bound state with only one heavy quark, the latter acts as a “static colour source”, and as it only interacts with soft degrees of freedom, it is nearly on-shell, and its momentum can be parametrised as

$$p^\mu = m_b v^\mu + k^\mu,$$

where  $v$  is the 4-velocity of the heavy quark with  $v^2 = 1$ , and  $k \sim \mathcal{O}(\Lambda_{\text{QCD}})$  is the “residual” momentum, if a frame is chosen in which the heavy quark is near-stationary. (For simplicity its rest frame is often chosen, in which case  $v^\mu = (1, 0, 0, 0)$ .) If one decomposes the Dirac spinor of the heavy quark in such a way that

$$\begin{aligned} Q(x) &= e^{-im_b v \cdot x} (h_v(x) + H_v(x)), \\ \text{with } h_v(x) &= e^{im_b v \cdot x} \frac{1 + \not{v}}{2} Q(x) \\ \text{and } H_v(x) &= e^{im_b v \cdot x} \frac{1 - \not{v}}{2} Q(x), \end{aligned} \quad (3.8)$$

$h_v(x)$  and  $H_v(x)$  can be identified as, respectively, the large massless component, and the small component of the heavy-quark Dirac spinor with mass  $2m_b$ . This can be seen if we substitute (3.8) into the Dirac Lagrangian

$$\begin{aligned} \mathcal{L} &= \bar{Q} (i\not{D} - m_b) Q \\ &= \bar{h}_v i v \cdot D h_v + \bar{H}_v (-i v \cdot D - 2m_b) H_v + \bar{h}_v i \not{\vec{D}} H_v + \bar{H}_v i \not{\vec{D}} h_v, \end{aligned} \quad (3.9)$$

where  $i \not{\vec{D}} = i\not{D} - \not{v} (i v \cdot D)$ . Power-counting shows that indeed  $H_v \sim \mathcal{O}\left(\frac{\Lambda_{\text{QCD}}}{m_b}\right) h_v$ . To achieve the desired effective theory, the heavy degrees of freedom need to be integrated out, and in this context it is the  $H_v$  field, which cannot be excited through soft interactions. This is done by using its equation of motion. The effective Lagrangian becomes

$$\mathcal{L}_{\text{HQET}} = \bar{h}_v i v \cdot D h_v + \frac{1}{2m_b} \bar{h}_v i \not{\vec{D}} i \not{\vec{D}} h_v + \dots; \quad (3.10)$$

the form of the leading term illuminates both the flavour and spin symmetries that have resulted from taking the heavy-quark limit. These are broken already by the second,  $\mathcal{O}(1/m_b)$  term in (3.10).

In its current form so far the HQET lacks the full QCD gauge invariance, as hard quarks and gluons have been integrated out and the remaining  $h_v$  field represents only the soft fluctuations of the heavy quark field about its mass shell. To remedy this, a modified set of gauge transformation rules can be defined, that also scale correctly with the soft-quark and soft-gluon fields in the power-counting.

On the other hand, the effective theory can be further simplified by decoupling soft gluons from the heavy field, by performing a field re-definition of  $h_v$ :

$$h_v(x) = Y_v(x) h_v^{(0)}(x); \quad (3.11)$$

the object which satisfies our need turns out to be in the form of a time-like Wilson line in the direction of  $v$ , defined as:

$$Y_v(x) = P \exp \left( ig_s \int_{-\infty}^0 dt v \cdot A_s(x + tv) \right), \quad (3.12)$$

where  $P$  is the path-ordering symbol. With its property to “convert” a covariant derivative into a normal, partial derivative, the HQET Lagrangian takes the final form of

$$\mathcal{L}_{\text{HQET}} = \bar{h}_v^{(0)} i v \cdot \partial h_v^{(0)} + \mathcal{O}(1/m_b). \quad (3.13)$$

At leading order this seems like a simple, if a bit useless, free-quark theory. The truth is more complicated once external interaction currents are taken into account, taking back into the picture soft quarks in a non-trivial way. The two issues of modified gauge transformation rules and decoupling of soft interactions from the leading quark fields will be discussed in some more detail in the following discussion on SCET.

We mention HQET here not only because of its usage in defining the heavy effective field in a heavy-to-light transition like  $\Lambda_b \rightarrow \Lambda \ell^+ \ell^-$ , but also because it is a precursor in some ways to the more complicated effective theory, SCET, to be discussed



and used imminently. Ideas can be gleaned from how HQET simplifies treatments of heavy-to-heavy hadronic decays. Using the heavy-quark symmetry projectors, a larger number of matrix elements of currents in QCD reduce to a smaller set in HQET, the Isgur-Wise functions [35, 36] which depend on the variable  $v \cdot v'$  only; for example in the decay  $\Lambda_b \rightarrow \Lambda_c e \bar{\nu}$ , taking both  $m_b, m_c \rightarrow \infty$ , there is only one independent hadronic form factor remaining, and for (heavy-to-light)  $\Lambda_b \rightarrow \Lambda$  decays, two. Beyond the strict HQET limit there are both  $1/m_b$  and  $\alpha_s$  corrections. This idea of a consistent power-counting (in the inverse of a large characteristic scale) can be taken further; by applying it to other suitable situations, one hopes to extract symmetries that decomplexify QCD calculations.

### 3.3 Soft-Collinear Effective Theory (SCET)

In various QCD processes inclusive and exclusive, jet-like dynamics play a crucial part; in both jet hadronic physics and flavour transitions, light particles with energies much larger than their invariant masses abound, and their dynamics are essentially Minkowskian. For instance, in the heavy-to-light decay of  $\Lambda_b \rightarrow \Lambda \ell^+ \ell^-$  (which example will provide the terminology in the following discussion for variables and expressions), the  $\Lambda$  hadron would move close to on the light cone, and the  $s$  quark, when receiving most of the energy from the decaying heavy  $b$  quark (in the large recoil limit), is collinear with its hadron. Light degrees of freedom are also present. In the reference frame of the heavy, decaying hadron, we can assume the  $\Lambda$  momentum  $p'$  to be large in one light-cone direction  $n_-^\mu$  and small in the opposite  $n_+^\mu$ . In general one requires  $n_+ \cdot n_- = 2$  and  $n_\pm^2 = 0$ , but they are commonly chosen as  $n_\pm^\mu = (1, 0, 0, \pm 1)$ . So,

$$p'^\mu = n_+ p' \frac{n_-^\mu}{2} + n_- p' \frac{n_+^\mu}{2} + p'_\perp{}^\mu; \quad (3.14)$$

the components scale as  $(n_+ p', p'_\perp, n_- p') \sim Q(1, \lambda^{1/2}, \lambda)$ , where  $Q$  is a large characteristic scale we identify as  $Q \sim m_b \sim E_\Lambda$ , and  $\lambda \sim \Lambda_{\text{QCD}}/m_b$ . We can see  $p'^2 = (n_+ p')(n_- p') + p'_\perp{}^2 \sim m_b \Lambda_{\text{QCD}} = \mu_{\text{hc}}^2$  – an intermediate energy scale, distinct

from the hard (virtuality  $m_b^2$ ) and soft ( $\Lambda_{\text{QCD}}^2$ ) scales. The  $\Lambda$  particle also contains soft degrees of freedoms such as the light spectator quarks, whose momenta scale as  $(n_+k, k_\perp, n_-k) \sim Q(\lambda, \lambda, \lambda)$ .

SCET sets out to take into account both soft and hard-collinear (as we shall name the intermediate scale which displays the momentum scaling as  $p'$  described above) momentum-scaling, by assigning them independent effective fields. It was first formulated by Bauer, Fleming, Pirjol, Stewart (BFPS) [37, 38]<sup>1</sup>, and further developed by Beneke, Chapovsky, Diehl, Feldmann (BCDF) [41, 42] and others including [43, 44], and exists in a few versions with slight differences in terminology and technicalities. The original BFPS “label” formulation makes an effort at letting the SCET procedures emulate HQET, so that a hard-collinear momentum is made to comprise of a “label” for its large component, and other “residual” dynamical components, a bit like  $p = m_b v + k$  for a heavy quark in HQET. Projection operators that only act on the large labels replace conventional derivatives, resulting in a hybrid position/momentum-space representation. On the other hand, the BCDF formulation, to which we shall stick in this work, works consistently in the position space and explicitly retains all momentum components of all fields.

SCET shares the same ideas as the method of regions in QCD calculations, but better facilitates systematic power-counting and corrections. The construction of the SCET will in certain aspects mimic that of HQET – which is now enlisted to describe heavy fields, and integrate out hard degrees of freedom irrelevant to SCET physics. Let us start by considering the hard-collinear quark field. In  $\psi_{\text{hc}}$  can be identified

---

<sup>1</sup>It serves as a formal extension of the older “Large-Energy Effective Theory” (LEET) [39, 40] which does not include hard-collinear gluon fields and hence cannot fully account for hard-scattering gluon-exchange contributions.

the large and small 2-component spinors, using the appropriate SCET projectors:

$$\begin{aligned}\psi_{\text{hc}}(x) &= \xi(x) + \eta(x), & \text{where } \xi(x) &= \frac{\not{n}_- \not{n}_+}{4} \psi_{\text{hc}}(x), \\ & & \text{and } \eta(x) &= \frac{\not{n}_+ \not{n}_-}{4} \psi_{\text{hc}}(x).\end{aligned}\quad (3.15)$$

One can demonstrate by power-counting (in terms of  $\lambda$ ) that  $\xi$  indeed generates the leading contribution.  $\eta$  can be “integrated out” by using its equation of motion, whose form

$$\eta(x) = -\frac{\not{n}_+}{2} \frac{1}{in_+ \cdot D + i\epsilon} i\not{D}_\perp \xi(x) \quad (3.16)$$

reveals one aspect where SCET and HQET differ: while the latter gives a Lagrangian which is close to local, SCET remains a non-local theory, as seen from the appearance of inverse differential operators unaccompanied by a large mass, unlike in HQET. Putting this into the QCD Lagrangian  $\bar{\psi} i\not{D} \psi$ , with  $\psi = \xi + \eta + q$  where we have added back the soft quark field  $q$ , we end up with the first semblance of a SCET effective Lagrangian:

$$\begin{aligned}\mathcal{L}_{\text{SCET}} &= \bar{\xi} \left( in_- D + i\not{D}_\perp \frac{1}{in_+ D + i\epsilon} i\not{D}_\perp \right) \frac{\not{n}_+}{2} \xi + \bar{q} i\not{D}_s q \\ &\quad + \bar{\xi} g_s \not{A}_{\text{hc}} q + \bar{q} g_s \not{A}_{\text{hc}} \xi - \bar{q} g_s \not{A}_{\text{hc}} \frac{1}{in_+ D} \frac{\not{n}_+}{2} g_s \not{A}_{\text{hc}} q \\ &\quad - \bar{\xi} i\not{D}_\perp \frac{1}{in_+ D} \frac{\not{n}_+}{2} g_s \not{A}_{\text{hc}} q - \bar{q} g_s \not{A}_{\text{hc}} \frac{1}{in_+ D} \frac{\not{n}_+}{2} i\not{D}_\perp \xi,\end{aligned}\quad (3.17)$$

where (as below)  $iD_{s,\text{hc}}^\mu = i\partial^\mu + g_s A_{s,\text{hc}}^\mu$ . The purely hard-collinear and purely soft Lagrangian terms (on the first line of (3.17)) are leading ( $\mathcal{O}(1)$ ) while the interaction terms involving both sectors start at  $\mathcal{O}(\lambda^{1/2})$ . Any terms that are kinematically forbidden do not appear in the SCET Lagrangian; for instance, one hard-collinear quark line cannot be connected to two soft quark lines as momentum must be conserved. Note that the integration measure  $\int d^4x$  should be treated as scaling as  $\lambda^{-2}$  and  $\lambda^{-4}$  for the two leading terms respectively.

As SCET aims at a formalised treatment of effective QCD fields based on indi-

vidual momentum configurations<sup>2</sup>, the Lagrangian should be constructed such that it contains only terms that explicitly have a single, homogeneous  $\lambda$ -scaling, to facilitate calculation at each order of  $\lambda$  without risk of double counting. To this end, in (3.17)  $\bar{\xi} in_- D \frac{\not{n}_+}{2} \xi$  should be re-written as

$$\bar{\xi} in_- D_{\text{hc}} \frac{\not{n}_+}{2} \xi + \bar{\xi} g_s n_- \cdot A_s \frac{\not{n}_+}{2} \xi, \quad (3.18)$$

while the inverse covariant derivative should be expanded as

$$\frac{1}{in_+ D} = \frac{1}{in_+ D_{\text{hc}}} - \frac{1}{in_+ D_{\text{hc}}} g_s n_+ \cdot A_s \frac{1}{in_+ D_{\text{hc}}} + \mathcal{O}(\lambda^4). \quad (3.19)$$

Other terms in the Lagrangian can similarly be separated.

### Multi-pole expansion of soft fields

On the other hand, though all momentum components of the soft fields scale as  $\lambda$ , one has to be careful with interaction terms between hard-collinear and soft fields; as the hard-collinear scaling naturally dominates the vertex momentum, the soft field varies more slowly in some directions than would have led to a leading result, and this results in an inhomogeneous contribution. In order again to disentangle the leading and sub-leading terms, one performs a multi-pole expansion on soft fields, expanding the position arguments so that

$$\phi_s(x) = \left( 1 + x_\perp \cdot \partial_\perp + x_+ \cdot \partial + \frac{1}{2} x_{\mu\perp} x_{\nu\perp} \partial^\mu \partial^\nu \right) \phi_s(x_-) + \mathcal{O}(\lambda^3 \phi_s), \quad (3.20)$$

where  $x_\mp^\mu \equiv (n_\pm x) n_\mp^\mu / 2$ , as they scale like  $(x_-, x_\perp, x_+) \sim (\lambda^{-1}, \lambda^{-1/2}, 1)$ . From now on, in all interaction terms one should take care to evaluate all soft fields at light-cone position  $x_-$  (while hard-collinear fields remain at general  $x$ .) In any case, there are no such interaction terms at leading order in  $\lambda$  in the SCET Lagrangian.

---

<sup>2</sup>In some physical situations, the hard-collinear and soft momentum modes are not sufficient, as there are other configurations involving momenta scaling as  $Q(1, \lambda, \lambda^2)$  (“collinear”) and  $Q(\lambda^2, \lambda^2, \lambda^2)$  (“ultrasoft”), for example. This more complicated formulation is termed SCET-II, which will rarely be mentioned again, as opposed to SCET-I presented and used in this work.

### Gauge transformation rules

After setting up separate effective fields with different momentum scalings and integrating out some degrees of freedom, the full QCD gauge invariance is lost, leaving only a “residual” gauge invariance described by a modified set of gauge transformation rules, whose gauge operators  $U_{\text{hc}}$  and  $U_s$  also follow corresponding scaling properties.

$$\begin{aligned}
 \text{Hard-collinear: } A_{\text{hc}} &\rightarrow U_{\text{hc}} A_{\text{hc}} U_{\text{hc}}^\dagger + \frac{i}{g} U_{\text{hc}} \left[ D_s, U_{\text{hc}}^\dagger \right], & \xi_{\text{hc}} &\rightarrow U_{\text{hc}} \xi_{\text{hc}}, \\
 A_s &\rightarrow A_s, & q &\rightarrow q, \\
 \text{Soft: } A_{\text{hc}} &\rightarrow U_s A_{\text{hc}} U_s^\dagger, & \xi_{\text{hc}} &\rightarrow U_s \xi_{\text{hc}}, \\
 A_s &\rightarrow U_s A_s U_s^\dagger + \frac{i}{g_s} U_s \left[ \partial, U_s^\dagger \right], & q &\rightarrow U_s q. \tag{3.21}
 \end{aligned}$$

Soft fields must not transform under hard-collinear transformations, as  $A_{\text{hc}}$  would ruin the soft scaling. Meanwhile this does not happen the other way round, and the soft gauge field acts as a kind of slowly varying background field for the hard-collinear fields, though this does cause  $A_{\text{hc}}$  to transform inhomogeneously under its own gauge transformation.

### Wilson lines

Already briefly mentioned in the discussion of HQET, Wilson lines are used in multiple facets of SCET and HQET.

All interactions between soft and hard-collinear fields at leading order can be removed, similar to what happens in the case of HQET, by imposing a re-definition of the  $\xi$  field, using a “soft” Wilson line  $Y_{n_-}(x_-)$  in the appropriate direction, defined as with  $Y_v(x)$  in (3.12) with  $n_-$  replacing  $v$ :

$$\xi(x) = Y_{n_-}(x_-) \xi^{(0)}(x) \quad \text{and} \quad A_{\text{hc}}^\mu(x) = Y_{n_-}(x_-) A_{\text{hc}}^{(0)\mu}(x) Y_{n_-}^\dagger(x_-). \tag{3.22}$$

The leading purely hard-collinear term in the SCET Lagrangian now simplifies to  $\bar{\xi}^{(0)}(x) i n_- D_{\text{hc}}^{(0)}(x) \xi^{(0)}(x)$ .

Wilson lines can also help to remove the unsavoury inverse covariant differential operators from the Lagrangian, by harnessing its effect on a field or object  $\phi(x)$ :

$$\frac{1}{i n_+ D_{\text{hc}}} \phi(x) = W_{\text{hc}} \frac{1}{i n_+ \partial} W_{\text{hc}}^\dagger \phi(x) = -i W_{\text{hc}}(x) \int_{-\infty}^0 dt \left[ W_{\text{hc}}^\dagger \phi \right](x + t n_+), \quad (3.23)$$

where the hard-collinear Wilson line is defined by

$$W_{\text{hc}}(x) = P \exp \left( i g_s \int_{-\infty}^0 dt n_+ \cdot A_{\text{hc}}(x + t n_+) \right). \quad (3.24)$$

The leading-order SCET Lagrangian becomes:

$$\begin{aligned} \mathcal{L}_{\text{SCET}} = & \bar{\xi}^{(0)}(x) i n_- \cdot D_{\text{hc}}^{(0)} \frac{\not{n}_+}{2} \xi^{(0)}(x) \\ & - \left[ \bar{\xi}^{(0)} i \overleftarrow{D}_{\text{hc}\perp}^{(0)} W_{\text{hc}}^{(0)} \right](x) \frac{\not{n}_+}{2} i \int_{-\infty}^0 dt \left[ W_{\text{hc}}^{\dagger(0)} i \not{D}_{\text{hc}\perp}^{(0)} \xi^{(0)} \right](x + t n_+). \end{aligned} \quad (3.25)$$

Wilson lines are also immensely useful in building gauge-invariant objects and operators like external currents. For example, the full QCD heavy-to-light (hard-collinear) current  $\bar{q} \Gamma b$  is not matched directly to  $\bar{\xi} \Gamma h_v$ , but to  $\bar{\xi} W_{\text{hc}} \Gamma h_v$ , which is the combination that preserves gauge invariance. Moreover, this object actually sums up an infinite geometric series of leading-order hard-collinear gluon emissions from the heavy quark before the decay vertex. Such leading-order couplings with  $n_- A_{\text{hc}}$  are large, so unlike  $A_{\text{hc}\perp}$  and  $n_- A_{\text{hc}}$  they cannot be written as an expansion; they have to be summed by exponentiation, and a hard-collinear Wilson line turns out to be the right object for this purpose. Such off-shell heavy-quark lines are not part of SCET and HQET by construction, and must be reproduced as an effective current.

Beyond tree level, the general matching expression is a bit more complicated but very interesting. A list of explicit current matchings can be found in [45]. In general, the matching is given by

$$\begin{aligned}
\bar{\psi}_{\text{hc}}(x) \Gamma b(x) &\rightarrow \sum_i \int dt \tilde{C}_i(t, \mu) (\bar{\xi} W_{\text{hc}})(x + t n_+) \Gamma_i h_v(x_-) \\
&= \sum_i C_i(n_+ \cdot P^{\text{hc}}, \mu) \left( \bar{\xi}^{(0)} W_{\text{hc}}^{(0)} \right)(x) \Gamma_i [Y_{n_-}^\dagger(x_-) Y_v(x_-)] h_v^{(0)}(x_-),
\end{aligned} \tag{3.26}$$

where we have used translational invariance and the decoupled hard-collinear quark fields again.  $P^{\text{hc}}$  refers to the total net hard-collinear momentum. In other words it can be said that QCD operators match to a sum of products of SCET operators, which reproduce correct physics below the scales integrated out, and Wilson coefficients that encode the short-distance effects. Even though the final expression of (3.26) looks like it has cleanly separated into the heavy and hard-collinear parts, with a sterile heavy field and a hard-collinear  $\bar{\xi}^{(0)} W_{\text{hc}}^{(0)}$  which is decoupled from soft interactions, the object  $[Y_{n_-}^\dagger(x_-) Y_v(x_-)]$  has arisen – this constitutes a cusp singularity at position  $x_-$  where the two Wilson lines of different directions meet. This is a universal object of geometric origin and gives rise to a logarithmic term in the anomalous scaling dimension of the effective current, and knowledge of its value to sufficiently high orders is important for RG resummation of large Sudakov logarithms.

In Chapter 5, use of Wilson lines (to maintain gauge invariance in hard-collinear fields) will be implicitly assumed and not written out every time.

### Renormalisation-group evolution of Wilson coefficients

The matching between QCD and SCET heavy-to-light currents leads to Wilson coefficients which are renormalisation-scale-dependent. In the RG equation

$$\frac{d}{d \ln \mu} C_i(\mu) = \gamma(\mu) C_i(\mu), \tag{3.27}$$

the anomalous dimension has the general structure

$$\gamma(\mu) = -\Gamma_{\text{cusp}}(\alpha_s) \ln \frac{\mu}{\mu_{\text{hard}}} + \gamma'(\alpha_s) \tag{3.28}$$

which includes an explicit logarithmic dependence on the energy scale together with the cusp anomalous dimension [44] mentioned above; this is a special property of the RG structure in SCET.<sup>3</sup> The solution has been found [37] to satisfy the universal evolution

$$C_i(\mu) = C_i(m_b) \exp \left[ -\frac{4\pi C_F}{\beta_0^2 \alpha_s(m_b)} \left( \frac{1}{z} - 1 + \ln z \right) + f_1(z) \right], \quad (3.29)$$

where

$$z = \frac{\alpha_s(\mu)}{\alpha_s(m_b)} = \left( 1 + \frac{\beta_0}{2\pi} \alpha_s(m_b) \ln \frac{\mu}{m_b} \right)^{-1}.$$

The first term in the exponential is responsible for summing up “double logarithms” of the form  $\alpha_s^n \ln^{n+1}(\mu/m_b)$  while  $f_1(z)$  (whose full form can be found in [37]) sums up next-to-leading-log terms,  $\alpha_s^n \ln^n(\mu/m_b)$ , performing the necessary job of resumming large logarithms that arise naturally in effective theories where large disparate scales would otherwise have invalidated ordinary perturbative expansions.

## 3.4 Factorisation

The factorisation theorem, in the context of heavy-to-light flavour transitions, was originally introduced by Beneke, Buchalla, Neubert, Sachrajda (BBNS) for use in non-leptonic two-body  $B$  decays [46–48]. It proposes that certain contributions to decay amplitudes can be separated into universal non-perturbative hadronic parameters and perturbatively calculable, process-dependent kernels, in the heavy-quark limit  $m_b \rightarrow \infty$ . This stays true to the goal in general in effective theories to systematically segregate high- and low-energy physics.

In a clearly oversimplifying scenario called “naïve factorisation”, a decay like  $B \rightarrow \pi \pi$  can be written as:

$$\langle \pi^+ \pi^- | (\bar{u}b)_{V-A} (\bar{d}u)_{V-A} | \bar{B}_d \rangle \rightarrow \langle \pi^- | (\bar{d}u)_{V-A} | 0 \rangle \langle \pi^+ | (\bar{u}b)_{V-A} | \bar{B}_d \rangle, \quad (3.30)$$

---

<sup>3</sup>  $\mu_{\text{hard}}$  is a high scale like  $m_b$  or the large recoil energy.



where the two objects on the right-hand side are essentially a decay constant and a transition form factor. This result is problematic in view of the mismatch in renormalisation-scale dependence, and it also obviously neglects possible gluon interactions between the two pions and final-state rescattering effects.

To put this into a more rigorous framework in which the above is the leading term at the head of a series of corrections (in  $\alpha_s$  and  $1/m_b$ ), more generalised factorisation formulæ are needed. Staying in the case of  $B$  to two light mesons  $M_1, M_2$ , the formula reads:

$$\begin{aligned} \langle M_1 M_2 | \mathcal{O}_i | \bar{B} \rangle = & \sum_j F_j^{B \rightarrow M_1}(m_2^2) \int_0^1 du T_{ij}^I(u) \Phi_{M_2}(u) + (M_1 \leftrightarrow M_2) \\ & + \int_0^1 d\xi du dv T_i^{II} \Phi_B(\xi) \Phi_{M_1}(v) \Phi_{M_2}(u); \end{aligned} \quad (3.31)$$

the  $\Phi_i$ s are the universal non-perturbative objects that describe the mesons, and  $T^{I,II}$  are perturbatively calculable functions which contain to an arbitrary order in  $\alpha_s$  possible contributions due to hard-scattering interactions. At leading order in  $\alpha_s$ , only the first line of (3.31) remains and  $T^I$  is independent of  $u$  – reproducing the naïve factorisation result. However, another type of contribution to the amplitude is still missing from this equation: when the partons only undergo soft interactions, its contribution remain a genuinely non-perturbative, “non-factorisable” quantity, commonly encased in a form factor.

The validity, and to what order in  $\alpha_s$  specifically, of the factorisation theorem has to be proved for each decay on a case-to-case basis. In any case, the idea to take from this approach is that factorisable terms can be identified which can be decomposed into simpler objects than the original transition matrix element.

The original BBNS approach as introduced above concerns non-leptonic decays; as in this work we are principally interested in semi-leptonic  $b$  decays in which a heavy hadron  $H$  decays into a light energetic particle  $L$ , we will turn our attention from now on to a more suited language. Note that this new situation is palpably

simpler than before, as gluon exchange between final states are now impossible. One schematic way of writing the contribution to a particular form factor is:

$$\langle L|\bar{q}\Gamma_i b|H\rangle = C_i(\mu_I)\xi_L(\mu_I) + \phi_H(\mu_{II}) \otimes T_i(\mu_{II}) \otimes \phi_L(\mu_{II}), \quad (3.32)$$

again valid at leading order in  $1/m_b$ . In the first term on the right-hand side,  $C_i = 1 + \mathcal{O}(\alpha_s)$  includes the hard effects (like hard-vertex renormalisations) due to heavy degrees of freedoms already integrated out using effective theory, and  $\mu_I$  is a factorisation scale below  $m_b$ .  $\xi_L$  is the soft overlap form factor mentioned earlier. It arises from the “Feynman mechanism” where a soft particle receives many small boosts to become a higher-energy particle (with no hard-gluon exchanges present.) There are arguments as to why it ought to be suppressed relative to hard-scattering contributions – Sudakov suppression, related to the fact that one quark carries hard-collinear momentum while the spectator quark(s) remains soft, forcing the hadron to live in the end-point region – but numerically the situation is not so clear-cut and it appears that the soft term counts just as importantly as hard-scattering terms in heavy-to-light decays. (For a discussion of Sudakov effects see e.g. [49].) In the strict heavy-quark limit,  $\xi_L$  is expected to be independent of the Dirac structure of the decay current (analogous to the Isgur-Wise functions in heavy-to-heavy decays [50]). In the “QCD factorisation” (QCDF) approach to calculating matrix elements (which leads naturally the related discoveries discussed at the beginning of this section),  $\xi_L$  is formally classified as a non-factorisable, non-perturbative object and must strictly be treated as an input rather than calculated, as ill-defined loop diagrams appear.

The other term in (3.32) – proportional to  $\alpha_s$  as all hard-scattering contributions are – is factorised, at a factorisation scale of  $\mu_{II} < \mu_{hc}$ ; it exists as a convolution of light-cone distribution amplitudes (LCDAs), universal non-perturbative objects treated as inputs describing the distribution of momentum within the initial and final hadrons (see Section 4.2), while  $T_i$  is a perturbatively calculable process-dependent hard-scattering kernel, encoding both hard-collinear interaction effects and hard corrections. This “factorisable” term is readily calculated using the so-called QCDF framework for mesonic transitions [51, 52]. An alternative approach, SCET-based

light-cone sum rules (which will be used in this work), is attuned to deal with both the soft and hard-scattering factorisable contributions, but at the cost of introducing extra auxiliary parameters and the always tricky approximation of the hadronic spectrum, in place of light-hadron LCDAs. At the end of the day, no method has been found to be truly ideal in this challenging area of matrix-element calculation, and light-cone sum rules in SCET and QCD factorisation (and other alternative methods) are best considered complementary bedfellows.

### 3.5 QCD Sum Rules (on the Light Cone)

The technique of QCD sum rules (for a good review see [53]) is one of the most effective tools to determine non-perturbative parameters of low-lying hadronic states, of which it may otherwise be difficult to get theoretical estimates. A sum rule, in short, is a relation linking a finite number of hadronic parameters, derived by connecting two representations of the same object, a correlation function of two quark currents.

The attractions of QCD sum rules are many. Results attained using this technique are universal – a parameter derived from one sum rule can then be used as an input in another, along with other inputs known from experimental measurements or theoretical calculations of all kinds. Manipulating sum-rule expressions in combination often results in cancellation of inputs and hence of systematic uncertainties. Meanwhile the method has its limitations – there is no systematic, rigorous “textbook” way to proceed; every case has to be considered and analysed individually, preferably with the benefit of experience. Sum rules are often restrained by irreducible systematic errors; nevertheless it remains a route that enjoys reasonable simplicity and allows one to keep track of sources of uncertainties.

Shifman, Vainshtein, Zakharov [54] originally put forward the QCD sum rules in the 1970s (hereby known as the SVZ sum rules). A correlation function of the

time-ordered product of two quark currents is defined between QCD vacuum states, as an analytic function of the momentum-transfer variable  $q^2$  (which can for instance refer to the virtuality of the photon that leads to the creation of a pair of quarks, as in the following sample correlation function:)

$$\Pi_{\mu\nu}(q) = i \int d^4x e^{iq \cdot x} \langle 0 | T \{ j_\mu(x) j_\nu(0) \} | 0 \rangle = (q_\mu q_\nu - q^2 g_{\mu\nu}) \Pi(q^2), \quad (3.33)$$

where  $j_\mu = \bar{q} \gamma_\mu q$ . The currents involved have the right quantum numbers corresponding to the states and process at hand. Light-cone sum rules (LCSRs) (see e.g. [55–57]) is a modification most suited to describing heavy-to-light flavour processes, where the starting point is a time-ordered product of two appropriate currents sandwiched between the vacuum state and an on-shell hadronic (or photonic) state. The other hadron is represented by an interpolating current. For instance, the  $B \rightarrow \pi$  decay would involve a correlation function of the  $b \rightarrow u$  current and the  $b-d$  pseudoscalar interpolating current (see Figure 3.2):

$$\Pi_\mu(q) = i m_b \int d^4x e^{iq \cdot x} \langle \pi(p_\pi) | T \{ \bar{u}(0) \gamma_\mu b(0) \bar{b}(x) i \gamma_5 d(x) \} | 0 \rangle. \quad (3.34)$$

The quark decay current is designed to project out the form factor being estimated. The correlation function displays vastly different behaviour depending on the value of  $q^2$ : at large negative  $q^2 \ll -\Lambda_{\text{QCD}}^2$ , the particles involved are highly virtual, and the short-distance physics is generally calculated within the framework of perturbation theory. If  $q^2$  is raised to positive values, the particles become real observed hadronic states; long-distance physics lurks into view, and the correlation function has to be expressed in terms of the hadronic spectrum. These two views of the same object are then connected through dispersive analysis.

In SVZ sum rules, the currents are sandwiched between QCD vacuum states. To fully account for the true non-perturbative vacuum effects, short-distance operator product expansion (OPE) is used to separate the correlation function into perturbatively calculable Wilson coefficients, and universal vacuum expectation values of field operators known as vacuum condensates. (In heavy flavour physics the OPE is facilitated by a natural scale  $m_b$ .) These objects, which have to be determined elsewhere

and imported into the sum rules as inputs, take care of the interactions with the background field of soft vacuum gluons and quarks. These condensates rank in importance in order of their mass dimensions; usually only the first few lowest-dimension terms are relevant. In LCSR, the correlation function is expanded near the light-cone as it is dominated by light-like distances in co-ordinate space (the validity of this is carefully demonstrated in [53]), resulting in an OPE-like procedure with the result that it is now expressible as the sum of a series of convolutions, where the perturbative process-dependent objects are not Wilson coefficients but hard-scattering kernels, and the non-perturbative inputs are light-cone distribution amplitudes, which are ordered by twist (see Section 4.2.1). A generic mesonic LCDA correlation function looks like:

$$\Pi(q^2, p^2) = \sum_n \int_0^1 du T^{(n)}(u, q^2, p^2, \mu) \phi^{(n)}(u, \mu), \quad (3.35)$$

where  $\phi^{(n)}$  is a LCDA term at twist  $n$ . Also note that a factorisation-scale dependence has entered both elements which must cancel after convolution.

On the hadronic side of the sum-rule derivation, the spectrum typically contains a small number of (for convenience in this discussion we shall assume this to be a single ground state reasonably far away from any other higher state) low-lying resonant states (corresponding to poles on the real axis of the  $q^2$  complex plane), and a continuum of higher-energy states (a cut, beginning at  $q^2 = s_{\text{cut}}$ ). By defining an appropriate contour, as shown in Figure 3.1, and taking its radius to infinity assuming the integrand vanishes sufficiently fast, Cauchy's formula gives a dispersion relation:

$$\Pi(q^2) = \int_{s_{\text{cut}}}^{\infty} ds \frac{\rho(s)}{s - q^2 - i\epsilon}, \quad (3.36)$$

where  $\rho(s)$ , the spectral density function, describes the specific physical spectrum at hand.

The hadronic content of the spectrum is, however, often poorly understood. To help isolate the contribution of the ground state in which one's interests lie, the unitarity relation is used to insert a complete set of states into the correlation function,

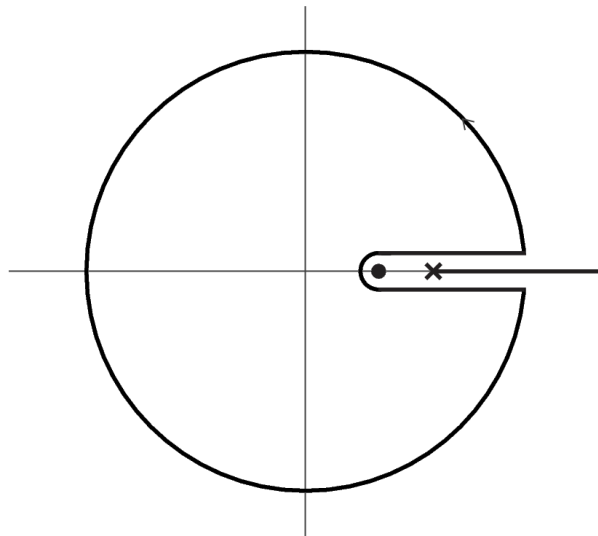


Figure 3.1: Contour on the complex  $q^2$ -plane used to get the dispersion relation. The circular dot represents a generic excited-state resonance (a pole on the real axis), and the cross shows the beginning of the continuum of higher-energy states (a cut).

from which one then extracts the ground state, represented as a  $\delta$ -function-like resonance whose normalisation  $f_M$  depends on the quark currents in the correlation function; everything else (mostly the continuum states) is shelved into a spectral function. Hence the total spectral density function can now be expressed as:

$$\rho(s) = f_M \delta(s - M^2) + \rho^*(s) \theta(s - s_{\text{cut}}). \quad (3.37)$$

To evade having to find knowledge of the heavier states in the spectrum, one invokes quark-hadron duality, which assumes at large enough  $q^2 > s_0$ , the integrated spectral function is equivalent to that calculated using OPE, as if hadrons could be approximated by a free-parton picture. This allows the integral in the OPE representation of the correlation function to be truncated above this “threshold parameter”  $s_0$ , which is typically taken as the location of the next highest resonance or the beginning of the continuum, above the ground state.

As we have seen, QCD sum rules are by construction really only ideal for studying low-lying hadronic states, in particular the ground state (isolated knowledge of higher

states are typically difficult to get, even if one uses tricks based on symmetries and so on to cancel out certain undesirable contributions.) A second, mathematical trick further pushes on the derivation to its natural conclusion: a Borel transformation,

$$\Pi(M_{\text{Bor}}^2) = \hat{\mathcal{B}}_{M_{\text{Bor}}^2} \Pi(q^2) = \lim_{\substack{-q^2, n \rightarrow \infty \\ -q^2/n = M_{\text{Bor}}^2}} \frac{(-q^2)^{n+1}}{n!} \left( \frac{d}{dq^2} \right)^n \Pi(q^2), \quad (3.38)$$

is performed, which eliminates any positive polynomials in  $q^2$  and suppresses higher states exponentially, achieving the overall effect of emphasising the contribution of nothing but the ground state.

These procedures introduce auxiliary parameters into the sum rules – the Borel parameter  $M_{\text{Bor}}^2$  and the hadronic threshold parameter  $s_0$  respectively, which unfortunately and inevitably carry their own associated uncertainties, as, for example, the hadronic spectrum of the interpolating current is more often than not not clear-cut in its structure beyond the lowest states. These parameters are not necessarily process-independent, but it is usually sensible to get at least an order-of-magnitude estimate from other sum rules. This issue must be considered carefully during the analysis on the reliability of the final sum-rule expression. With hope, there exist (a range of) values of them that lead to a stable sum rule. Despite this weakness the sum rule method is often still favoured for its simplicity compared to methods like lattice-based calculations.

Flavour physics-related parameters that have been successfully calculated using sum rules over the years include quark masses, meson decay constants, LCDA-related parameters like Gegenbauer moments, and also transition form factors (see e.g. [58–63] for achievements in decay form factors of  $B$  mesons over the years). In this work, we combine it with SCET to estimate form factors entering the decay  $\Lambda_b \rightarrow \Lambda \ell^+ \ell^-$  in the large-recoil limit.

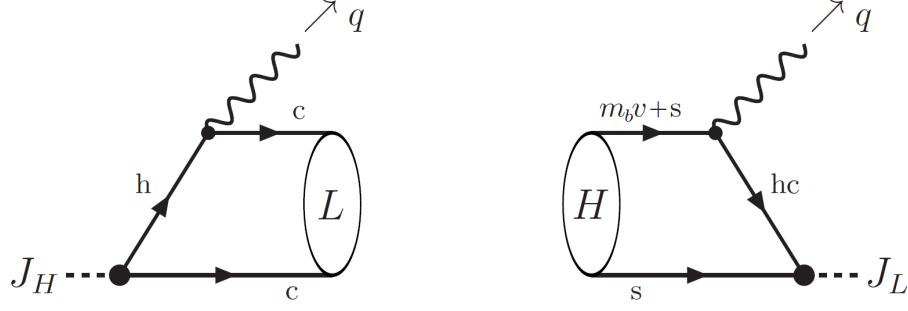


Figure 3.2: Sum-rule correlation diagrams, using the soft Feynman-mechanism term as an example, in conventional light-cone sum rules (left) and SCET LCSRs (right).

### 3.5.1 SCET LCSRs

For the quintessential exclusive heavy-to-light decay  $B \rightarrow \pi$ , it has been shown [64] that light-cone sum rules produce results that fit with symmetry relations derived from QCD factorisation for factorisable terms. However, while the traditional LCSR framework is able to assign momentum scalings to quark and gluon lines in individual diagrams reminiscent of SCET procedures, incorporating SCET into the LCSR framework in a fundamental way makes it more naturally accommodating with QCDF ideas, when it comes to identifying factorisable and non-factorisable contributions. With SCET as a formal underlying effective-theory framework to enforce explicit perturbative separation of scales, a modified version of the LCSR technique will facilitate better control of resummation of large logarithms, for both generic and end-point configurations via renormalisation-group methods.

Importantly, while traditional LCSRs do not require the heavy-quark limit to be taken at the beginning, and dispersive analysis is performed with finite heavy-quark masses, a SCET version of LCSRs allows the heavy-quark expansion from the outset, allowing power counting at the correlator level, with the analysis proceeding from there, ending with a systematic expansion of terms in  $1/m_b$  and  $\alpha_s$ .



The first technical modification comes from recognising that the hard degrees of freedom (virtuality  $\mathcal{O}(m_b^2)$ ) in the heavy-quark field are integrated out already into external coefficients. Hence it ought to be treated as an external source field and not forced to enter the correlator as a propagating particle. To this end, the heavy hadron is now made to enter the correlation function through its momentum-space light-cone distribution amplitudes, while the light hadron is represented by a choice of interpolating current with the correct quantum numbers. This swap in the manners of involvement of the initial and final hadrons of course leads to the issue of heavy-hadron LCDAs which require different treatment in a number of ways from their light counterparts (see Section 4.2).

\* \* \*

A generic “factorisable” term in a heavy-to-light decay, as represented by the second term in (3.32), could be visualised as in Figure 3.3: formally, it divides into 3 parts as clearly shown by the structure of the term  $\phi_H \otimes T_i \otimes \phi_L$ . This would require a calculation involving SCET-II, as the quark lines entering the light hadron are counted formally as having collinear momentum:  $p_c \sim Q(1, \lambda, \lambda^2)$ , but with the same virtuality as soft fields. Unfortunately this  $s \otimes hc \otimes c$  factorisation structure is idealistic and reality fails to factorise simply, due to complications between the latter 2 sectors.

Using SCET LCSRs where the separation of the scales  $m_b$ ,  $\mu_{hc}$  and  $\Lambda$  is already built in, and where the light hadron is interpolated by quark fields, one effectively sidesteps complications involving the collinear sector (and usage of SCET-II). Instead of having to consider both soft and collinear radiative corrections and end-point divergences related to the light LCDAs in relevant diagrams, one now only has soft ones from the heavy side. Another significant consequence is that with SCET LCSRs, one can even attempt to deal with the QCDF-designated non-factorisable term, and as seen in [65] and in equation (5.6), it ends up also as a convolution of a heavy LCDA and a kernel-like object – originating from the soft and hard-collinear regions respectively. Thus both factorisable and non-factorisable terms at their respective leading

orders in  $1/m_b$  and  $\alpha_s$  have been calculated; theoretically a systematic and consistent expansion exists but whether the corrections are technically feasible to be derived is another matter. In any case, it is pleasant to see the two types of contributions on equal footing calculationally speaking.

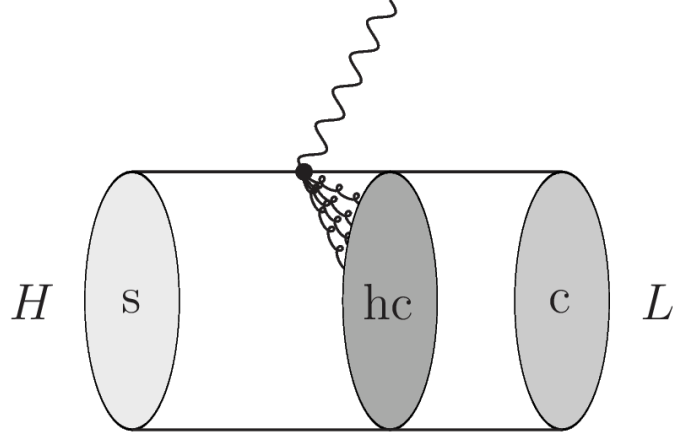


Figure 3.3: A factorisable exclusive heavy-to-light process in QCDF/SCET.

# Chapter 4

## Light-Cone Distribution

## Amplitudes and Decay Form

## Factors for Heavy Baryons

To begin this chapter we motivate flavour research on heavy baryons, in particular the  $\Lambda_b$  particle and its decays; we also discuss two issues which will play important rôles in the SCET sum-rule calculations for  $\Lambda_b \rightarrow \Lambda \ell^+ \ell^-$  in Chapter 5 – the light-cone distribution amplitudes for  $\Lambda_b$  in HQET and relevant form-factor parametrisations.

### 4.1 Baryon versus Meson

Experimentally observed fermionic bound states of quarks exist as either mesons or baryons. The  $B$  meson is the simplest possible hadron containing a heavy quark – a single  $b$  quark and a single light quark. Due to the simplifying power of the high mass of the  $b$ , much has been achieved in terms of data on CKM parameters and CP violation, through measurements of decay rates, angular distributions, mixing parameters and so on, with related technological advances on the theory side.

However,  $B$  mesons exist as pseudoscalar bound states; although angular analyses

can be used to extract helicity information out of rehadronisation processes, using decays of half-integer-spin baryons one has a more direct link to the helicity structure of the weak effective Hamiltonian, for instance whether extra wrong-chirality effective operators suppressed or forbidden in the Standard Model, like an extra operator  $O'_{7\gamma}$  (3.4) where  $(1 + \gamma_5)$  is replaced by  $(1 - \gamma_5)$ , might be at play. In any case baryonic decays have a complementary analysing power to mesonic ones, and their hadronic systematic uncertainties are not the same. A natural candidate for consideration is the decay  $\Lambda_b \rightarrow \Lambda \ell^+ \ell^-$ , whose initial state, the  $\Lambda_b$  baryon, is one of the simplest 3-quark heavy bound states, with the valence structure of a heavy  $b$  quark and the 2 lightest quarks  $u$  and  $d$ , a ground state with  $J^P = \frac{1}{2}^+$  and mass  $M_{\Lambda_b} = 5.6 \text{ GeV}$  [66]. Utilising heavy-quark symmetry leads to considerable theoretical simplification (see Section 3.2 and [35, 67]); within the baryon the dynamics reduce to soft interactions between light degrees of freedom and an external static colour source. In particular, it enjoys an  $SU(2)$  spin symmetry; the spin degrees of freedom “decouple” in the heavy-quark limit, with the light  $u d$  pair forming as a spin- and isospin-singlet “diquark” object, and the overall baryonic state shares the same spin= $\frac{1}{2}$  with the heavy  $b$  quark.

At  $e^+e^-$  colliders,  $\Lambda_b$  baryons retain a significant portion of the longitudinal polarisation that originates from the bottoms produced through  $Z$  decays; at  $p\bar{p}$  hadron colliders the transverse-polarised are less negligible (for more information about  $\Lambda_b$  polarisation from hadronic collisions see e.g. Section 6 of [68]). This is enormously helpful in the study of helicity structure of the effective Hamiltonian mentioned above, through angular analysis of the  $\Lambda_b$  spin and the  $\Lambda$  momentum [69]. Even for unpolarised  $\Lambda_b$  particles, information can be gathered through an angular analysis of the self-analysing secondary decay  $\Lambda \rightarrow p \pi^-$ , or lepton asymmetries.

There are obvious downsides to using baryons in the search for new physics, various additional difficulties compared to mesonic investigations. Immediately one knows that the theoretical calculations become more intricate as there are more light degrees of freedom in bound states, leading to larger theoretical uncertainties. In

addition, baryons like  $\Lambda_b$  suffer the disadvantage of a lower production rate. Compared to the  $B$  meson, the production rate of  $\Lambda_b$  through  $b$  hadronisation is smaller by about an order of magnitude (see e.g. [70]).

On the semi-leptonic decay  $B \rightarrow K^{(*)}\ell^+\ell^-$  much work has been done in past experiments in particular BaBar [71] and Belle [72]. The observation of the baryonic equivalent is not expected at these B-factories, however, due to a practical issue: both of these B-factories, Belle and BaBar, are by definition specialist machines for producing  $B$  mesons, with the centre-of-mass energy tuned at just above  $\Upsilon(4S)$ <sup>1</sup>. For baryonic  $b$  decays one has to rely on hadronic colliders. It was at CDF Tevatron that  $\Lambda_b \rightarrow \Lambda\mu^+\mu^-$  was first observed and measured in 2011 with a  $\mathcal{O}(10^{-6})$  branching ratio. The bright side is that, given the power of current hadron colliders especially the LHCb, the issue of small data is increasingly overcome. Data for the same decay from LHCb were announced in June 2013 with a slightly bigger yield. The available data are summarised in Table 4.1.

Experiment & Published year	Yield /events	Branching ratio/ $10^{-6}$ ( $\pm\text{stat}\pm\text{sys}$ )	Remarks
CDF 2011 [73]	$24 \pm 5$	$1.73 \pm 0.42 \pm 0.55$	$\sqrt{s} = 1.96 \text{ TeV}$ , $6.8 \text{ fb}^{-1}$
CDF 2012 update [74]	$51 \pm 7$	$1.95 \pm 0.34 \pm 0.61$	full data set $9.6 \text{ fb}^{-1}$
LHCb 2013 [75]	$78 \pm 12$	$0.96 \pm 0.16 \pm 0.13$ $\pm 0.21$ from normalisation mode $\Lambda_b \rightarrow J/\psi \Lambda$	$\sqrt{s} = 7 \text{ TeV}$ , $1.0 \text{ fb}^{-1}$ data collected in 2011

Table 4.1: Currently available experimental data on the decay  $\Lambda_b \rightarrow \Lambda\mu^+\mu^-$ .

Given enough data, the study of baryonic heavy decays opens up possibilities previous unavailable for mesonic decays. In any case, with its non-zero spin and its completely separate hadronic make-up from  $B$  mesons, the  $\Lambda_b$  simply unlocks

<sup>1</sup>Though Belle has also explored the  $\Upsilon(10860)$  resonance and some lower ones.

an excellent extra set of independent channels to complement  $B$  processes, allowing comparison and additional constraints on BSM models. As brought up at the end of Chapter 2, any new independent decay channel will be considered valuable, if the community moves towards a Bayesian statistical approach to New Physics discovery, which will require as many observables as possible in order to be able to draw constraints on parameters in each new model. The hard-to-detect nature of baryonic decays are no longer valid arguments with the recent advent of powerful hadron colliders, but there is still a long way to go. The investigation of  $\Lambda_b$  decays looks bright as long as we continue to build upon theoretical work to keep uncertainties under control and manageably small for confronting high-statistics data.

\* \* \*

As we have probably mentioned, the focus is on the decay  $\Lambda_b \rightarrow \Lambda \ell^+ \ell^-$  in this work, specifically to calculate its transition form factors using SCET light-cone sum rules, which requires a description of the  $\Lambda_b$  baryon in terms of light-cone distribution amplitudes. In the following section we introduce LCDAs and a new study of  $\Lambda_b$  LCDAs which have received relatively little attention until recently.

## 4.2 $\Lambda_b$ Light-Cone Distribution Amplitudes

### 4.2.1 Introduction

Light-cone distribution amplitudes (LCDAs) are matrix elements of non-local QCD light-cone operators between the vacuum and the multi-quark bound state under consideration. They encode information about the (longitudinal) momentum distribution among partons within a hadronic state, and have been probed to various levels of depth for mesons and baryons, light and heavy, for use in both flavour physics and beyond. First put forward by Brodsky, Lepage [76], Chernyak, Zhitnitsky [77, 78] and others in the context of QCD hard exclusive processes, the study of LCDAs can be viewed as a field of research unto itself; as the constituents of a hadronic bound state

are held together through soft interactions of order  $\Lambda_{\text{QCD}}$ , LCDAs are non-trivial objects not calculable perturbatively by nature, and they are modelled and estimated accordingly, using methods like lattice calculations and sum rules, and also investigated experimentally.

The name reflects that the operators involved are defined at light-like separations; e.g. the 3 quark fields in (4.2) and (4.3) lie on the same light-cone direction. Due to this non-local nature, to restore manifest gauge invariance to the matrix element, one has to include gauge links in the form of Wilson lines:

$$[x, y] = P \exp \left\{ ig_s \int_0^1 dt (x - y)^\mu A_\mu(tx + (1 - t)y) \right\}, \quad (4.1)$$

where  $P$  signifies path-ordering. In this chapter we focus only on the  $\Lambda_b$  LCDAs defined by 3-particle operators, in which the  $b$  quark enters as an effective heavy-quark field, and the light diquark is interpolated by different possible Dirac structures.

In general, usage of LCDAs facilitate the ideas of QCD factorisation. As seen in the previous chapter, LCDAs feature in factorisation theorems, in which exclusive heavy-to-light decays contain factorisable parts that use LCDAs as non-perturbative universal inputs. In sum-rule approaches, LCDAs are indispensable ingredients for calculating the same decays, which depending on the exact approach may allow treatments of both factorisable and non-factorisable contributions. Another advantage is that the renormalisation-group (RG) evolution behaviour of the operators that define LCDAs translate directly into RG equations for the LCDAs themselves. Their usefulness and ease-of-use are a good driving force behind keen research into LCDAs – their basic parametrisation, modelling and RG behaviour.

Conventional QCD sum rules on the light cone require the knowledge of DAs of light mesons, and these were the first to be examined at length. Using conformal symmetry of massless QCD, the matrix elements of such light-cone non-local operators are subjected to short-distance expansion, using local conformal operators as

a basis [53, 79]. It can be shown that this results in an infinite series of terms suppressed by increasing inverse powers of the large momentum transfer, linked to the twist (=dimension−spin) of the conformal operators, and hence LCDAs of the lowest twist(s) are the most crucial ones to be included in related calculations. The voluminous<sup>2</sup> literature on light-meson LCDAs began from early studies in twist-2 LCDAs of  $\pi$  [76, 77], to twist-2 and higher LCDAs of chiefly pseudoscalar and vector mesons like  $\pi, \rho, K, K^{(*)}, \phi$ , using sum-rule and related methods [80–83], lattice-based methods [84] and various others, e.g. [85].

With more partonic content baryonic LCDAs are obviously more challenging and research is thin in comparison, with most of it focussed on the nucleon [86, 87]. Strange baryons have also been studied [88, 89].

Interest in LCDAs of heavy-light hadrons flared after their worth in the QCD factorisation approach to heavy-to-light decays was realised. They naturally require a different treatment from their all-light counterparts, starting not from conformal massless QCD but from a definition and parametrisation of matrix elements within heavy-quark effective theory. Now, twist itself has no clear definition within HQET (though could still be assigned to the light-quark spinors, as in [90]); in the case of SCET (sum rules), which we shall adopt in Chapter 5, the power-counting officially follows from the effective field operators and is in terms of  $1/m_b$  and  $1/n_+p'$ , and is not in direct correspondence with a twist expansion; meanwhile the soft multi-pole expansion takes the place of the light-cone expansion in conventional twist-counting. LCDAs of  $B$  mesons were first explored in [91] and have been studied in papers such as [51, 92, 93]; for particular focus on their RG properties see e.g. [94–97].

\* \* \*

This leads us ultimately to the construction of LCDAs of heavy-light baryons,

---

<sup>2</sup>The citations here represent but a small selection of results published on this vast topic, often by the same experts building on previous work.



which will inevitably build on the expertise in all of the above. For the relatively simple  $\Lambda_b$  ( $J^P = 1/2^+$ ) baryons, their LCDAs have been looked at in [98, 99] but were first carefully classified and modelled in the important paper [90], upon which other work has been built [100]. Now we present a new study of these LCDAs and corresponding models.

### 4.2.2 LCDAs for Heavy Baryons: A New Study

Light-cone distribution amplitudes for  $\Lambda_b$  baryons in HQET contain the hadronic information entering factorisation theorems for exclusive  $\Lambda_b$  transitions in the heavy-quark limit (see e.g. [1, 101]). Following [90], we define the following position-space LCDAs related to the leading 3-particle operators:

$$\begin{aligned}\epsilon^{abc} \langle 0 | (u^a(\tau_1 n_-) C \gamma_5 \not{n}_- d^b(\tau_2 n_-)) h_v^c(0) | \Lambda_b(v, s) \rangle &= f_{\Lambda_b}^{(2)} \tilde{\phi}_2(\tau_1, \tau_2) u_{\Lambda_b}(v, s), \\ \epsilon^{abc} \langle 0 | (u^a(\tau_1 n_-) C \gamma_5 \not{n}_+ d^b(\tau_2 n_-)) h_v^c(0) | \Lambda_b(v, s) \rangle &= f_{\Lambda_b}^{(2)} \tilde{\phi}_4(\tau_1, \tau_2) u_{\Lambda_b}(v, s),\end{aligned}\quad (4.2)$$

for diquark currents with an odd number of Dirac matrices, and

$$\begin{aligned}\epsilon^{abc} \langle 0 | (u^a(\tau_1 n_-) C \gamma_5 d^b(\tau_2 n_-)) h_v^c(0) | \Lambda_b(v, s) \rangle &= f_{\Lambda_b}^{(1)} \tilde{\phi}_3^s(\tau_1, \tau_2) u_{\Lambda_b}(v, s), \\ \epsilon^{abc} \langle 0 | (u^a(\tau_1 n_-) C \gamma_5 i \sigma_{\mu\nu} n_+^\mu n_-^\nu d^b(\tau_2 n_-)) h_v^c(0) | \Lambda_b(v, s) \rangle &= 2 f_{\Lambda_b}^{(1)} \tilde{\phi}_3^\sigma(\tau_1, \tau_2) u_{\Lambda_b}(v, s),\end{aligned}\quad (4.3)$$

for those an even number of Dirac matrices. Gauge links of the form (4.1) required to ensure gauge invariance have been omitted for simplicity.

### Light-Cone Projectors for the 3-Particle Fock State

The above definitions can be cast into a manifestly Lorentz-invariant form by defining the most general non-local matrix elements in co-ordinate space as

$$\begin{aligned}\epsilon^{abc} \langle 0 | (u_\alpha^a(z_1) d_\beta^b(z_2)) h_v^c(0) | \Lambda_b(v, s) \rangle \\ \equiv \frac{1}{4} \left\{ f_{\Lambda_b}^{(1)} \left[ \tilde{M}^{(1)}(v, z_1, z_2) \gamma_5 C^T \right]_{\beta\alpha} + f_{\Lambda_b}^{(2)} \left[ \tilde{M}^{(2)}(v, z_1, z_2) \gamma_5 C^T \right]_{\beta\alpha} \right\} u_{\Lambda_b}(v, s),\end{aligned}\quad (4.4)$$

in which the part containing an odd number of Dirac matrices,  $M^{(1)}$ , has been separated from the part with an even number,  $M^{(2)}$ . These are:

$$\begin{aligned} \tilde{M}^{(2)}(v, z_1, z_2) = & \not{v} \tilde{\Phi}_2(t_1, t_2, z_1^2, z_2^2, z_1 \cdot z_2) + \frac{\tilde{\Phi}_X(t_1, t_2, z_1^2, z_2^2, z_1 \cdot z_2)}{4t_1 t_2} (\not{z}_2 \not{v} \not{z}_1 - \not{z}_1 \not{v} \not{z}_2) \\ & + \frac{\tilde{\Phi}_{42}^{(i)}(t_1, t_2, z_1^2, z_2^2, z_1 \cdot z_2)}{2t_1} \not{z}_1 + \frac{\tilde{\Phi}_{42}^{(ii)}(t_1, t_2, z_1^2, z_2^2, z_1 \cdot z_2)}{2t_2} \not{z}_2, \end{aligned} \quad (4.5)$$

$$\begin{aligned} \tilde{M}^{(1)}(v, z_1, z_2) = & \tilde{\Phi}_3^{(0)}(t_1, t_2, z_1^2, z_2^2, z_1 \cdot z_2) + \frac{\tilde{\Phi}_Y(t_1, t_2, z_1^2, z_2^2, z_1 \cdot z_2)}{4t_1 t_2} (\not{z}_2 \not{z}_1 - \not{z}_1 \not{z}_2) \\ & + \frac{\tilde{\Phi}_3^{(i)}(t_1, t_2, z_1^2, z_2^2, z_1 \cdot z_2)}{2t_1} \not{v} \not{z}_1 + \frac{\tilde{\Phi}_3^{(ii)}(t_1, t_2, z_1^2, z_2^2, z_1 \cdot z_2)}{2t_2} \not{z}_2 \not{v}, \end{aligned} \quad (4.6)$$

where  $t_i = v \cdot z_i$ . Considering isospin invariance for the light-quark fields (exchanging  $z_1 \leftrightarrow z_2$  and taking care of the charge-conjugation properties of Dirac matrices), one requires the above LCDAs to have the following symmetries and relations:

$$\begin{aligned} \tilde{\Phi}_2(t_1, t_2, z_1^2, z_2^2, z_1 \cdot z_2) &= \tilde{\Phi}_2(t_2, t_1, z_2^2, z_1^2, z_1 \cdot z_2), \\ \tilde{\Phi}_{42}^{(i)}(t_1, t_2, z_1^2, z_2^2, z_1 \cdot z_2) &= \tilde{\Phi}_{42}^{(ii)}(t_2, t_1, z_2^2, z_1^2, z_1 \cdot z_2), \\ \tilde{\Phi}_X(t_1, t_2, z_1^2, z_2^2, z_1 \cdot z_2) &= \tilde{\Phi}_X(t_2, t_1, z_2^2, z_1^2, z_1 \cdot z_2), \end{aligned} \quad (4.7)$$

and

$$\begin{aligned} \tilde{\Phi}_3^{(0)}(t_1, t_2, z_1^2, z_2^2, z_1 \cdot z_2) &= \tilde{\Phi}_3^{(0)}(t_2, t_1, z_2^2, z_1^2, z_1 \cdot z_2), \\ \tilde{\Phi}_3^{(i)}(t_1, t_2, z_1^2, z_2^2, z_1 \cdot z_2) &= \tilde{\Phi}_3^{(ii)}(t_2, t_1, z_2^2, z_1^2, z_1 \cdot z_2), \\ \tilde{\Phi}_Y(t_1, t_2, z_1^2, z_2^2, z_1 \cdot z_2) &= \tilde{\Phi}_Y(t_2, t_1, z_2^2, z_1^2, z_1 \cdot z_2). \end{aligned} \quad (4.8)$$

### The Projector $\tilde{M}^{(2)}$ (odd number of Dirac matrices)

Here one expands  $z_1$  and  $z_2$  around the light-cone, using  $n_- z_i \ll z_i^\perp \ll n_+ z_i$ , to obtain

$$\begin{aligned} \tilde{M}^{(2)}(v, z_1, z_2) \longrightarrow & \frac{\not{n}_+}{2} \tilde{\phi}_2(\tau_1, \tau_2) + \frac{\not{n}_-}{2} \left( \tilde{\phi}_2(\tau_1, \tau_2) + \tilde{\phi}_{42}^{(i)}(\tau_1, \tau_2) + \tilde{\phi}_{42}^{(ii)}(\tau_1, \tau_2) \right) \\ & + \frac{\tilde{\phi}_{42}^{(i)}(\tau_1, \tau_2)}{2\tau_1} \not{z}_1^\perp + \frac{\tilde{\phi}_{42}^{(ii)}(\tau_1, \tau_2)}{2\tau_2} \not{z}_2^\perp \\ & + \tilde{\phi}_X(\tau_1, \tau_2) \left( \frac{\not{z}_1^\perp}{2\tau_1} - \frac{\not{z}_2^\perp}{2\tau_2} \right) \left( \frac{\not{n}_- \not{n}_+}{4} - \frac{\not{n}_+ \not{n}_-}{4} \right) + \mathcal{O}(z_{i\perp}^2, n_- z_i), \end{aligned} \quad (4.9)$$

where again  $\tau_i = \frac{n+z_i}{2}$  are the Fourier-conjugate variables to the momentum components  $\omega_i = n_- k_i$  of the associated light-quark fields, such that

$$\phi_2(\omega_1, \omega_2) \equiv \int \frac{d\tau_1}{2\pi} e^{i\omega_1 \tau_1} \int \frac{d\tau_2}{2\pi} e^{i\omega_2 \tau_2} \tilde{\phi}_2(\tau_1, \tau_2) \quad \text{etc.} \quad (4.10)$$

Comparison with the definition in (4.2) yields the relation

$$\tilde{\phi}_{42}^{(i)}(\tau_1, \tau_2) + \tilde{\phi}_{42}^{(ii)}(\tau_1, \tau_2) = \tilde{\phi}_4(\tau_1, \tau_2) - \tilde{\phi}_2(\tau_1, \tau_2), \quad (4.11)$$

while the asymmetric combination of  $\tilde{\phi}_{42}^{(i)}$  and  $\tilde{\phi}_{42}^{(ii)}$  and also  $\tilde{\phi}_X$  do not contribute in the collinear limit  $z_i^2 \rightarrow 0$ . After Fourier transformation, the general momentum-space representation for (4.9), including first-order terms off the light-cone, reads:

$$\begin{aligned} M^{(2)}(\omega_1, \omega_2) = & \frac{\not{n}_+}{2} \phi_2(\omega_1, \omega_2) + \frac{\not{n}_-}{2} \phi_4(\omega_1, \omega_2) \\ & - \frac{1}{2} \gamma_\mu^\perp \int_0^{\omega_1} d\eta_1 \left( \phi_{42}^{(i)}(\eta_1, \omega_2) - \phi_X(\eta_1, \omega_2) \right) \frac{\not{n}_+ \not{n}_-}{4} \frac{\partial}{\partial k_{1\mu}^\perp} \\ & - \frac{1}{2} \gamma_\mu^\perp \int_0^{\omega_1} d\eta_1 \left( \phi_{42}^{(i)}(\eta_1, \omega_2) + \phi_X(\eta_1, \omega_2) \right) \frac{\not{n}_- \not{n}_+}{4} \frac{\partial}{\partial k_{1\mu}^\perp} \\ & - \frac{1}{2} \gamma_\mu^\perp \int_0^{\omega_2} d\eta_2 \left( \phi_{42}^{(ii)}(\omega_1, \eta_2) - \phi_X(\omega_1, \eta_2) \right) \frac{\not{n}_- \not{n}_+}{4} \frac{\partial}{\partial k_{2\mu}^\perp} \\ & - \frac{1}{2} \gamma_\mu^\perp \int_0^{\omega_2} d\eta_2 \left( \phi_{42}^{(ii)}(\omega_1, \eta_2) + \phi_X(\omega_1, \eta_2) \right) \frac{\not{n}_+ \not{n}_-}{4} \frac{\partial}{\partial k_{2\mu}^\perp}. \end{aligned} \quad (4.12)$$

### The Projector $\tilde{M}^{(1)}$ (even number of Dirac matrices)

Similarly, for the projector with an even number of Dirac matrices, one obtains

$$\begin{aligned} \tilde{M}^{(1)}(v, z_1, z_2) \longrightarrow & \tilde{\phi}_3^{(0)}(\tau_1, \tau_2) + \tilde{\phi}_3^{(i)}(\tau_1, \tau_2) \frac{\not{n}_+ \not{n}_-}{4} + \tilde{\phi}_3^{(ii)}(\tau_1, \tau_2) \frac{\not{n}_- \not{n}_+}{4} \\ & + \tilde{\phi}_3^{(i)}(\tau_1, \tau_2) \frac{\not{n}_1^\perp \not{n}_1^\perp}{2\tau_1} + \tilde{\phi}_3^{(ii)}(\tau_1, \tau_2) \frac{\not{n}_2^\perp \not{n}_2^\perp}{2\tau_2} \\ & + \tilde{\phi}_Y(\tau_1, \tau_2) \left( \frac{\not{n}_2^\perp \not{n}_-}{2\tau_2} + \frac{\not{n}_- \not{n}_1^\perp}{2\tau_1} \right) + \mathcal{O}(z_{i\perp}^2, n_- z_i), \end{aligned} \quad (4.13)$$

where from (4.3) one now has

$$\begin{aligned} \tilde{\phi}_3^s(\tau_1, \tau_2) &= \frac{2\tilde{\phi}_3^{(0)}(\tau_1, \tau_2) + \tilde{\phi}_3^{(i)}(\tau_1, \tau_2) + \tilde{\phi}_3^{(ii)}(\tau_1, \tau_2)}{2}, \\ \tilde{\phi}_3^\sigma(\tau_1, \tau_2) &= \frac{\tilde{\phi}_3^{(ii)}(\tau_1, \tau_2) - \tilde{\phi}_3^{(i)}(\tau_1, \tau_2)}{2}. \end{aligned} \quad (4.14)$$

It is sometimes more convenient to define, following [90],

$$\begin{aligned}\tilde{\phi}_3^{+-}(\tau_1, \tau_2) &\equiv 2 \left( \tilde{\phi}_3^s(\tau_1, \tau_2) + \tilde{\phi}_3^\sigma(\tau_1, \tau_2) \right) = 2 \left( \tilde{\phi}_3^{(0)}(\tau_1, \tau_2) + \tilde{\phi}_3^{(ii)}(\tau_1, \tau_2) \right), \\ \tilde{\phi}_3^{-+}(\tau_1, \tau_2) &\equiv 2 \left( \tilde{\phi}_3^s(\tau_1, \tau_2) - \tilde{\phi}_3^\sigma(\tau_1, \tau_2) \right) = 2 \left( \tilde{\phi}_3^{(0)}(\tau_1, \tau_2) + \tilde{\phi}_3^{(i)}(\tau_1, \tau_2) \right).\end{aligned}\quad (4.15)$$

The expansion of the corresponding momentum-space projector takes the general form

$$\begin{aligned}M^{(1)}(\omega_1, \omega_2) &= \frac{\not{p}_- \not{p}_+}{8} \phi_3^{+-}(\omega_1, \omega_2) + \frac{\not{p}_+ \not{p}_-}{8} \phi_3^{-+}(\omega_1, \omega_2) \\ &\quad - \frac{1}{2} \int_0^{\omega_1} d\eta_1 \phi_3^{(i)}(\eta_1, \omega_2) \not{p} \gamma_\mu^\perp \frac{\partial}{\partial k_{1\mu}^\perp} - \frac{1}{2} \int_0^{\omega_2} d\eta_2 \phi_3^{(ii)}(\omega_1, \eta_2) \gamma_\mu^\perp \not{p} \frac{\partial}{\partial k_{2\mu}^\perp} \\ &\quad - \frac{1}{2} \int_0^{\omega_1} d\eta_1 \phi_Y(\eta_1, \omega_2) \not{p}_- \gamma_\mu^\perp \frac{\partial}{\partial k_{1\mu}^\perp} - \frac{1}{2} \int_0^{\omega_2} d\eta_2 \phi_Y(\omega_1, \eta_2) \gamma_\mu^\perp \not{p}_- \frac{\partial}{\partial k_{2\mu}^\perp}.\end{aligned}\quad (4.16)$$

### Wandzura-Wilczek Relations

Wandzura-Wilczek (WW) relations [102] have been shown to link certain LCDA terms for particles like  $B$  mesons in HQET [51, 103] and light vector mesons [81]. In the WW approximation where LCDAs for higher Fock states with dynamical gluons are neglected, the matrices  $\tilde{M}^{(1,2)}(z_1, z_2)$  (4.5, 4.6) would fulfil the equations of motion for free light-quark fields,

$$\gamma^\mu \frac{i\partial}{\partial z_2^\mu} \tilde{M}^{(1,2)}(v, z_1, z_2) = \frac{i\partial}{\partial z_1^\mu} \tilde{M}^{(1,2)}(v, z_1, z_2) \gamma^\mu \approx 0. \quad (4.17)$$

This translates into differential equations for the LCDAs in the collinear limit. These can be obtained by expanding the above equation around the light-cone, and solving for the derivatives with respect to the arguments  $(z_i^2, z_1 \cdot z_2)$  off the light cone. Alternatively, one can start from the expanded form of  $\tilde{M}^{(1,2)}$  and consider the projected equations of motion

$$\frac{\not{p}_+ \not{p}_-}{4} \gamma_\mu \frac{i\partial}{\partial z_2^\mu} \tilde{M}^{(1,2)}(v, z_1, z_2) \Big|_{z_{1,2}^\perp=0} = \frac{i\partial}{\partial z_1^\mu} \tilde{M}^{(1,2)}(v, z_1, z_2) \gamma_\mu \frac{\not{p}_- \not{p}_+}{4} \Big|_{z_{1,2}^\perp=0} \approx 0. \quad (4.18)$$

This yields the following WW relations for the LCDAs in  $\tilde{M}^{(2)}$ :

$$\begin{aligned}\tilde{\phi}_{42}^{(i)}(\tau_1, \tau_2) + \tilde{\phi}_X(\tau_1, \tau_2) + \tau_1 \frac{\partial}{\partial \tau_1} \tilde{\phi}_4(\tau_1, \tau_2) &\approx 0, \\ \tilde{\phi}_{42}^{(ii)}(\tau_1, \tau_2) + \tilde{\phi}_X(\tau_1, \tau_2) + \tau_2 \frac{\partial}{\partial \tau_2} \tilde{\phi}_4(\tau_1, \tau_2) &\approx 0.\end{aligned}\quad (4.19)$$

For the Fourier-transformed LCDAs this implies

$$\begin{aligned}\phi_{42}^{(i)}(\omega_1, \omega_2) + \phi_X(\omega_1, \omega_2) - \frac{\partial}{\partial \omega_1} (\omega_1 \phi_4(\omega_1, \omega_2)) &\approx 0, \\ \phi_{42}^{(ii)}(\omega_1, \omega_2) + \phi_X(\omega_1, \omega_2) - \frac{\partial}{\partial \omega_2} (\omega_2 \phi_4(\omega_1, \omega_2)) &\approx 0,\end{aligned}\quad (4.20)$$

or, equivalently,

$$\begin{aligned}\phi_{42}^{(i)}(\omega_1, \omega_2) - \phi_{42}^{(ii)}(\omega_1, \omega_2) &\approx \frac{\partial}{\partial \omega_1} (\omega_1 \phi_4(\omega_1, \omega_2)) - \frac{\partial}{\partial \omega_2} (\omega_2 \phi_4(\omega_1, \omega_2)), \\ 2\phi_X(\omega_1, \omega_2) + \phi_4(\omega_1, \omega_2) - \phi_2(\omega_1, \omega_2) &\approx \frac{\partial}{\partial \omega_1} (\omega_1 \phi_4(\omega_1, \omega_2)) + \frac{\partial}{\partial \omega_2} (\omega_2 \phi_4(\omega_1, \omega_2)).\end{aligned}\quad (4.21)$$

The latter relations reveal that, once the functions  $\phi_2$  and  $\phi_4$  – which are the relevant LCDAs for the collinear limit – are known,  $\phi_X$  and the asymmetric combination of  $\phi_{42}^{(i,ii)}$  can be calculated from the WW approximation. At the same time, one could also conclude that given the number of WW relations derived is smaller than the number of LCDAs in the Lorentz decomposition (4.5), the LCDA terms relevant for the collinear limit in (4.2) remain independent.

In a similar way, for the terms in  $\tilde{M}^{(1)}$  one obtains the relations

$$\begin{aligned}\tilde{\phi}_3^{(i)}(\tau_1, \tau_2) + \tau_1 \frac{\partial}{\partial \tau_1} \left( \tilde{\phi}_3^{(0)}(\tau_1, \tau_2) + \tilde{\phi}_3^{(i)}(\tau_1, \tau_2) \right) &\approx 0, \\ \tilde{\phi}_3^{(ii)}(\tau_1, \tau_2) + \tau_2 \frac{\partial}{\partial \tau_2} \left( \tilde{\phi}_3^{(0)}(\tau_1, \tau_2) + \tilde{\phi}_3^{(ii)}(\tau_1, \tau_2) \right) &\approx 0,\end{aligned}\quad (4.22)$$

or, in momentum space,

$$\begin{aligned}\phi_3^{(i)}(\omega_1, \omega_2) - \frac{\partial}{\partial \omega_1} \left( \omega_1 \phi_3^{(0)}(\omega_1, \omega_2) + \omega_1 \phi_3^{(i)}(\omega_1, \omega_2) \right) &\approx 0, \\ \phi_3^{(ii)}(\omega_1, \omega_2) - \frac{\partial}{\partial \omega_2} \left( \omega_2 \phi_3^{(0)}(\omega_1, \omega_2) + \omega_2 \phi_3^{(ii)}(\omega_1, \omega_2) \right) &\approx 0.\end{aligned}\quad (4.23)$$

Notice that in this case, the function  $\phi_Y$  does not appear in the WW relations, and therefore remains independent, whereas the functions  $\phi_3^s$  and  $\phi_3^\sigma$  appearing in the collinear limit are related by

$$-\omega_1 \frac{\partial}{\partial \omega_1} \phi_3^{-+}(\omega_1, \omega_2) \approx -\omega_2 \frac{\partial}{\partial \omega_2} \phi_3^{+-}(\omega_1, \omega_2) \approx 2\phi_3^{(0)}(\omega_1, \omega_2). \quad (4.24)$$

### 4.2.3 Construction in Momentum Space

Momentum-space projectors of the LCDAs are especially useful as they find straightforward application in the diagrammatic analysis of exclusive matrix elements, whether in QCD factorisation or sum-rule correlation functions (as seen in [51] etc.) Here we construct on-shell projectors for the  $\Lambda_b$  baryon from 3-particle “wave-functions” directly from a momentum-space representation (the meson case is similarly investigated in [2]); to keep the discussion simple, corrections to the WW relation are neglected in the rest of this discussion.

The most general form of the momentum-space projector can be written as:

$$\begin{aligned} M^{(1)}(v, k_1, k_2) &= \tilde{\psi}_s(x_1, x_2, K^2) \not{k}_2 \not{k}_1, \\ M^{(2)}(v, k_1, k_2) &= \tilde{\psi}_v(x_1, x_2, K^2) \not{k}_2 \not{v} \not{k}_1, \end{aligned} \quad (4.25)$$

where  $x_i = 2v \cdot k_i$  and  $K^2 = (k_1 + k_2)^2$ , and  $\psi_s$  and  $\psi_v$  are two independent wave-functions. The equations of motion,  $\not{k}_2 M^{(1,2)}(v, k_1, k_2) = M^{(1,2)}(v, k_1, k_2) \not{k}_1 = 0$ , are again trivially fulfilled for on-shell quarks with  $k_i^2 = 0$ . In addition to the WW approximation, the potential  $K^2$ -dependence is neglected for simplicity, even though the invariant mass of the diquark system can in principle be arbitrary, i.e.  $K^2 \neq 0$ . This approximation corresponds to the case where the wave-function only depends on the total invariant mass of the 3 quarks in the  $\Lambda_b$  baryon, i.e.  $(m_b v + k_1 + k_2)^2 \simeq m_b^2 + m_b(x_1 + x_2)$ .

#### The Projector $M^{(2)}$ (odd number of Dirac matrices)

To compare with the general definition of LCDAs, we consider the convolution of their momentum-space projectors with a hard-scattering kernel that is at most linear in  $k_{i\perp}$ . One obtains:

$$\begin{aligned}
& \int \widetilde{dk}_1 \int \widetilde{dk}_2 \operatorname{Tr} \left[ (T_0(\omega_1, \omega_2) + k_{i\perp}^\mu T_\mu^i(\omega_1, \omega_2)) M^{(2)}(v, k_1, k_2) \right] \\
&= \int d\omega_1 d\omega_2 \int_{\omega_1}^\infty dx_1 \int_{\omega_2}^\infty dx_2 \left\{ \right. \\
& \quad \operatorname{Tr} \left[ T_0(\omega_1, \omega_2) \left( \omega_1 \omega_2 \frac{\not{n}_+}{2} + (x_1 - \omega_1)(x_2 - \omega_2) \frac{\not{n}_-}{2} \right) \right] \\
& \quad - \operatorname{Tr} \left[ T_\mu^1(\omega_1, \omega_2) \left( \omega_1 \omega_2 (x_1 - \omega_1) \frac{\not{n}_+ \not{n}_-}{4} + \omega_1 (x_1 - \omega_1)(x_2 - \omega_2) \frac{\not{n}_- \not{n}_+}{4} \right) \frac{\gamma_\perp^\mu}{2} \right] \\
& \quad - \operatorname{Tr} \left[ T_\mu^2(\omega_1, \omega_2) \frac{\gamma_\perp^\mu}{2} \left( \omega_1 \omega_2 (x_2 - \omega_2) \frac{\not{n}_- \not{n}_+}{4} + \omega_2 (x_1 - \omega_1)(x_2 - \omega_2) \frac{\not{n}_+ \not{n}_-}{4} \right) \right] \\
& \quad \left. \right\} \psi_v(x_1, x_2), \tag{4.26}
\end{aligned}$$

where we have used for the momentum integrations a Lorentz-invariant integration measure  $\widetilde{dk}_i$  for an on-shell massless particle, defined such that it already reflects the light-cone kinematics in a hard-scattering process (with the azimuthal angle in the transverse plane integrated out):

$$\widetilde{dk}_i \equiv d|k_{i\perp}|^2 \frac{d\omega_i}{\omega_i} = \frac{d^3 k_i}{\pi v \cdot k_i}, \quad \text{where} \quad k_i^\mu = \omega_i \frac{n_+^\mu}{2} + k_{i\perp}^\mu + \frac{|k_{i\perp}|^2}{\omega} \frac{n_-^\mu}{2}. \tag{4.27}$$

Comparison with the position-space expressions in the collinear limit as above yields

$$\begin{aligned}
\phi_2(\omega_1, \omega_2) &= \int_{\omega_1}^\infty dx_1 \int_{\omega_2}^\infty dx_2 \omega_1 \omega_2 \psi_v(x_1, x_2), \\
\phi_4(\omega_1, \omega_2) &= \int_{\omega_1}^\infty dx_1 \int_{\omega_2}^\infty dx_2 (x_1 - \omega_1)(x_2 - \omega_2) \psi_v(x_1, x_2), \tag{4.28}
\end{aligned}$$

together with

$$\begin{aligned}
\phi_{42}^{(i)}(\omega_1, \omega_2) &= \frac{1}{2} \int_{\omega_1}^\infty dx_1 \int_{\omega_2}^\infty dx_2 x_2 (x_1 - 2\omega_1) \psi_v(x_1, x_2), \\
\phi_{42}^{(ii)}(\omega_1, \omega_2) &= \frac{1}{2} \int_{\omega_1}^\infty dx_1 \int_{\omega_2}^\infty dx_2 x_1 (x_2 - 2\omega_2) \psi_v(x_1, x_2), \\
\phi_X(\omega_1, \omega_2) &= \frac{1}{2} \int_{\omega_1}^\infty dx_1 \int_{\omega_2}^\infty dx_2 (x_1 - 2\omega_1)(x_2 - 2\omega_2) \psi_v(x_1, x_2). \tag{4.29}
\end{aligned}$$

Some of these terms, following the pattern in (4.12), feature in the calculation of  $\Delta\xi_\Lambda$  in Chapter 5; for convenience here we define the concise notations

$$\begin{aligned} G(\omega_1, \omega_2) &\equiv \int_0^{\omega_1} d\eta_1 \left( \phi_{42}^{(i)}(\eta_1, \omega_2) - \phi_X(\eta_1, \omega_2) \right), \\ H(\omega_1, \omega_2) &\equiv \int_0^{\omega_2} d\eta_2 \left( \phi_{42}^{(ii)}(\omega_1, \eta_2) + \phi_X(\omega_1, \eta_2) \right). \end{aligned} \quad (4.30)$$

It can be checked that the LCDAs constructed in this way satisfy the WW relations derived earlier. Note that our simplified ansatz relates all LCDAs to  $x_i$ -moments of only two fundamental wave-functions,  $\psi_v$  and  $\psi_s$  (see below). The functional form of  $\psi_v$  can be reconstructed, for instance, from

$$\psi_v(\omega_1, \omega_2) = \frac{d^2}{d\omega_1 d\omega_2} \left( \frac{\phi_2(\omega_1, \omega_2)}{\omega_1 \omega_2} \right) = \frac{d^4 \phi_4(\omega_1, \omega_2)}{d\omega_1^2 d\omega_2^2}. \quad (4.31)$$

With a more general ansatz these relations would be modified by non-trivial  $K^2$ -dependence of the wave-functions. In the simplest case, one could again model the wave-functions by assuming an exponential dependence on  $(x_1 + x_2)$ :

$$\psi_v(x_1, x_2) \rightarrow \frac{\exp\left(-\frac{x_1+x_2}{\omega_0}\right)}{\omega_0^6}; \quad (4.32)$$

this yields

$$\phi_2(\omega_1, \omega_2) \rightarrow \frac{\omega_1 \omega_2}{\omega_0^4} e^{-(\omega_1+\omega_2)/\omega_0}, \quad \phi_4(\omega_1, \omega_2) \rightarrow \frac{1}{\omega_0^2} e^{-(\omega_1+\omega_2)/\omega_0}, \quad (4.33)$$

and

$$\begin{aligned} \phi_{42}^{(i)}(\omega_1, \omega_2) &\rightarrow \frac{(\omega_0 - \omega_1)(\omega_0 + \omega_2)}{2\omega_0^4} e^{-(\omega_1+\omega_2)/\omega_0}, \\ \phi_{42}^{(ii)}(\omega_1, \omega_2) &\rightarrow \frac{(\omega_0 + \omega_1)(\omega_0 - \omega_2)}{2\omega_0^4} e^{-(\omega_1+\omega_2)/\omega_0}, \\ \phi_X(\omega_1, \omega_2) &\rightarrow \frac{(\omega_0 - \omega_1)(\omega_0 - \omega_2)}{2\omega_0^4} e^{-(\omega_1+\omega_2)/\omega_0}. \end{aligned} \quad (4.34)$$

In particular,

$$\begin{aligned} \phi_{42}^{(i)}(\omega_1, \omega_2) - \phi_{42}^{(ii)}(\omega_1, \omega_2) &\rightarrow \frac{\omega_2 - \omega_1}{\omega_0^3} e^{-(\omega_1+\omega_2)/\omega_0}, \\ G(\omega_1, \omega_2) &= \frac{\omega_1 \omega_2}{\omega_0^3} e^{-(\omega_1+\omega_2)/\omega_0}, \quad H(\omega_1, \omega_2) = \frac{\omega_2}{\omega_0^2} e^{-(\omega_1+\omega_2)/\omega_0}. \end{aligned} \quad (4.35)$$



For comparison, a free-parton picture with  $x_1 + x_2 = 2\bar{\Lambda} = M_{\Lambda_b} - m_b$  would correspond to

$$\psi_v(x_1, x_2) \rightarrow \frac{15}{4\bar{\Lambda}^5} \delta(x_1 + x_2 - 2\bar{\Lambda}), \quad (4.36)$$

which yields

$$\begin{aligned} \phi_2(\omega_1, \omega_2) &\rightarrow \frac{15\omega_1\omega_2(2\bar{\Lambda} - \omega_1 - \omega_2)}{4\bar{\Lambda}^5} \theta(2\bar{\Lambda} - \omega_1 - \omega_2), \\ \phi_4(\omega_1, \omega_2) &\rightarrow \frac{5(2\bar{\Lambda} - \omega_1 - \omega_2)^3}{8\bar{\Lambda}^5} \theta(2\bar{\Lambda} - \omega_1 - \omega_2). \end{aligned} \quad (4.37)$$

To illustrate these results, we compare the forms of the LCDA  $\phi_2(\omega_1, \omega_2)$  resulting from: (i) the exponential ansatz in (4.33), (ii) the free-parton approximation (4.37), and (iii) the model from equation (38) in [90]. For this purpose, we consider the functions

$$f_2(\omega) \equiv \omega \int_0^1 du \phi_2(u\omega, \bar{u}\omega) = \begin{cases} \frac{\omega^3}{6\omega_0^4} e^{-\omega/\omega_0} & (4.33) \text{ with } \omega_0 = \frac{2\bar{\Lambda}}{5} = 0.4 \text{ GeV} \\ \frac{\omega^3}{6\epsilon_0^4} e^{-\omega/\epsilon_0} & [90] \text{ with } \epsilon_0 = 0.2 \text{ GeV} \\ \frac{5\omega^3(2\bar{\Lambda}-\omega)}{8\bar{\Lambda}^5} \theta(2\bar{\Lambda} - \omega) & (4.37) \text{ with } \bar{\Lambda} = 1 \text{ GeV} \end{cases}, \quad (4.38)$$

and

$$g_2(u) \equiv \int_0^\infty d\omega \phi_2(u\omega, \bar{u}\omega) = \begin{cases} \frac{2u\bar{u}}{\omega_0} & (4.33) \text{ with } \omega_0 = 0.4 \text{ GeV} \\ u\bar{u} \left( \frac{2}{\epsilon_0} + \frac{3a_2(5(u-\bar{u})^2-1)}{\epsilon_1} \right) & [90] \text{ with } \begin{cases} \epsilon_0 = 0.2 \text{ GeV} \\ \epsilon_1 = 0.65 \text{ GeV} \\ a_2 = 1/3 \end{cases} \\ \frac{5u\bar{u}}{\bar{\Lambda}} & (4.37) \text{ with } \bar{\Lambda} = 1 \text{ GeV} \end{cases}. \quad (4.39)$$

The parameter  $\omega_0$  in the first case has been related to the value of  $\bar{\Lambda}$  in the third case, such that the  $\langle \omega^{-1} \rangle$  moment of  $f_2$  is identical in both cases. The model in [90] prefers a central value for  $\omega_0$  that is significantly smaller – and which we suspect may be too small for the light degrees of freedom in a realistic baryon – and takes into account a (rather small) non-trivial shape for the function  $g_2(u)$  from the next-to-leading term in the Gegenbauer expansion. Figure 4.1 illustrates the shapes of  $f_2(\omega)$  and  $g_2(u)$  using these 3 models.

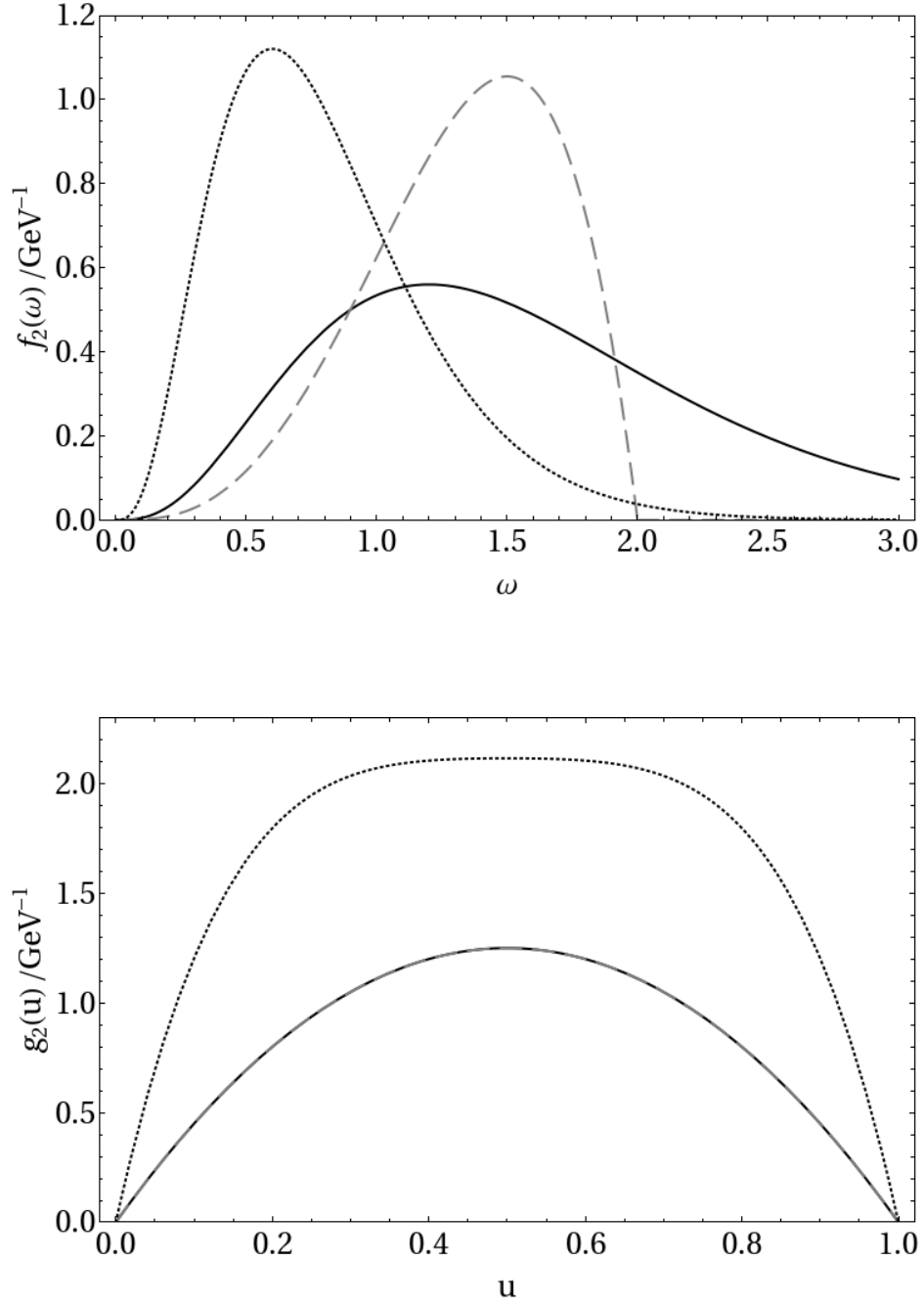


Figure 4.1: The functions  $f_2(\omega)$  and  $g_2(u)$  in 3 different models for the LCDA  $\phi_2(\omega_1, \omega_2)$ : Exponential ansatz (4.33) (solid lines); free-parton approximation (4.37) (dashed); model in [90] (dotted).

### The Projector $M^{(1)}$ (even number of Dirac matrices)

Again we consider the convolution of the projector with a hard-scattering kernel:

$$\begin{aligned}
& \int \widetilde{dk}_1 \int \widetilde{dk}_2 \operatorname{Tr} \left[ (T_0(\omega_1, \omega_2) + k_{i\perp}^\mu T_\mu^i(\omega_1, \omega_2)) M^{(1)}(v, k_1, k_2) \right] \\
&= \int d\omega_1 d\omega_2 \int_{\omega_1}^\infty dx_1 \int_{\omega_2}^\infty dx_2 \left\{ \right. \\
& \quad \operatorname{Tr} \left[ T_0(\omega_1, \omega_2) \left( \omega_2 (x_1 - \omega_1) \frac{\not{n}_+ \not{n}_-}{4} + \omega_1 (x_2 - \omega_2) \frac{\not{n}_- \not{n}_+}{4} \right) \right] \\
& \quad - \operatorname{Tr} \left[ T_\mu^1(\omega_1, \omega_2) \left( \omega_1 \omega_2 (x_1 - \omega_1) \frac{\not{n}_+}{2} + \omega_1 (x_1 - \omega_1) (x_2 - \omega_2) \frac{\not{n}_-}{2} \right) \frac{\gamma_\perp^\mu}{2} \right] \\
& \quad - \operatorname{Tr} \left[ T_\mu^2(\omega_1, \omega_2) \frac{\gamma_\perp^\mu}{2} \left( \omega_1 \omega_2 (x_2 - \omega_2) \frac{\not{n}_+}{2} + \omega_2 (x_1 - \omega_1) (x_2 - \omega_2) \frac{\not{n}_-}{2} \right) \right] \\
& \quad \left. \right\} \psi_s(x_1, x_2). \tag{4.40}
\end{aligned}$$

Comparison with the coordinate-space expression (4.16) yields

$$\begin{aligned}
\phi_3^{-+}(\omega_1, \omega_2) &= 2 \left( \phi_3^{(0)}(\omega_1, \omega_2) + \phi_3^{(i)}(\omega_1, \omega_2) \right) = 2 \int_{\omega_1}^\infty dx_1 \int_{\omega_2}^\infty dx_2 \omega_2 (x_1 - \omega_1) \psi_s(x_1, x_2), \\
\phi_3^{+-}(\omega_1, \omega_2) &= 2 \left( \phi_3^{(0)}(\omega_1, \omega_2) + \phi_3^{(ii)}(\omega_1, \omega_2) \right) = 2 \int_{\omega_1}^\infty dx_1 \int_{\omega_2}^\infty dx_2 \omega_1 (x_2 - \omega_2) \psi_s(x_1, x_2),
\end{aligned} \tag{4.41}$$

and

$$\begin{aligned}
\phi_3^{(0)}(\omega_1, \omega_2) &= \int_{\omega_1}^\infty dx_1 \int_{\omega_2}^\infty dx_2 \omega_1 \omega_2 \psi_s(x_1, x_2), \\
\phi_Y(\omega_1, \omega_2) &= \frac{1}{2} \int_{\omega_1}^\infty dx_1 \int_{\omega_2}^\infty dx_2 (2\omega_1 - x_1) (2\omega_2 - x_2) \psi_s(x_1, x_2).
\end{aligned} \tag{4.42}$$

The wave-function  $\psi_s$  in our approximation can again be reconstructed from

$$\psi_s(x_1, x_2) = \frac{d^2}{d\omega_1 d\omega_2} \left( \frac{\phi_3^{(0)}(\omega_1, \omega_2)}{\omega_1 \omega_2} \right)_{\omega_i \rightarrow x_i}; \tag{4.43}$$

with the exponential model for the wave-function

$$\psi_s(x_1, x_2) \rightarrow \frac{\exp\left(-\frac{x_1+x_2}{\omega_0}\right)}{\omega_0^6}, \tag{4.44}$$

one obtains:

$$\begin{aligned}\phi_3^{-+}(\omega_1, \omega_2) &\rightarrow \frac{2\omega_2}{\omega_0^3} e^{-(\omega_1+\omega_2)/\omega_0}, \\ \phi_3^{+-}(\omega_1, \omega_2) &\rightarrow \frac{2\omega_1}{\omega_0^3} e^{-(\omega_1+\omega_2)/\omega_0},\end{aligned}\tag{4.45}$$

and

$$\begin{aligned}\phi_3^{(0)}(\omega_1, \omega_2) &\rightarrow \frac{\omega_1\omega_2}{\omega_0^4} e^{-(\omega_1+\omega_2)/\omega_0}, \\ \phi_Y(\omega_1, \omega_2) &\rightarrow \frac{(\omega_1 - \omega_0)(\omega_2 - \omega_0)}{2\omega_0^4} e^{-(\omega_1+\omega_2)/\omega_0}.\end{aligned}\tag{4.46}$$

In the free-parton picture they take the form

$$\begin{aligned}\phi_3^{-+}(\omega_1, \omega_2) &\rightarrow \frac{15\omega_2(2\bar{\Lambda} - \omega_1 - \omega_2)^2}{4\bar{\Lambda}^5} \theta(2\bar{\Lambda} - \omega_1 - \omega_2), \\ \phi_3^{+-}(\omega_1, \omega_2) &\rightarrow \frac{15\omega_1(2\bar{\Lambda} - \omega_1 - \omega_2)^2}{4\bar{\Lambda}^5} \theta(2\bar{\Lambda} - \omega_1 - \omega_2),\end{aligned}\tag{4.47}$$

and so on.

#### 4.2.4 Renormalisation-Group Behaviour

The behaviour of baryonic LCDAs in renormalisation groups has been explored in [90], following the important work done on mesonic  $B$  LCDAs in [94, 96], which finds that the logarithmic Fourier transform with respect to  $\ln(\omega/\mu)$  of the leading LCDA,

$$\varphi_B^+(\theta, \mu) = \int_0^\infty \frac{d\omega}{\omega} \left(\frac{\omega}{\mu}\right)^{-i\theta} \phi_B^+(\omega, \mu),\tag{4.48}$$

has the RG equation solution of:

$$\varphi_B^+(\theta, \mu) = e^{V-2\gamma_E g} \left(\frac{\mu}{\mu_0}\right)^{i\theta} \frac{\Gamma(1-i\theta)\Gamma(1+i\theta-g)}{\Gamma(1+i\theta)\Gamma(1-i\theta+g)} \varphi_B^+(\theta+ig, \mu_0),\tag{4.49}$$

to leading order. (RG functions  $V = V(\mu, \mu_0)$  and  $g = g(\mu, \mu_0)$  can be found in [96].) After going back to momentum space, ultimately one gets the desired analytic relation between the LCDA at different energy scales, as a convolution integral involving hypergeometric functions and the same LCDA at a lower scale  $\mu_0$ .

In [2] an alternative representation to the RG-evolution solution is proposed, starting from the ansatz

$$\varphi_B^+(\theta, \mu) = \frac{\Gamma(1-i\theta)}{\Gamma(1+i\theta)} \int_0^\infty \frac{d\omega'}{\omega'} \rho_B^+(\omega', \mu) \left(\frac{\mu}{\omega'}\right)^{i\theta}, \quad (4.50)$$

which makes use of a “spectral function”  $\rho_B^+(\omega', \mu)$ , whose own relatively simple RG properties in turn allow a straightforward relation between the momentum-space LCDA at scale  $\mu$  and this dual function at  $\mu_0$ , through a convolution with Bessel functions:

$$\begin{aligned} \phi_B^+(\omega, \mu) &= \int_0^\infty \frac{d\omega'}{\omega'} \sqrt{\frac{\omega}{\omega'}} J_1\left(2\sqrt{\frac{\omega}{\omega'}}\right) \rho_B^+(\omega', \mu) \\ &= e^V \int_0^\infty \frac{d\omega'}{\omega'} \sqrt{\frac{\omega}{\omega'}} J_1\left(2\sqrt{\frac{\omega}{\omega'}}\right) \left(\frac{\mu_0}{\hat{\omega}'}\right)^{-g} \rho_B^+(\omega', \mu_0). \end{aligned} \quad (4.51)$$

In the baryonic case, in complete analogy to the above, one finds for the LCDA  $\phi_2(\omega_1, \omega_2, \mu)$ :

$$\varphi_2(\theta_1, \theta_2, \mu) = \frac{\Gamma(1-i\theta_1)\Gamma(1-i\theta_2)}{\Gamma(1+i\theta_1)\Gamma(1+i\theta_2)} \int_0^\infty \frac{d\omega'_1}{\omega'_1} \int_0^\infty \frac{d\omega'_2}{\omega'_2} \rho_2(\omega'_1, \omega'_2, \mu) \left(\frac{\mu}{\omega'_1}\right)^{i\theta_1} \left(\frac{\mu}{\omega'_2}\right)^{i\theta_2}, \quad (4.52)$$

such that

$$\phi_2(\omega_1, \omega_2, \mu) = \int_0^\infty \frac{d\omega'_1}{\omega'_1} \int_0^\infty \frac{d\omega'_2}{\omega'_2} \sqrt{\frac{\omega_1\omega_2}{\omega'_1\omega'_2}} J_1\left(2\sqrt{\frac{\omega_1}{\omega'_1}}\right) J_1\left(2\sqrt{\frac{\omega_2}{\omega'_2}}\right) \rho_2(\omega'_1, \omega'_2, \mu). \quad (4.53)$$

Using the exponential ansatz for  $\phi_2$  would again correspond to a simple exponential dual spectrum function:

$$\rho_2(\omega'_1, \omega'_2, \mu_0) \rightarrow \frac{1}{\omega'_1\omega'_2} \exp\left[-\frac{\omega_0}{\omega'_1} - \frac{\omega_0}{\omega'_2}\right]. \quad (4.54)$$

Apart from having one more momentum variable, the baryonic case is complicated by a non-trivial Efremov-Radyushkin-Brodsky-Lepage (ERBL) term which arises from gluon exchange between the light quarks in the heavy baryon. Neglecting this term the RG evolution will retain its simplicity, with:

$$\frac{d\rho_2(\omega'_1, \omega'_2, \mu)}{d \ln \mu} = - \left[ \Gamma_{\text{cusp}}(\alpha_s) \ln \frac{\mu}{\sqrt{\hat{\omega}'_1 \hat{\omega}'_2}} + \gamma_2(\alpha_s) \right] \rho_2(\omega'_1, \omega'_2, \mu), \quad (4.55)$$

solved by

$$\rho_2(\omega'_1, \omega'_2, \mu) = e^{V_2} \left( \frac{\mu_0}{\sqrt{\hat{\omega}'_1 \hat{\omega}'_2}} \right)^{-g} \rho_2(\omega'_1, \omega'_2, \mu_0). \quad (4.56)$$

A more detailed discussion on the above approach can be found in [2].

\* \* \*

We have presented a relatively simple-to-use framework for the momentum-space representation of the heavy baryonic LCDAs of  $\Lambda_b$ , which is inspired by separation of momentum regions à la SCET and QCD factorisation, through the use of light-cone expansion of the matrix projectors; we await its applications in related calculations of heavy-to-light and heavy-to-heavy decays. Future extensions to the current work may address the effects of going beyond the pure WW approximation, and allowing a non-zero diquark invariant mass  $K^2 = (k_1 + k_2)^2$ , which will inevitably reduce the transparency currently achieved.

### 4.3 Helicity-based Parametrisation for $\Lambda_b \rightarrow \Lambda$ Form Factors

Form factors are scalar functions defined as part of Lorentz decompositions of matrix elements of bilinear quark currents (vector, axial-vector and tensor). For the baryonic decay  $\Lambda_b \rightarrow \Lambda$ , there are 10 of these independent physical form factors. Here we put forward a Lorentz-invariant parametrisation that already incorporates symmetry relations arising from HQET and SCET and hence is convenient to work with; in other words, expressions of physical observables and other quantities (partial rates, unitary bounds for example, c.f. [104, 105]) look conspicuously simplified and easier to follow, compared to some previous, more traditionally looking parametrisations, as provided for instance in [101, 106]. Concretely, the improvements come in two aspects: (i) The form factors are now defined on a helicity basis; and (ii) they are normalised to the limit of point-like hadrons.

In the following,  $q = s(x)$  and  $b = b(x)$  denote the light- and heavy-quark fields respectively in  $b \rightarrow s$  transitions. Starting with the vector decay current, we define:

$$\begin{aligned} \langle \Lambda(p', s') | \bar{q} \gamma_\mu b | \Lambda_b(p, s) \rangle = & \bar{u}_\Lambda(p', s') \left\{ f_0(q^2) (M_{\Lambda_b} - m_\Lambda) \frac{q_\mu}{q^2} \right. \\ & + f_+(q^2) \frac{M_{\Lambda_b} + m_\Lambda}{s_+} \left( p_\mu + p'_\mu - \frac{q_\mu}{q^2} (M_{\Lambda_b}^2 - m_\Lambda^2) \right) \\ & \left. + f_\perp(q^2) \left( \gamma_\mu - \frac{2m_\Lambda}{s_+} p_\mu - \frac{2M_{\Lambda_b}}{s_+} p'_\mu \right) \right\} u_{\Lambda_b}(p, s), \end{aligned} \quad (4.57)$$

$$\text{where} \quad s_\pm = (M_{\Lambda_b} \pm m_\Lambda)^2 - q^2. \quad (4.58)$$

At the limit of vanishing momentum transfer  $q^2 \rightarrow 0$ , one finds an additional kinematic constraint  $f_0(0) = f_+(0)$ . The individual form factors  $f_0$ ,  $f_+$  and  $f_\perp$  in (4.57) are defined such that they correspond to time-like (scalar), longitudinal and transverse polarisations with respect to the momentum transfer  $q^\mu$  respectively (cf. [104, 105]). Meanwhile the normalisation is chosen in such a way that for  $f_0, f_+, f_\perp \rightarrow 1$ , the expression for a transition between point-like baryons is recovered, i.e.  $\langle \Lambda | \bar{q} \Gamma b | \Lambda_b \rangle \rightarrow \bar{u}_\Lambda \Gamma u_{\Lambda_b}$ . It transpires that the form factor  $f_0$  corresponds to the scalar decay current, as it can also be obtained by applying the equations of motion to (4.57):

$$\begin{aligned} \langle \Lambda(p', s') | \bar{q} b | \Lambda_b(p, s) \rangle &= \frac{q^\mu}{m_b - m_q} \langle \Lambda(p', s') | \bar{q} \gamma_\mu b | \Lambda_b(p, s) \rangle \\ &= f_0(q^2) \frac{M_{\Lambda_b} - m_\Lambda}{m_b - m_q} \bar{u}_\Lambda(p', s') u_{\Lambda_b}(p, s). \end{aligned} \quad (4.59)$$

Expressions for the axial-vector and pseudoscalar currents can be directly obtained by appropriately changing the relative sign between the light- and heavy-baryon mass, leading to the definitions:

$$\begin{aligned} \langle \Lambda(p', s') | \bar{q} \gamma_\mu \gamma_5 b | \Lambda_b(p, s) \rangle = & -\bar{u}_\Lambda(p', s') \gamma_5 \left\{ g_0(q^2) (M_{\Lambda_b} + m_\Lambda) \frac{q_\mu}{q^2} \right. \\ & + g_+(q^2) \frac{M_{\Lambda_b} - m_\Lambda}{s_-} \left( p_\mu + p'_\mu - \frac{q_\mu}{q^2} (M_{\Lambda_b}^2 - m_\Lambda^2) \right) \\ & \left. + g_\perp(q^2) \left( \gamma_\mu + \frac{2m_\Lambda}{s_-} p_\mu - \frac{2M_{\Lambda_b}}{s_-} p'_\mu \right) \right\} u_{\Lambda_b}(p, s), \end{aligned} \quad (4.60)$$

where there is again the kinematic constraint  $g_0(0) = g_+(0)$  at the large-recoil limit  $q^2 \rightarrow 0$ , and

$$\begin{aligned} \langle \Lambda(p', s') | \bar{q} \gamma_5 b | \Lambda_b(p, s) \rangle &= \frac{q^\mu}{m_b + m_q} \langle \Lambda(p', s') | \bar{q} \gamma_5 \gamma_\mu b | \Lambda_b(p, s) \rangle \\ &= g_0(q^2) \frac{M_{\Lambda_b} + m_\Lambda}{m_b + m_q} \bar{u}_\Lambda(p', s') \gamma_5 u_{\Lambda_b}(p, s). \end{aligned} \quad (4.61)$$

Finally, for the tensor and pseudo-tensor currents, we define:

$$\begin{aligned} &\langle \Lambda(p', s') | \bar{q} i \sigma_{\mu\nu} q^\nu b | \Lambda_b(p, s) \rangle \\ &= -\bar{u}_\Lambda(p', s') \left\{ h_+(q^2) \frac{q^2}{s_+} \left( p_\mu + p'_\mu - \frac{q_\mu}{q^2} (M_{\Lambda_b}^2 - m_\Lambda^2) \right) \right. \\ &\quad \left. + (M_{\Lambda_b} + m_\Lambda) h_\perp(q^2) \left( \gamma_\mu - \frac{2m_\Lambda}{s_+} p_\mu - \frac{2M_{\Lambda_b}}{s_+} p'_\mu \right) \right\} u_{\Lambda_b}(p, s), \end{aligned} \quad (4.62)$$

$$\begin{aligned} &\langle \Lambda(p', s') | \bar{q} i \sigma_{\mu\nu} \gamma_5 q^\nu b | \Lambda_b(p, s) \rangle \\ &= -\bar{u}_\Lambda(p', s') \gamma_5 \left\{ \tilde{h}_+(q^2) \frac{q^2}{s_-} \left( p_\mu + p'_\mu - \frac{q_\mu}{q^2} (M_{\Lambda_b}^2 - m_\Lambda^2) \right) \right. \\ &\quad \left. + (M_{\Lambda_b} - m_\Lambda) \tilde{h}_\perp(q^2) \left( \gamma_\mu + \frac{2m_\Lambda}{s_-} p_\mu - \frac{2M_{\Lambda_b}}{s_-} p'_\mu \right) \right\} u_{\Lambda_b}(p, s). \end{aligned} \quad (4.63)$$

Again, the normalisation of the form factors  $h_{\perp,+}$  and  $\tilde{h}_{\perp,+}$  has been fixed by the case of point-like hadrons. This leads to a total of 10 independent form factors for the general case, after the equations of motion have been taken into account. Appendix B.1 summarises how this set of form factors are related to those defined in [106].

In terms of these helicity form factors, the differential decay width for  $\Lambda_b \rightarrow \Lambda \mu^+ \mu^-$  takes a particularly simple form (see Appendix A). Another alternative parametrisation, based on the large and small projections of spinors of energetic or massive fermions, has been drawn up in Appendix B.2, also motivated by a desire to align them with known symmetry relations from HQET and SCET.

### 4.3.1 HQET Limit

In the heavy-quark limit  $m_b \rightarrow \infty$ , baryonic heavy-to-light transition form factors have been known to reduce to just 2 independent functions [67, 99, 107]; the heavy-baryon velocity  $v^\mu$  can be used to project out the large spinor components  $h_v^{(b)} = \not{v} h_v^{(b)}$



of the heavy  $b$ -quark field. In terms of this “reduced” 2-component field, we see the result of spin symmetry:

$$\begin{aligned} \langle \Lambda(p', s') | \bar{q} \Gamma b | \Lambda_b(p, s) \rangle &\rightarrow \langle \Lambda(p', s') | \bar{q} \Gamma h_v^{(b)} | \Lambda_b(v, s) \rangle \\ &\simeq \bar{u}_\Lambda(p', s') (A(v \cdot p') + \not{v} B(v \cdot p')) \Gamma u_{\Lambda_b}(v, s). \end{aligned} \quad (4.64)$$

Here  $\Gamma$  is an arbitrary Dirac matrix, and  $p^\mu = M_{\Lambda_b} v^\mu \simeq m_b v^\mu$ .  $|\Lambda_b(v, s)\rangle$  is a heavy-baryon state, and  $u_{\Lambda_b}(v, s) = \not{v} u_\Lambda(v, s)$  is a heavy-baryon spinor in HQET. In the heavy-quark limit, where  $m_\Lambda, v \cdot p' \ll m_b$ , it can be shown that the 10 helicity form factors are simply related to the 2 HQET form factors in (4.64) as follows:

$$\begin{aligned} f_0(q^2) &\simeq g_+(q^2) \simeq g_\perp(q^2) \simeq \tilde{h}_+(q^2) \simeq \tilde{h}_\perp(q^2) \simeq A(v \cdot p') + B(v \cdot p'), \\ g_0(q^2) &\simeq f_+(q^2) \simeq f_\perp(q^2) \simeq h_+(q^2) \simeq h_\perp(q^2) \simeq A(v \cdot p') - B(v \cdot p'). \end{aligned} \quad (4.65)$$

These relations are valid in the region of small recoil, where

$$q^2 = M_{\Lambda_b}^2 - 2M_{\Lambda_b} v \cdot p' + m_\Lambda^2 \sim \mathcal{O}(m_b^2)$$

is large. Note that  $f_0$  and  $g_0$  in (4.65) have been derived from the (axial-)vector current. Using the (pseudo)scalar current leads to results differing by terms of order  $1/m_b$ .

### 4.3.2 SCET Limit

In the kinematic region of large recoil energy  $E_\Lambda$  of the  $\Lambda$  baryon in the rest frame of the decaying  $\Lambda_b$ , further simplifications can be achieved (see e.g. [40, 51]). This can be more formally shown using SCET. One projects out the large components of the collinear quark field,  $\xi \equiv \frac{\not{n}_- \not{n}_+}{4} q$ , where  $n_\pm^\mu$  are light-like vectors used as a projector as described in Section 3.3, and considers the matrix element of the leading current of this effective hard-collinear  $s$  field and the effective heavy  $b$  field. In the large- $E_\Lambda$  limit, one can approximate  $p'^\mu \simeq n_+ p' \frac{n_-^\mu}{2}$  and take  $m_\Lambda \rightarrow 0$ . This amounts to

$$\begin{aligned} &\langle \Lambda(p', s') | \bar{\xi} W \Gamma Y^\dagger h_v^{(b)} | \Lambda_b(v, s) \rangle \\ &= \bar{u}_\Lambda(p', s') (A(q^2) + \not{v} B(q^2)) \frac{\not{n}_+ \not{n}_-}{4} \Gamma u_{\Lambda_b}(v, s) \\ &= A(q^2) \bar{u}_\Lambda(p', s') \frac{\not{n}_+ \not{n}_-}{4} \Gamma u_{\Lambda_b}(v, s) + B(q^2) \bar{u}_\Lambda(p', s') \frac{\not{n}_-}{2} \Gamma u_{\Lambda_b}(v, s), \end{aligned} \quad (4.66)$$

where  $W$  and  $Y$  are the appropriate Wilson lines in SCET included to render the definitions of the form factors invariant under collinear and soft gauge transformations respectively (see Section 3.3). In the following their inclusion will no longer be explicitly shown. (This actually corresponds to using the light-cone gauges for collinear and soft gluon fields). Exploiting the approximate equations of motion for  $\bar{u}_\Lambda(p', s') \not{n}_- \simeq 0$ , (4.66) simplifies to

$$\langle \Lambda(p', s') | \bar{\xi} \Gamma h_v^{(b)} | \Lambda_b(v, s) \rangle \simeq \xi_\Lambda(n_+ p') \bar{u}_\Lambda(p', s') \Gamma u_{\Lambda_b}(v, s), \quad (4.67)$$

in which only a single form factor,  $\xi_\Lambda$ , remains. This defines the so-called “soft”  $\Lambda_b \rightarrow \Lambda$  form factor. It can be shown that  $\xi_\Lambda(n_+ p') \simeq A(v \cdot p')$  which appears in the HQET expression (4.64), while the contributions from  $B(v \cdot p')$  are negligible. Therefore we see that in the SCET limit, where

$$q^2 = M_{\Lambda_b}^2 - M_{\Lambda_b} n_+ p' + m_\Lambda^2 \left( 1 - \frac{M_{\Lambda_b}}{n_+ p'} \right)$$

is small, all helicity form factors defined in (4.57, 4.60, 4.62, 4.63) are equal to  $\xi_\Lambda(n_+ p')$ .

$$\begin{aligned} f_0(q^2) &\approx f_+(q^2) \approx f_\perp(q^2) \approx h_+(q^2) \approx h_\perp(q^2) \\ &\approx g_0(q^2) \approx g_+(q^2) \approx g_\perp(q^2) \approx \tilde{h}_+(q^2) \approx \tilde{h}_\perp(q^2) \approx \xi_\Lambda(n_+ p'). \end{aligned} \quad (4.68)$$

### 4.3.3 Hard-Scattering Corrections

Hard-scattering gluon exchange constitutes a leading correction to the form-factor relations described above, and can be described by new form-factor terms, which take into account the corresponding sub-leading SCET currents containing one additional (transverse) hard-collinear gluon field (see [41, 52]). If one neglects additional hard-vertex corrections for simplicity, the form factors relate to matrix elements of local SCET currents. In the duo limit  $m_b, n_+ p' \rightarrow \infty$ , these matrix elements can again be reduced to one single form factor, which we opt to define as follows:

$$\langle \Lambda(p', s') | \bar{\xi} \tilde{\Gamma} g A_\mu^\perp h_v^{(b)} | \Lambda_b(v, s) \rangle \equiv M_{\Lambda_b} \Delta \xi_\Lambda(n_+ p') \bar{u}_\Lambda(p', s') \gamma_\mu^\perp \tilde{\Gamma} u_{\Lambda_b}(v, s), \quad (4.69)$$

where the basis of independent Dirac matrices can be reduced to  $\tilde{\Gamma} = \frac{\not{n}_+}{2} \{1, \gamma_\nu^\perp, \gamma_5\}$ , thanks to the fields now being two-component effective spinors. Due to the heavy-quark spin symmetry, the Dirac matrix in the effective decay current couples trivially

to the heavy-baryon spinor. The matching of the various decay currents in QCD onto SCET currents is process-independent and can be taken into account by appropriate Wilson coefficients. Relevant results are summarised in Appendix C.

\* \* \*

It is these quantities,  $\xi_\Lambda(n_+p')$  (4.67) and  $\Delta\xi_\Lambda(n_+p')$  (4.69), the universal soft form factor and the hard-scattering factorisable correction, that will be calculated using SCET LCSRs and analysed in the following chapter.

## Chapter 5

# $\Lambda_b \rightarrow \Lambda \ell^+ \ell^-$ Soft Form Factor and Correction from Hard-Collinear Gluon Exchange

As already discussed in the preceding chapters,  $\Lambda_b \rightarrow \Lambda \ell^+ \ell^-$  offers a relatively novel channel to study rare exclusive semi-leptonic and radiative  $b \rightarrow s$  decays; experimental observation and theoretical prediction are to be checked side by side and reconciled for refining SM parameters and spotting BSM effects. The CDF experiment has already measured a branching ratio of the order of  $10^{-6}$  for  $l = \mu$  [73]; here we make a step to predict experimentally accessible observables using the technique of SCET light-cone sum rules which has already well served the analogous case of  $B$  mesons.

It has been pointed out in Section 4.3 that in the heavy-quark limit, 2 independent transition form factors remain for  $\Lambda_b \rightarrow \Lambda \ell^+ \ell^-$ , reducing to just one in the additional kinematical limit of large recoil energy. This corresponds to the scenario where only soft interactions occur within the hadronic system  $\Lambda_b \rightarrow \Lambda$ , and our immediate goal here is to estimate this universal “soft” form factor,  $\xi_\Lambda$ .

Some corrections to this leading term (in both  $\alpha_s$  and  $1/m_b$  expansions) are expected to be factorisable – expressible as a convolution of universal non-perturbative

parameters and process-dependent kernels, as observed in analogous heavy  $B$  meson decays. We estimate the  $\mathcal{O}(\alpha_s)$  hard-scattering correction, in terms of a form factor  $\Delta\xi_\Lambda$  as defined in Section 4.3.3, that breaks the form-factor symmetry relations (see Appendix C.3). This term concerns the exchange of a hard-collinear gluon between the decay vertex and either of the soft light quarks.

Following related work on the  $B \rightarrow \pi(\rho)$  form factors in [65, 108], the calculations are built upon the SCET LCSR framework. A suitably defined SCET correlation function between the decay current and an interpolating current with the quantum numbers of the light hadron ( $\Lambda$ ) is analysed using the dispersion relation. The heavy baryon is represented by its LCDAs in momentum space (Section 4.2). The operational details and philosophy behind this set of procedures have been discussed in Chapter 3.

The leading diagrams for the correlation functions involving  $\xi_\Lambda$  and  $\Delta\xi_\Lambda$  are displayed in Figures 5.1 and 5.2. Note that in the case of  $\Delta\xi_\Lambda$ , the light quark which is uninvolved in the hard-scattering process remains a soft spectator and stays in the kinematic end-point region in phase space; the diagram represents an intermediate or hybrid case where only some of the constituents undergo calculable short-distance interactions.<sup>1</sup> This means that, unlike in the mesonic case, the QCD factorisation approach cannot be directly implemented, as the kernel  $T_i(\mu_{\text{hc}})$  in eq.(3.32), i.e. the part of the factorisable term that is not LCDAs, is only supposed to encode physics above the hard-collinear scale. This strengthens our case of approaching our calculations using the method of SCET sum rules.

The sum rules that result from the dispersive analysis are investigated numerically, in particular their various dependences on hadronic input parameters and the associated theoretical uncertainties. The expression for the ratio  $\Delta\xi_\Lambda/\xi_\Lambda$  is free of a

---

<sup>1</sup>A similar discussion for the electromagnetic form factors for the nucleon can be found in [109].

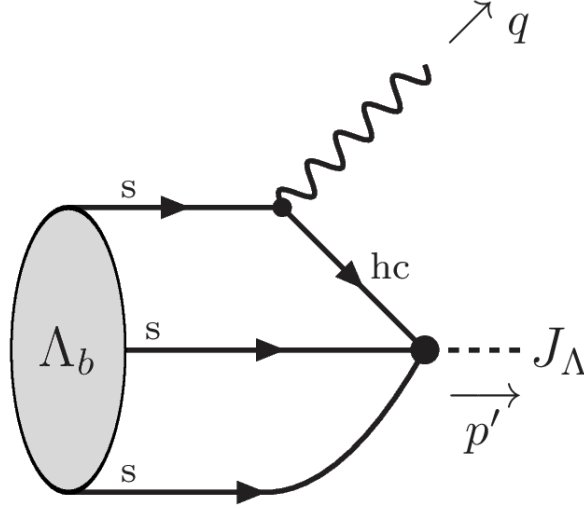


Figure 5.1: SCET correlation function relevant to the soft form factor  $\xi_\Lambda$ . The  $\Lambda$  baryon is represented by an interpolating current  $J_\Lambda$  and the  $\Lambda_b$  by LCDAs (4.2). The uppermost of the 3 quark lines coming out of the  $\Lambda_b$  represents the heavy  $b$  quark which decays into an  $s$  quark at the radiative vertex; the remaining lines denote the  $u$  and the  $d$ .

number of these inputs and uncertainties by cancellation, and hence presents itself as a desirable object to be made good use of when designing observables. We also provide estimates for the partial branching fractions for  $\Lambda_b \rightarrow \Lambda \mu^+ \mu^-$ , at small  $q^2$  where the SCET limit is valid.

## 5.1 $\xi_\Lambda$ : Soft Form Factor

A correlation function needs to be constructed to describe the transition from  $\Lambda_b$  (momentum  $p$ ) to  $\Lambda$  (momentum  $p'$ ) in a semi-leptonic process. But before this a choice has to be made on the interpolating current with the right quantum numbers to stand for the final-state baryon, based on what is expected to lead to an overall non-suppressed result. An appropriate choice is

$$J_\Lambda(x) \equiv \epsilon^{abc} \left( u^a(x) C \gamma_5 \not{p}_+ d^b(x) \right) s^c(x), \quad (5.1)$$

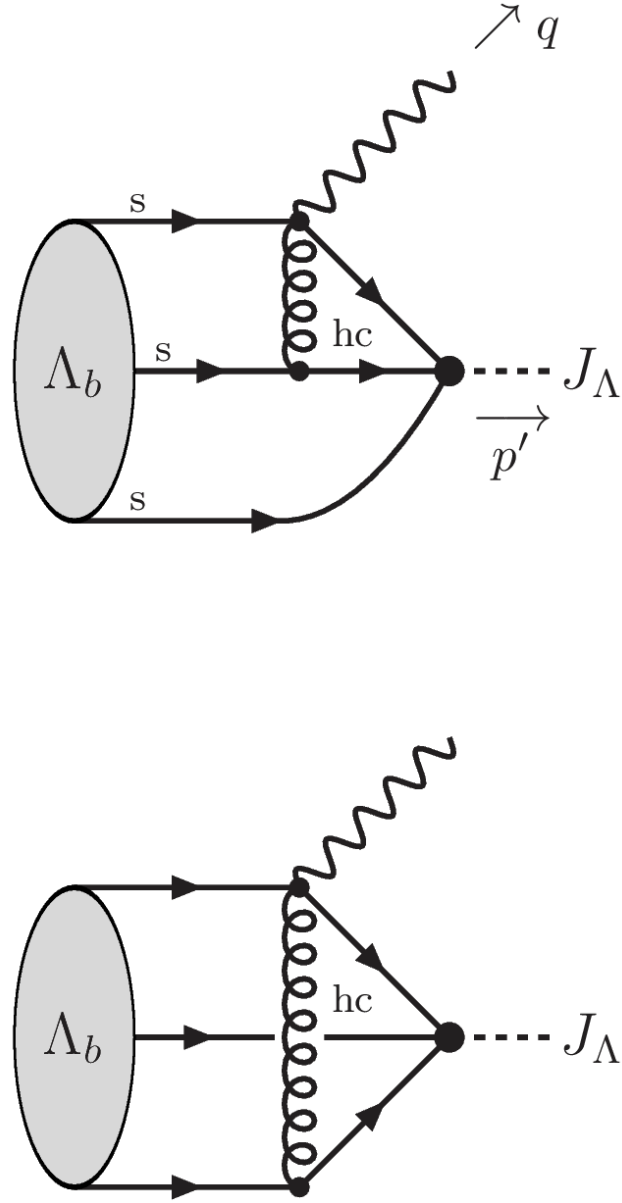


Figure 5.2: SCET correlation functions relevant to the form factor  $\Delta\xi_\Lambda$  (defined in (4.69)) for the  $\mathcal{O}(\alpha_s)$  hard-scattering correction. The quarks and gluon in the loop have hard-collinear momenta.

which is normalised by the matrix element

$$\langle 0 | \frac{\not{p}_\pm \not{p}'_\pm}{4} J_\Lambda(0) | \Lambda(p', s') \rangle = f_\Lambda \cdot n_+ p' \frac{\not{p}_\pm \not{p}'_\pm}{4} u_\Lambda(p', s'), \quad (5.2)$$

corresponding to a leading term in the large-energy limit. Note that the  $C\gamma_5$  reflects the scalar nature of the “diquark” object formed by the  $u$  and  $d$  quarks within the partonic structure of the  $\Lambda_b$  baryon. For our eventual numerical analysis, we use  $f_\Lambda \simeq (6.0 \pm 0.3) \times 10^{-3} \text{ GeV}^2$  for the  $\Lambda$ -baryon decay constant, derived from a sum-rule estimate [88].<sup>2</sup> The light quarks are decomposed into soft and hard-collinear fields to match the above current onto SCET. At tree level, it is sufficient to calculate the correlation function in QCD and perform the appropriate kinematic limits for the propagators.

$\Pi_\Lambda$  is in general a function of momentum transfer  $q^2 = (p - p')^2$ ; working in the frame where the heavy quark is stationary with  $v^\mu = (1, 0, 0, 0)$  and the transverse momentum of the final baryon  $p'_\perp$  vanishes, one can pick the independent kinematic variables to be the large and small momentum components,  $n_+ p' \sim \mathcal{O}(m_b)$  and  $n_- p' \sim \mathcal{O}(\Lambda_{\text{QCD}}) < 0$  respectively. First, one considers  $\Pi_\Lambda$  as a function of  $n_- p'$ . The quark fields inside  $\Pi_\Lambda$  are effective fields with their small irrelevant spinor components already removed using respective effective-theory projectors:

$$\Pi_\Lambda(n_- p') \equiv i \int d^4x e^{ip'x} \langle 0 | T \left[ \frac{\not{p}_- \not{p}_+}{4} J_\Lambda(x) \left[ \bar{s}(0) \frac{\not{p}_+ \not{p}_-}{4} \Gamma \frac{1 + \not{p}}{2} b(0) \right] \right] | \Lambda_b(p) \rangle. \quad (5.3)$$

The time-ordered product of the two currents can be calculated in perturbation theory. Substituting in (5.1), the two  $s$ -quark fields present are contracted to a propagator, while the  $u$  and  $d$  quarks start as and remain as spectators with soft momenta, as seen in the diagram for the leading soft  $\xi_\Lambda$  (Figure 5.1). Employing the kinematic limits in the QCD diagram, and performing a Fourier transform such that  $\omega_{1,2} = n_- k_{1,2}$  correspond to the relevant light-cone momenta of the  $u$  and  $d$  quarks,

---

<sup>2</sup>In comparison, the nucleon decay constant is estimated to be  $f_N \simeq 5.6 \times 10^{-3} \text{ GeV}^2$  in [86].



the correlation function at leading order is given by:

$$\begin{aligned}
\Pi_\Lambda(n_{-p'}) &\simeq \int \frac{d\omega_1 d\omega_2}{\omega_1 + \omega_2 - n_{-p'} - i\epsilon} \langle 0 | \epsilon^{abc} (u^a(\omega_1) C \gamma_5 \not{p}_+ d^b(\omega_2)) \frac{\not{p}_-}{2} \Gamma h_v^c | \Lambda_b(v, s) \rangle \\
&= \int \frac{d\omega_1 d\omega_2}{\omega_1 + \omega_2 - n_{-p'} - i\epsilon} \frac{f_{\Lambda_b}^{(2)}}{4} [M^{(2)}(\omega_1, \omega_2) \gamma_5 C^{-1}]_{\beta\alpha} (C \gamma_5 \not{p}_+)_{\alpha\beta} \frac{\not{p}_-}{2} \Gamma u_{\Lambda_b}(v, s) \\
&= \int \frac{d\omega_1 d\omega_2}{\omega_1 + \omega_2 - n_{-p'} - i\epsilon} \frac{f_{\Lambda_b}^{(2)}}{4} \text{Tr} \left[ \left( \frac{\not{p}_+}{2} \phi_2(\omega_1, \omega_2) + \frac{\not{p}_-}{2} \phi_4(\omega_1, \omega_2) + \dots \right) \not{p}_+ \right] \frac{\not{p}_-}{2} \Gamma u_{\Lambda_b}(v, s) \\
&= f_{\Lambda_b}^{(2)} \int \frac{d\omega_1 d\omega_2 \phi_4(\omega_1, \omega_2)}{\omega_1 + \omega_2 - n_{-p'} - i\epsilon} \frac{\not{p}_-}{2} \Gamma u_{\Lambda_b}(v, s) \tag{5.4}
\end{aligned}$$

In the second line, the momentum-space projector for the heavy  $\Lambda_b$  baryon,  $M^{(2)}$  as defined in Section 4.2, is recalled; only the LCDA  $\phi_4$  remains due to the choice of the interpolating current.

At leading order, the result for the correlation function only involves the sum of the spectator-quark momenta, so the partially integrated version of the LCDA can be used:

$$\psi_4(\omega) \equiv \omega \int_0^1 du \phi_4^{\text{alt}}(\omega, u). \tag{5.5}$$

Hence, the perturbative calculation of the correlation function results in:

$$\Pi_\Lambda(n_{-p'}) \simeq f_{\Lambda_b}^{(2)} \int_0^\infty \frac{d\omega \omega \int_0^1 du \phi_4^{\text{alt}}(\omega, u)}{\omega - n_{-p'} - i\epsilon} \frac{\not{p}_-}{2} \Gamma u_{\Lambda_b}(v, s). \tag{5.6}$$

Note that this takes the form of a convolution of a LCDA and a kernel, despite the term being classified as “non-factorisable” in traditional QCD factorisation.

The quantity is evaluated again using the hadronic spectrum, which we assume is dominated by the ground-state  $\Lambda$ . Starting from (5.3), one finds:

$$\begin{aligned}
\Pi_\Lambda(n_{-p'}) &\simeq \sum_{s'} \frac{\not{p}_- \not{p}_+}{4} \frac{\langle 0 | J_\Lambda | \Lambda(p', s') \rangle \langle \Lambda(p', s') | \bar{q} \frac{\not{p}_+ \not{p}_-}{4} \Gamma h_v^{(b)} | \Lambda_b(v) \rangle}{m_\Lambda^2 - p'^2} \\
&= \frac{f_\Lambda \cdot n_{+p'} \cdot \xi_\Lambda(n_{+p'})}{m_\Lambda^2 - n_{+p'} \cdot n_{-p'}} \sum_{s'} \frac{\not{p}_- \not{p}_+}{4} u_\Lambda(p', s') \bar{u}_\Lambda(p', s') \frac{\not{p}_+ \not{p}_-}{4} \Gamma u_{\Lambda_b}(v, s) \\
&= \frac{f_\Lambda \cdot n_{+p'} \cdot \xi_\Lambda(n_{+p'})}{m_\Lambda^2 / n_{+p'} - n_{-p'}} \frac{\not{p}_-}{2} \Gamma u_{\Lambda_b}(v, s). \tag{5.7}
\end{aligned}$$

The perturbative (5.3) and hadronic (5.7) sides of the sum rule are equated. One performs the standard sum-rule procedures of subtracting the continuum part of the hadronic spectrum assuming quark-hadron duality above  $\omega_s$ , as well as Borel-transforming the expression with respect to  $n_+p'$  with Borel parameter  $\omega_M$ .<sup>3</sup> This produces the useful leading-order sum rule:

$$e^{-m_\Lambda^2/(\omega_M n_+p')} f_\Lambda \cdot n_+p' \cdot \xi_\Lambda(n_+p') = f_{\Lambda_b}^{(2)} \int_0^{\omega_s} d\omega \psi_4(\omega) e^{-\omega/\omega_M}, \quad (5.8)$$

which takes an analogous form to one for the  $B \rightarrow \pi, \rho$ , with the distribution amplitude for the spectator anti-quark in the  $B$ -meson replaced by an object that is effectively a wave-function for the spectator diquark, in the  $\Lambda_b$  baryon.

The formal scaling of this tree-level result for  $\xi_\Lambda$  with the large-energy variable  $n_+p'$  at the limit  $\omega_s, \omega_M \sim \frac{\Lambda^2}{n_+p'} \ll \langle \omega \rangle$ , where  $\langle \omega \rangle$  is the typical light-cone momentum of the light diquark, can be derived by expanding the  $\Lambda_b$  LCDA around  $\omega = 0$  in the integrand. This yields

$$\xi_\Lambda(n_+p') \simeq \frac{f_{\Lambda_b}^{(2)} \omega_M^2 \psi_4'(0)}{f_\Lambda \cdot n_+p'} e^{m_\Lambda^2/(\omega_M n_+p')} \left( 1 - e^{-\omega_s/\omega_M} \left( 1 + \frac{\omega_s}{\omega_M} \right) \right), \quad (5.9)$$

where  $\psi_4'(0) \sim 1/\omega_0^2$  with  $\omega_0 \sim \langle \omega \rangle$  (see Section 4.2 for details of the LCDA model used here). In this limit, the soft  $\Lambda_b \rightarrow \Lambda$  form factor scales as  $1/n_+p'^3$  with the large energy of the final-state baryon. Compared to the mesonic case [65, 108], one encounters an additional factor of  $1/n_+p'$ , which physically can be traced back to the phase-space suppression of the additional spectator quark. Technically, the difference between the mesonic and baryonic case stems from the fact that the  $B$ -meson LCDA  $\phi_B^-(\omega)$  does not vanish at the end point, while  $\psi_4(\omega)$  vanishes linearly.

\* \* \*

Radiative corrections (due to hard-collinear – virtuality  $\mathcal{O}(m_b \Lambda_{\text{QCD}})$  – gluon loops; hard – virtuality  $\mathcal{O}(m_b^2)$  – effects have entered external Wilson coefficients  $C_i$ )

---

<sup>3</sup>Note that the parameters are related to QCDF ones as  $\omega_s = s_0/n_+p'$  and  $\omega_M = M_{\text{Bor}}^2/n_+p'$ .

to the leading-order sum rule leads to additional dependence of the form factors on  $n_+p'$  with logarithmically enhanced perturbative coefficients. There are universal corrections which can be factorised into (i) hard-vertex corrections absorbed into Wilson coefficients of SCET decay currents, (ii) a jet function, absorbing the hard-collinear emissions from the strange-quark propagator in SCET, and (iii) contributions arising from the soft evolution of the relevant LCDAs. To  $\mathcal{O}(\alpha_s)$  (see Figure 1(a1-a4) of [108] for relevant diagrams), one obtains an analogous result as discussed for the mesonic case [65, 108]:

$$F_i(q^2) \simeq C_i(n_+p', \mu) \cdot \frac{f_{\Lambda_b}^{(2)}}{f_\Lambda \cdot n_+p'} e^{m_\Lambda^2/(\omega_M n_+p')} \int_0^{\omega_s} d\omega' e^{-\omega'/\omega_M} \\ \times \left\{ \left[ 1 + \frac{\alpha_s C_F}{4\pi} \left( 7 - \pi^2 + 3 \ln \left[ \frac{\mu^2}{\omega' \cdot n_+p'} \right] + 2 \ln^2 \left[ \frac{\mu^2}{\omega' \cdot n_+p'} \right] \right) \right] \psi_4(\omega', \mu) \right. \\ \left. + \frac{\alpha_s C_F}{4\pi} \int_0^{\omega'} d\omega \left( 4 \ln \left[ \frac{\mu^2}{(\omega' - \omega) n_+p'} \right] + 3 \right) \frac{\psi_4(\omega', \mu) - \psi_4(\omega, \mu)}{\omega' - \omega} \right\}, \quad (5.10)$$

where  $F_i(q^2)$  denotes a generic form factor with the corresponding Wilson coefficient  $C_i$ . The leading (double-logarithmic)  $\mu$ -dependence is shown to cancel between the 3 terms on the right-hand side, using the renormalisation-group equations (see e.g. [37, 90, 93–95]),

$$\frac{d}{d \ln \mu} C_i(n_+p', \mu) = -\frac{\alpha_s C_F}{4\pi} \Gamma_{\text{cusp}}^{(1)} \ln \frac{\mu}{m_b} C_i(n_+p', \mu) + \dots, \quad (5.11)$$

$$\frac{d}{d \ln \mu} \psi_4(\omega, \mu) = -\frac{\alpha_s C_F}{4\pi} \Gamma_{\text{cusp}}^{(1)} \ln \frac{\mu}{\omega} \psi_4(\omega, \mu) + \dots, \quad (5.12)$$

with the cusp anomalous dimension  $\Gamma_{\text{cusp}}^{(1)} = 4$ . Evaluating the terms in curly brackets in (5.10) at a factorisation scale of order  $\mu^2 \sim \omega_s \cdot n_+p'$  and evolving the Wilson coefficients down to that scale, one achieves the resummation of the leading Sudakov double logarithms.

There are also additional process-dependent corrections to (5.10) arising from hard-collinear gluon exchange between the strange quark and the “spectator” quarks in SCET (Figure 1(b1-b2) of [108]). These involve a sub-leading term in the SCET Lagrangian (3.17). (These corrections are not to be confused with that to be calculated in the upcoming section, which concerns a differently defined decay current.)

As shown in [65, 108], these will lead to logarithmically enhanced terms which are sensitive to the end-point behaviour of  $\psi_4(\omega, \mu)$ . The explicit derivation of these terms is left for future work.

## 5.2 $\Delta\xi_\Lambda$ : Hard-Collinear Gluon-Exchange Correction

Sub-leading currents in the SCET Lagrangian induce violations of the form-factor symmetry relations that hold in the large-recoil limit. In a SCET correlation function to be subjected to dispersive analysis, the contribution involving the exchange of one hard-collinear gluon can be treated perturbatively. To obtain leading ( $\mathcal{O}(\alpha_s)$ ) corrections, we have defined the matrix element (4.69), in which the leading contribution arises from hard-collinear gluon exchange with either of the two light quarks in the baryons (Figure 5.2). From the perspective of the QCD factorisation approach, this diagram represents an intermediate case, where only some of the constituents undergo calculable short-distance interactions; the remaining spectator quark remains undisturbed and is thus forced to stay in the end-point region in phase space.

As in the sum-rule calculation of  $\xi_\Lambda$  above, we define a correlation function, where the SCET decay current features an additional transverse gluon field. Moreover, we use the projector  $\frac{\not{n}_+ \not{n}_-}{4}$  (contrary to the one used in (5.3)) to project out the sub-leading transverse momentum in the  $s$ -quark propagator.

$$\Pi_\Lambda^\mu(n, p') \equiv i \int d^4x e^{ip'x} \langle 0 | T \left[ \frac{\not{n}_+ \not{n}_-}{4} J_\Lambda(x) \left[ \bar{s}(0) \tilde{\Gamma} g_s A_\perp^\mu(0) b(0) \right] \right] | \Lambda_b(p) \rangle. \quad (5.13)$$

The momenta of the light quarks in the heavy baryon are as before denoted as  $k_{1,2}$ , and the relevant light-cone component  $\omega_i = n_- k_i$ .  $k = k_1 + k_2$ , while  $k_\perp$  is the transverse component. Also, as hinted in (5.5), the longitudinal momentum fraction variable  $u$  is introduced, such that in the diquark,  $\omega_1 = u\omega$  and  $\omega_2 = (1 - u)\omega \equiv \bar{u}\omega$ . Assuming isospin symmetry of strong interactions, the two diagrams (Figure 5.2)

under consideration are actually equivalent and lead to the identical results. Hence, denoting the gluon momentum as  $l$ , the correlation function for the sum of both cases can be expressed as:

$$\begin{aligned}\Pi_\Lambda^\mu(n_{-p'}) &= 2 \times i g_s^2 \frac{C_F}{2} \frac{f_{\Lambda_b}^{(2)}}{4} \int_0^\infty d\omega_1 \int_0^\infty d\omega_2 \\ &\times \int \frac{d^D l}{(2\pi)^D} \frac{1}{[l_\perp^2 + (n_+ l)(n_- l - u\omega)]} \frac{1}{[l_\perp^2 + (n_+ l + n_{+p'})(n_- l + n_{-p'} - \omega)]} \\ &\times \frac{1}{[l_\perp^2 + (n_+ l)(n_- l)]} \text{Tr}[M^{(2)}(k_1, k_2) C \gamma_5 \not{l}_+ (\not{k}_2 - \not{l}) \gamma_\perp^\mu] \\ &\times \frac{\not{l}_+ \not{l}_-}{4} (\not{l} - \not{k}_1 - \not{k}_2) \tilde{\Gamma} u_{\Lambda_b}(v, s). \quad (5.14)\end{aligned}$$

Here  $\omega_1$  denotes the light-cone momentum of the quark which remains a spectator. Square brackets around a propagator denominator imply a  $+i\epsilon$  prescription. The Dirac trace is straightforward:

$$\begin{aligned}\text{Tr}[M^{(2)}(k_1, k_2) C \gamma_5 \not{l}_+ (\not{k}_2 - \not{l}) \gamma_\perp^\mu] \\ = -4 \phi_4(\omega_1, \omega_2) l_\perp^\mu + 2 n_+ l \left( G(\omega_1, \omega_2) \frac{\partial}{\partial k_{1\mu}^\perp} + H(\omega_1, \omega_2) \frac{\partial}{\partial k_{2\mu}^\perp} \right). \quad (5.15)\end{aligned}$$

$G(\omega_1, \omega_2)$  and  $H(\omega_1, \omega_2)$  are defined in Section 4.2. This yields

$$\begin{aligned}\Pi^\mu(n_{-p'}) &= i \frac{g_s^2 C_F f_{\Lambda_b}^{(2)}}{4} \int d\omega_1 \int d\omega_2 \\ &\times \int \frac{d^D l}{(2\pi)^D} \frac{\frac{4l_\perp^2}{D-2} \phi_4(\omega_1, \omega_2) + 2 n_+ l [G(\omega_1, \omega_2) + H(\omega_1, \omega_2)]}{[l_\perp^2 + (n_+ l)(n_- l)][l_\perp^2 + (n_+ l)(n_- l - \omega_2)][l_\perp^2 + (n_{+p'} + n_+ l)(n_{-p'} + n_- l - \omega)]} \\ &\times \frac{\not{l}_+ \not{l}_-}{4} \gamma_\perp^\mu \tilde{\Gamma} u_{\Lambda_b}(v, s). \quad (5.16)\end{aligned}$$

Both terms in the numerator contribute at the same order in the SCET correlator, as  $l_\perp^2 \sim \omega \cdot n_+ l \sim m_b \Lambda_{\text{QCD}}$ . However, in the limit  $\omega_1 \rightarrow 0$ , the contributions from  $\phi_4$  and  $G$  formally give sub-leading contributions to the  $\Delta\xi_\Lambda$  sum rule (see (5.22)).

To tackle this complicated-looking integral involving the light-cone components of loop momentum  $l$  separately, we split

$$\frac{d^D l}{(2\pi)^D} \rightarrow \frac{1}{2} \frac{d n_+ l}{2\pi} \frac{d^{D-2} l_\perp}{(2\pi)^{D-2}} \frac{d n_- l}{2\pi};$$

the integral over  $n_-l$  can be performed using complex contour integration via Cauchy's theorem: we recognise that only when  $n_+p' > -n_+l > 0$  is this integral non-vanishing, as otherwise all 3 poles in (5.16) are on the same side of the real axis. One gets:

$$\begin{aligned}
\Pi^\mu(n_-p') &= \frac{g_s^2 C_F f_{\Lambda_b}^{(2)}}{4} \int d\omega_1 \int d\omega_2 \int \frac{dn_+l}{2\pi} \int \frac{d^{D-2}l_\perp}{(2\pi)^{D-2}} (n_+l + n_+p') \\
&\quad \times \frac{\frac{2l_\perp^2}{D-2} \phi_4(\omega_1, \omega_2) + n_+l [G(\omega_1, \omega_2) + H(\omega_1, \omega_2)]}{[(\omega - n_-p')(n_+l)(n_+l + n_+p') + l_\perp^2 n_+p'] [(\omega_1 - n_-p')(n_+l)(n_+l + n_+p') + l_\perp^2 n_+p']} \\
&\quad \times \theta(-n_+l) \theta(n_+l + n_+p') \gamma_\perp^\mu \tilde{\Gamma} u_{\Lambda_b}(v, s), \\
\Pi^\mu(n_-p') &= \frac{\alpha_s C_F f_{\Lambda_b}^{(2)}}{2} \int d\omega_1 \int d\omega_2 \int_0^1 dz \int \frac{d^{D-2}l_\perp}{(2\pi)^{D-2}} \\
&\quad \times \frac{\frac{l_\perp^2}{D-2} \phi_4(\omega_1, \omega_2) + n_+l [G(\omega_1, \omega_2) + H(\omega_1, \omega_2)]}{[l_\perp^2 - z(1-z)n_+p'(\omega - n_-p')] [l_\perp^2 - z(1-z)n_+p'(\omega_1 - n_-p')]} \gamma_\perp^\mu \tilde{\Gamma} u_{\Lambda_b}(v, s),
\end{aligned} \tag{5.17}$$

where we have defined the dimensionless variable  $z = -n_+l/n_+p'$  in going to the final line.

The (Euclidean)  $l_\perp^{D-2}$  integral is done using the standard method of Feynman parameters, while the  $z$ -integral is straightforward. The extraction of a non-vanishing imaginary part leads to further Heaviside functions. After Borelisation and continuum subtraction, the perturbative calculation of the correlation function for  $\Delta\xi_\Lambda$  is:

$$\begin{aligned}
\hat{B}\Pi_\Lambda^\mu(\omega_M) &= -\frac{\alpha_s C_F f_{\Lambda_b}^{(2)}}{4\pi} \int d\omega_1 \int d\omega_2 \int_0^{\omega_s} \frac{d\omega'}{\omega_M} e^{-\omega'/\omega_M} \\
&\quad \times \left\{ \frac{[\omega_2 + (\omega' - \omega)\theta(\omega - \omega')]\theta(\omega' - \omega_1)}{4\omega_2} \phi_4(\omega_1, \omega_2) \right. \\
&\quad \left. + \frac{\theta(\omega - \omega')\theta(\omega' - \omega_1)}{2\omega_2} [G(\omega_1, \omega_2) + H(\omega_1, \omega_2)] \right\} \\
&\quad \times \frac{\not{p}_+ \not{p}_-}{4} \gamma_\perp^\mu \tilde{\Gamma} u_{\Lambda_b}(v, s).
\end{aligned} \tag{5.18}$$

In the limit  $\omega_s, \omega_M \ll \langle \omega_{1,2} \rangle$ , where  $\langle \omega_{1,2} \rangle$  are the typical momenta of the light quarks in the heavy baryon, the integral can be simplified. Since  $\omega_1 \leq \omega' \leq \omega_s$ , one may approximate  $\omega_1 \simeq 0$  in the LCDAs. This reflects the physical assumption that

the hard-collinear scattering requires the active light quark to carry almost all of the momentum  $\omega$  of the diquark compound. In this limit,

$$\hat{B}\Pi_\Lambda^\mu(\omega_M) \simeq -\frac{\alpha_s C_F}{8\pi} \gamma_\perp^\mu \tilde{\Gamma} u_{\Lambda_b}(v, s) \underbrace{f_{\Lambda_b}^{(2)} \int_0^\infty \frac{d\omega}{\omega} H(0, \omega)}_{\Lambda_b} \times \underbrace{(\omega_M - e^{-\omega_s/\omega_M}(\omega_M + \omega_s))}_{J_\Lambda}. \quad (5.19)$$

As indicated the right-hand side factorises into an inverse moment of the heavy-baryon LCDA, and a function characterising the light baryon, in terms of the Borel and threshold parameters related to the spectrum of the interpolating current.

On the hadronic side of the sum rule, the contribution of the  $\Lambda$  baryon to the correlator is given by

$$\Pi_\Lambda^\mu = \frac{f_\Lambda m_\Lambda M_{\Lambda_b} \Delta\xi_\Lambda}{m_\Lambda^2/n_+p' - n_-p'} \gamma_\perp^\mu \tilde{\Gamma} u_{\Lambda_b}(v, s). \quad (5.20)$$

After Borel transformation, and putting everything together, the sum rule for  $\Delta\xi_\Lambda$  is derived:

$$\begin{aligned} & e^{-m_\Lambda^2/(\omega_M n_+p')} f_\Lambda M_{\Lambda_b} m_\Lambda/\omega_M \Delta\xi_\Lambda \\ &= -\frac{\alpha_s C_F f_{\Lambda_b}^{(2)}}{4\pi} \int d\omega_1 \int d\omega_2 \int_0^{\omega_s} \frac{d\omega'}{\omega_M} e^{-\omega'/\omega_M} \\ & \quad \times \left\{ \frac{(\omega_2 + (\omega' - \omega) \theta(\omega - \omega')) \theta(\omega' - \omega_1)}{4\omega_2} \phi_4(\omega_1, \omega_2) \right. \\ & \quad \left. + \frac{\theta(\omega - \omega') \theta(\omega' - \omega_1)}{2\omega_2} (G(\omega_1, \omega_2) + H(\omega_1, \omega_2)) \right\} \end{aligned} \quad (5.21)$$

$$\simeq -\frac{\alpha_s C_F}{8\pi} f_{\Lambda_b}^{(2)} \int_0^\infty \frac{d\omega}{\omega} H(0, \omega) \times (\omega_M - e^{-\omega_s/\omega_M}(\omega_M + \omega_s)). \quad (5.22)$$

In the large-recoil limit, the correction to the soft form factor scales as

$$\frac{\Delta\xi_\Lambda}{\xi_\Lambda} \sim \alpha_s \frac{\omega_0}{m_\Lambda} \frac{n_+p'}{M_{\Lambda_b}}.$$

Formally this has the same power-counting in terms of  $\Lambda_{\text{QCD}}/m_b$  (though note that the ratio  $\omega_0/m_\Lambda$  is numerically small), but its dependence on  $n_+p'$  is less pronounced

than for  $\xi_\Lambda$ . The decay constants of both baryons have dropped out of this ratio, while the sensitivity to the sum-rule parameters and the exact shape of the LCDAs of the  $\Lambda_b$  baryon remains.

### 5.3 Numerical Results

Here we numerically investigate the results of our sum rules regarding  $\Lambda_b \rightarrow \Lambda$  form factors (in the large-recoil limit). A small number of hadronic parameters play crucial parts in the numerics, bringing along their respective uncertainties. Our “default” choices for these are summarised in Table 5.1 for convenient reference throughout this section.

Parameter	Central value	Remarks
Threshold $s_0$ ( $\omega_s \equiv s_0/n_+p'$ )	2.55 GeV <sup>2</sup>	First excited-state resonance: $\Lambda(1600)$
Borel $M_{\text{Borel}}^2$ ( $\omega_M \equiv M_{\text{Bor}}^2/n_+p'$ )	2.5 GeV <sup>2</sup>	
Decay constant $f_\Lambda$	0.006 GeV <sup>2</sup>	Taken from [88]
Decay constant $f_{\Lambda_b}^{(2)}$	0.030 GeV <sup>3</sup>	Taken from [90]
$\Lambda_b$ LCDA parameter $\omega_0$	300 MeV	Our estimate

Table 5.1: Summary of hadronic input parameters

#### 5.3.1 Soft Form Factor

The numerical value of  $\xi_\Lambda$  is predicted from the leading-order sum rule (5.8). We shall also compare this with the approximated version (5.9). The default value for the



threshold parameter is taken from the position of the next highest  $b$ -baryon resonance<sup>4</sup> with  $I(J^P) = 0(1/2^+)$ . For the relevant LCDAs, we use our simple exponential model as discussed in Section 4.2.3. In the case of  $\xi_\Lambda$ , only the partially integrated function  $\psi_4(\omega)$  appears:

$$\psi_4(\omega) := \frac{\omega}{\omega_0^2} e^{-\omega/\omega_0},$$

illustrated in Figure 5.3. It makes physical sense to model the diquark as unlikely to possess too much or too little momentum.

Using the parameter values listed in Table 5.1, the soft form factor at maximal recoil ( $q^2 = 0, n_+ p' = M_{\Lambda_b}$ ) is estimated to be

$$\xi_\Lambda(n_+ p' = M_{\Lambda_b}) \simeq 0.38 \quad \text{central value, from (5.8),}$$

which is consistent within uncertainties with estimates derived from other methods in [106, 111]. We remark in passing, that the authors of [101] estimate the  $\Lambda_b \rightarrow \Lambda$  form factors with a similar set-up, but without performing the large-recoil limit in SCET explicitly. They quote a rather small value  $g_2(q^2 = 0) = 0.018 \pm 0.003$  for one of the form factors that, as we understand, should coincide with  $\xi_\Lambda(n_+ p' = M_{\Lambda_b})$  in the heavy-quark limit.

Figures 5.4 to 5.8 show the dependence of  $\xi_\Lambda(n_+ p' = M_{\Lambda_b})$  on the LCDA parameter  $\omega_0$ , the two auxiliary sum-rule parameters, and the energy dependence itself of  $\xi_\Lambda(n_+ p')$  away from the large-recoil limit.

The following observations and comments can be made:

- As seen from Figure 5.4, for values of  $\omega_0$  smaller than around 300 MeV (a value extracted from the analysis in [90]), the approximate formula (5.9) does not yield a reliable estimate, because numerically  $\omega_0 \simeq \omega_s \simeq \omega_M$ . In this case  $\xi_\Lambda$  is

---

<sup>4</sup>One should, however, be aware that one may encounter pollution from baryon states with opposite parity, see the recent discussion in [110].

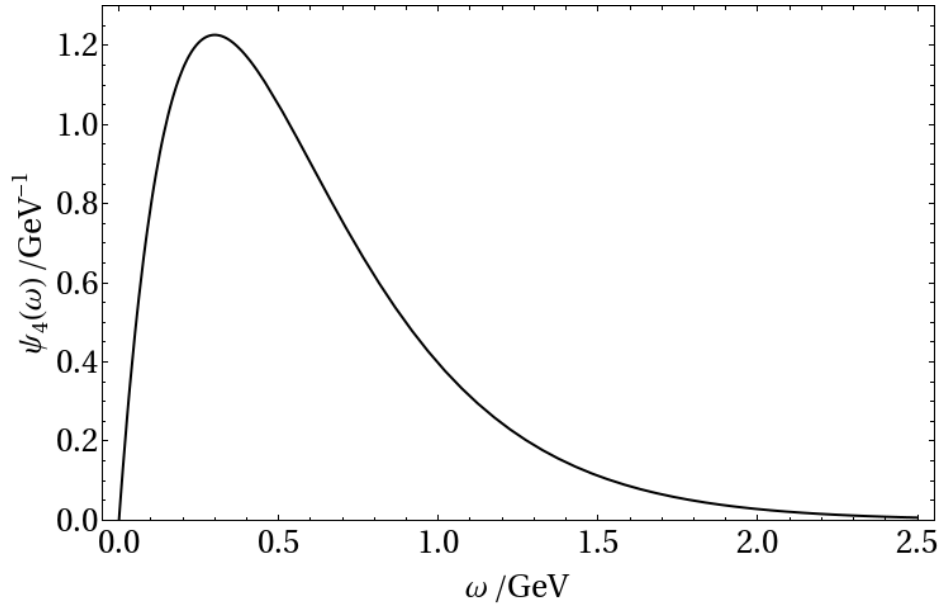


Figure 5.3: Functional form of the partially integrated LCDA  $\psi_4(\omega)$  in the exponential model, with  $\omega_0 = 300$  MeV.

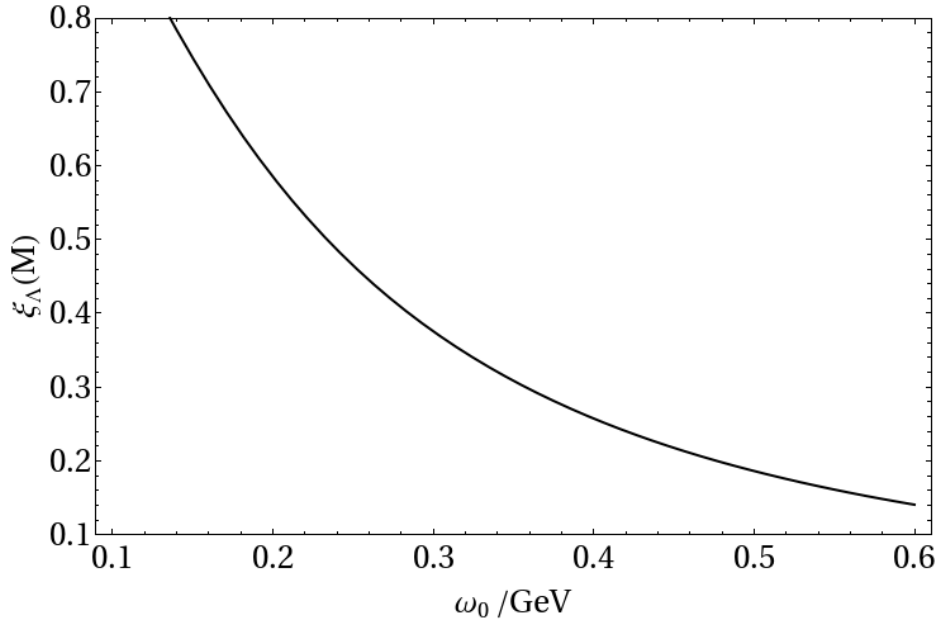


Figure 5.4: Dependence of  $\xi_\Lambda(n_+ p' = M_{\Lambda_b})$  on the value of  $\omega_0$ .

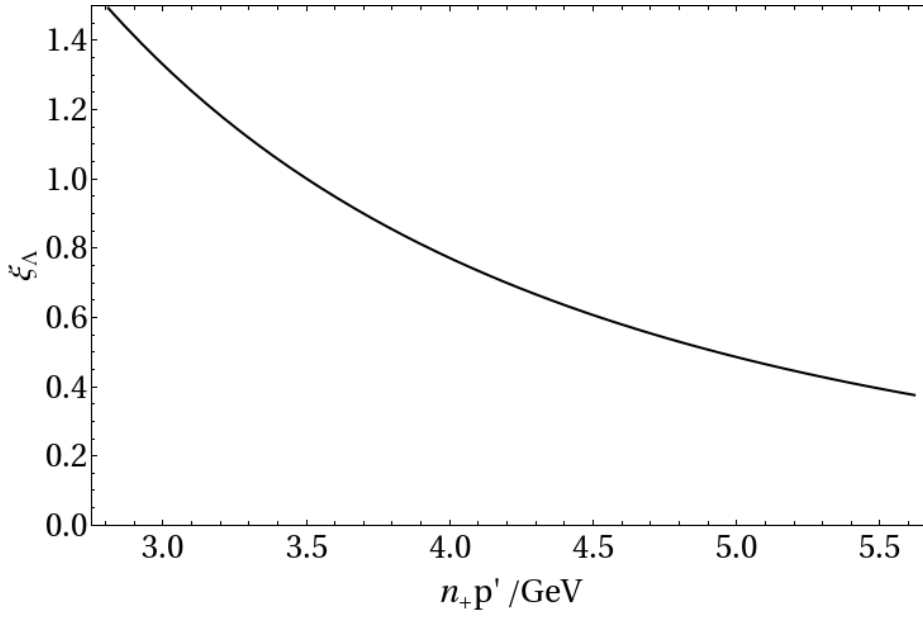


Figure 5.5: Dependence of the soft form factor on  $n_+p'$ , using the leading-order sum rule (5.8).

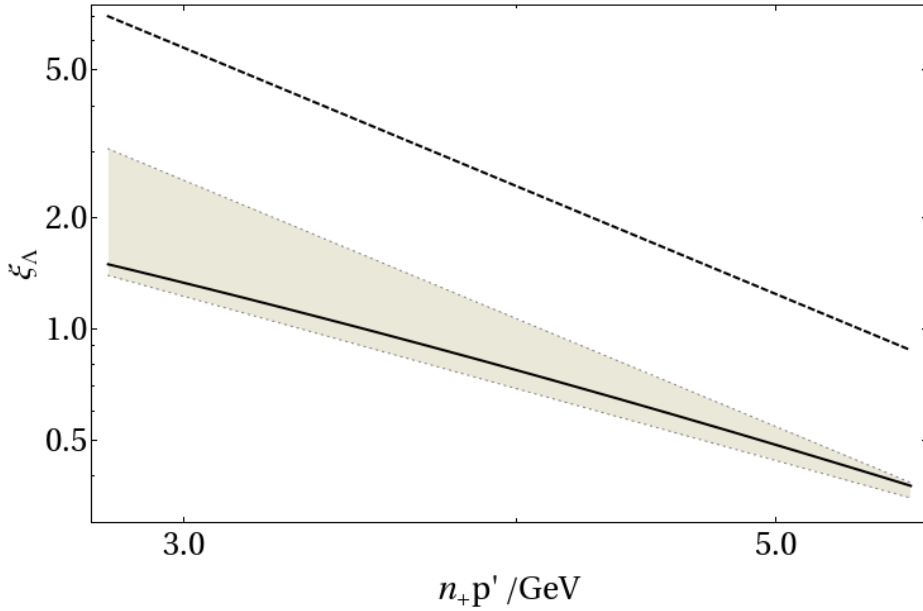


Figure 5.6: Results for the soft form factor using the leading-order sum rule (5.8) (solid line) and the approximate formula (5.9) (thick dashed line). The shaded band demonstrates the range between a pure  $1/n_+p'^2$  and a pure  $1/n_+p'^3$  behaviour. It is easy to see the leading-order result more closely resembles the former.

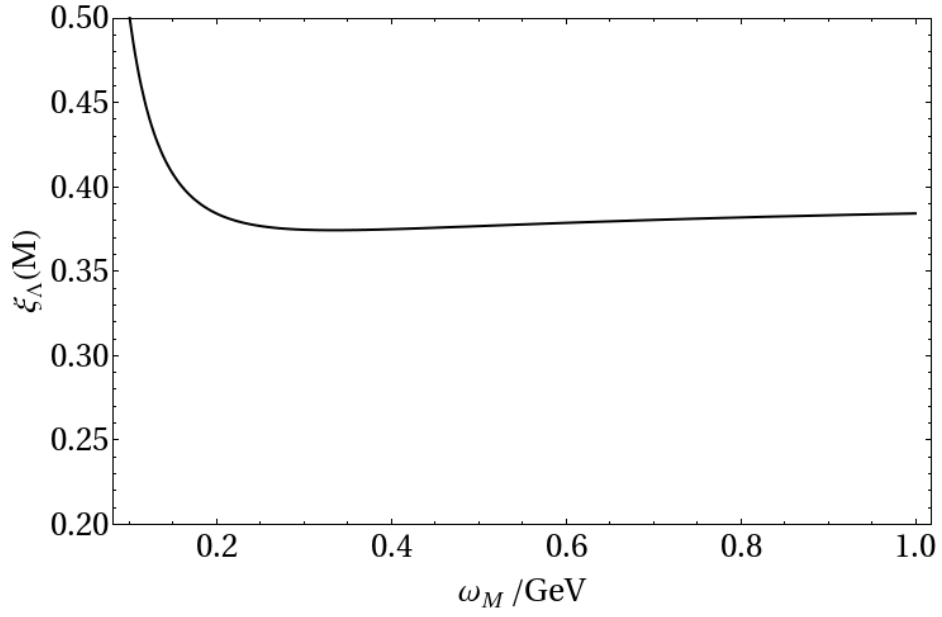


Figure 5.7: Dependence of the soft form factor on the Borel parameter at maximal recoil,  $n_+ p' = M_{\Lambda_b}$ .

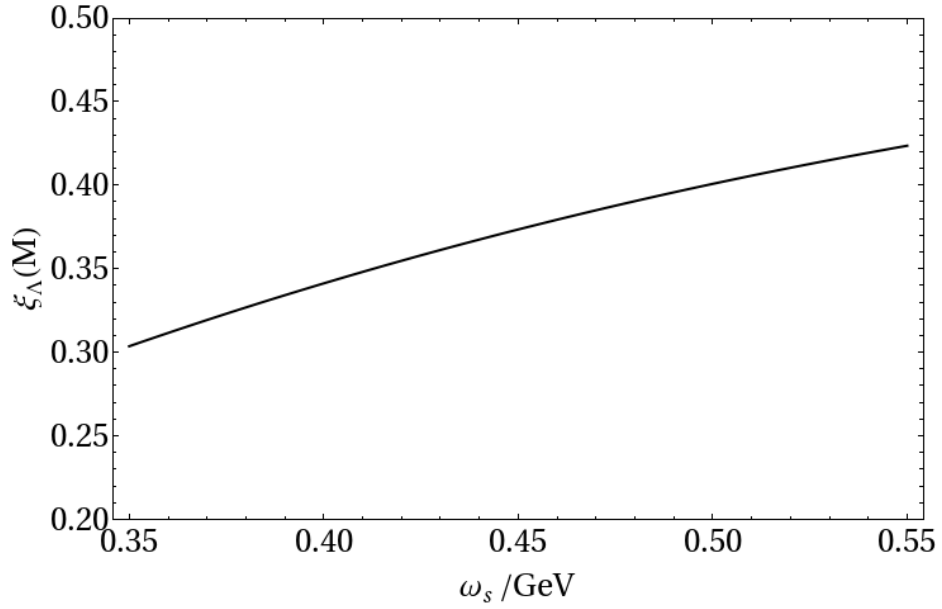


Figure 5.8: Dependence of the soft form factor on the threshold parameter at maximal recoil,  $n_+ p' = M_{\Lambda_b}$ .

overestimated by a factor of 2 or higher. However this might not be completely surprising physically, as in the first place one expects the value of  $\omega_0$  to be larger in the baryonic LCDA than in the mesonic equivalent.

- Generally, one observes that the sum-rule result for  $\xi_\Lambda$  is very sensitive to the shape of the LCDA, and the value of  $\omega_0$  in particular. Varying  $\omega_0$  in a reasonable range between 0.2 and 0.5 GeV induces a 50% uncertainty in  $\xi_\Lambda$ . More independent information on that parameter is clearly crucial for a higher-level precision in this kind of sum-rule analysis.
- As graphically revealed in Figure 5.6, for small values of  $\omega_0$ , the energy dependence of the form factor follows an approximate  $1/n_+p'^2$  behaviour, rather than a  $1/n_+p'^3$  behaviour as predicted by (5.9).
- The dependence on the Borel parameter  $\omega_M$  (Figure 5.7) is very weak (less than a few percent) and negligible compared to the other sources of uncertainties.
- The dependence on the threshold parameter  $\omega_s$  (Figure 5.8) is almost linear, so the leading-order sum-rule result depends in an essential way on the exact interpretation and modelling of the continuum contribution to the correlator; a more sophisticated analysis than picking the position of the first excited state may be required. Varying  $\omega_s$  in the range of 0.35 and 0.55 GeV induces a 10 – 20% uncertainty for  $\xi_\Lambda$  at maximal recoil.

Taking these observations at face value, we have to conclude that the normalisation of the  $\Lambda_b \rightarrow \Lambda$  form factors at large recoil still suffers from sizeable uncertainties, most seriously those related to  $\Lambda_b$  LCDAs and the threshold parameter. The energy dependence of the form factor also displays ambiguous behaviour, varying between  $\xi_\Lambda \sim 1/n_+p'^2$  to  $1/n_+p'^3$  depending on the size of LCDA parameter  $\omega_0$ . Independent study and verification of heavy-baryon LCDAs, in particular  $\psi_4(\omega)$ , would clearly be hugely useful for our current approach, as would further study on the lattice of  $\Lambda_b \rightarrow \Lambda$  form factors at intermediate momentum transfer (see Section 6.2).

### 5.3.2 Form-Factor Ratios

Beyond leading order the symmetry relations between the individual  $\Lambda_b \rightarrow \Lambda$  form factors receive perturbative and non-perturbative corrections. Staying in the large-recoil region, we turn our focus on the corrections springing from the exchange of one hard-collinear gluon, contained in the function  $\Delta\xi_\Lambda$  from (5.21). Using the same default numerical values of the hadronic inputs in Table 5.1 as before,  $\Delta\xi_\Lambda$  is estimated to be

$$\Delta\xi_\Lambda(n_+p' = M_{\Lambda_b}) \simeq -0.003 \quad \text{with} \quad \frac{\Delta\xi_\Lambda}{\xi_\Lambda} \simeq -0.8\%.$$

Note that for convenience the strong coupling constant has been fixed to  $\alpha_s \simeq 0.3$ , which corresponds nicely to a hard-collinear energy scale of  $\mu = 2 \text{ GeV}$ .

The ratio  $\Delta\xi_\Lambda/\xi_\Lambda$  is found to exhibit a mild linear dependence on the large recoil energy and a pronounced linear dependence on the LCDA parameter  $\omega_0$ , as seen in Figures 5.9 and 5.10. This is in qualitative agreement with the considerations after (5.22).

The dependence of  $\Delta\xi_\Lambda$  at maximal recoil on the sum-rule parameters is plotted in Figure 5.11. In comparison with  $\xi_\Lambda$ , the sensitivity of  $\Delta\xi_\Lambda$  to the Borel parameter  $\omega_M$  is similarly weak, while the dependence on the threshold parameter  $\omega_s$  is somewhat weaker. Due to the different systematics in (5.8) and (5.21) pertaining to the modelling of the continuum and the pollution from other hadronic resonances, the dependence of the ratio  $\Delta\xi_\Lambda/\xi_\Lambda$  on the sum-rule parameters is not straightforward to estimate numerically; however, as already pointed out, to one's delight both light and heavy baryonic decay constants do not feature in the expression. The overall dependence on the renormalisation scale used for the strong coupling constant has to be resolved by calculating higher-order radiative corrections to  $\Delta\xi_\Lambda$  in SCET.

Our result for the hard-collinear gluon-exchange correction  $\Delta\xi_\Lambda/\xi_\Lambda$  can be utilised to predict, in particular, ratios of individual form factors, which appear in physical decay observables. To illustrate this, using the definitions in the helicity-based

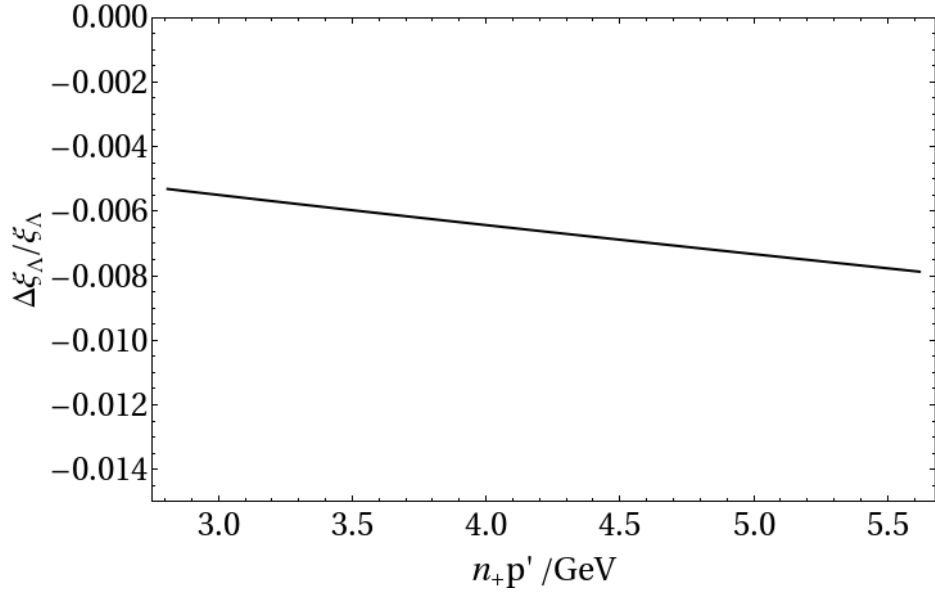


Figure 5.9: Energy dependence of the form-factor correction  $\Delta\xi_\Lambda/\xi_\Lambda$  from the exchange of one hard-collinear gluon estimated from leading-order SCET sum rules (5.8) and (5.21).

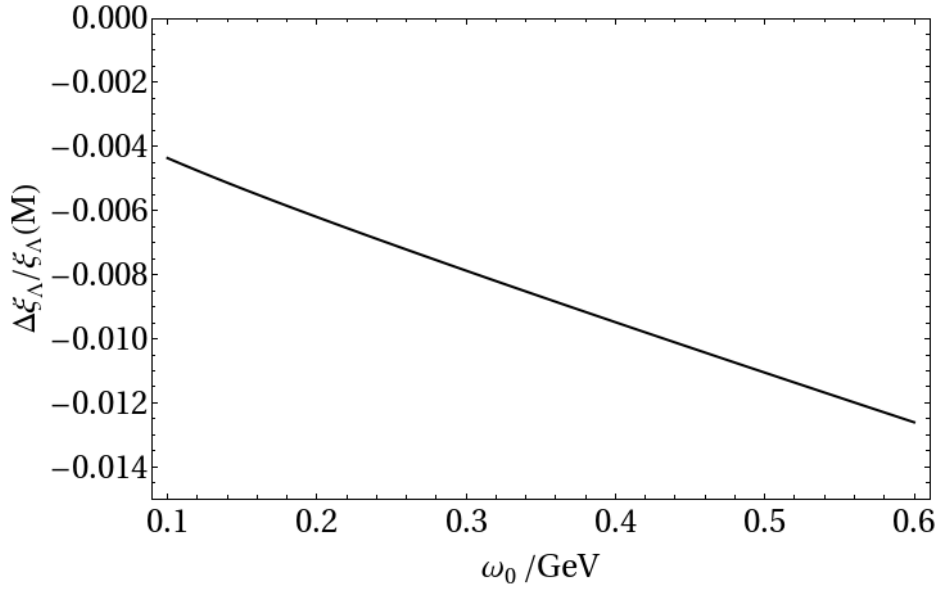


Figure 5.10: Dependence of  $\Delta\xi_\Lambda/\xi_\Lambda$  on the parameter  $\omega_0$  which characterises the  $\Lambda_b$  LCDA, at maximal recoil.

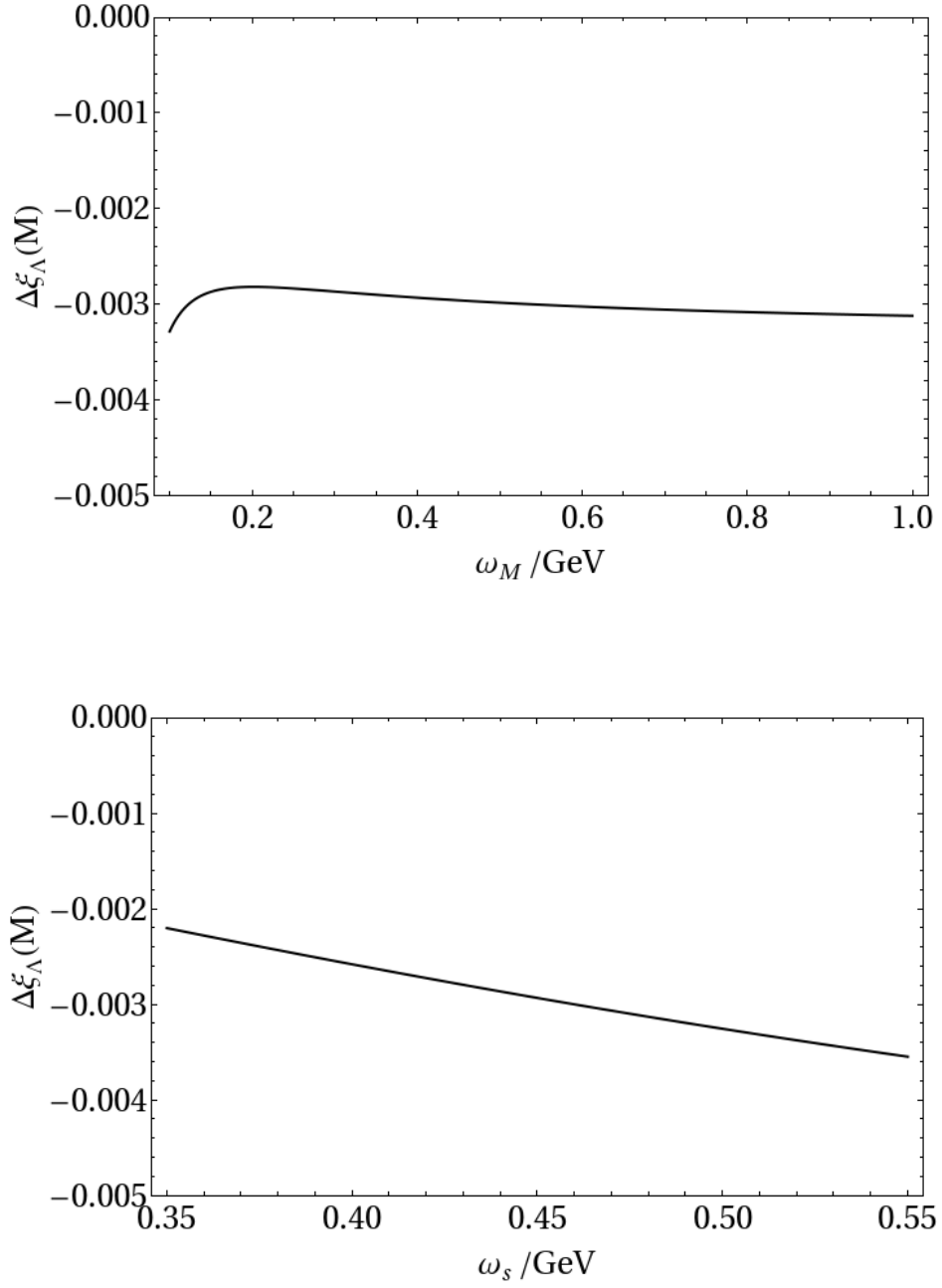


Figure 5.11: Dependence of  $\Delta\xi_\Lambda$  on the sum-rule parameters  $\omega_M$  and  $\omega_s$  at maximal recoil.



parametrisation expounded in Section 4.2, we discuss the ratios  $h_{\perp}/f_{\perp}$  and  $\tilde{h}_{\perp}/g_{\perp}$  as examples. These appear in the forward-backward asymmetry observable  $A_{FB}$  for  $\Lambda_b \rightarrow \Lambda \mu^+ \mu^-$ . Including the effect of hard-vertex corrections to  $\mathcal{O}(\alpha_s)$  accuracy (see Appendix C.2) (for which we use  $\alpha_s(m_b) \simeq 0.2$ ), Figure 5.12 is obtained which show the sizes and energy dependences of the two ratios. We observe that the corrections are dominated by the hard-gluon effects in the matching coefficients for the decay currents.

### 5.3.3 $\Lambda_b \rightarrow \Lambda \mu^+ \mu^-$ Observables

The general expressions for the double-differential  $\Lambda_b \rightarrow \Lambda \mu^+ \mu^-$  decay rate (neglecting corrections from “non-factorisable contributions” – see Chapter 6) are summarised in Appendix A. Our estimates for the form factors in the large-recoil region yield branching ratios which are compatible with the central experimental values reported in 2011 by CDF and its 2012 update [73] (and also compatible with an independent theoretical estimate [111]) within theoretical and experimental uncertainties. Yields from very recent results (June 2013) from LHCb [75] are on the low side compared to our estimates (and CDF results as well), but still fall within the same order of magnitude, though we keep in mind the small statistical significance of the data at low  $q^2$  bins and the presence of large theoretical uncertainties in our predictions. Figure 5.13 presents our results, including also data points and errors from both experiments. Note that hard-scattering spectator effects associated with  $\Delta\xi_{\Lambda}$  are sub-leading and so small, given the largeness of hadronic uncertainties, that we have chosen not to plot them in Figure 5.13.

The functions describing the transverse and longitudinal rates and the forward-backward asymmetry simplify considerably in the SCET limit, where all rates are proportional to the universal form factor  $\xi_{\Lambda}(n+p')$ , and when one takes  $m_{\Lambda} \ll M_{\Lambda_b}$ . To first approximation, this is especially auspicious as taking ratios of observables removes all references to the form factor itself, resulting in quantities free of hadronic

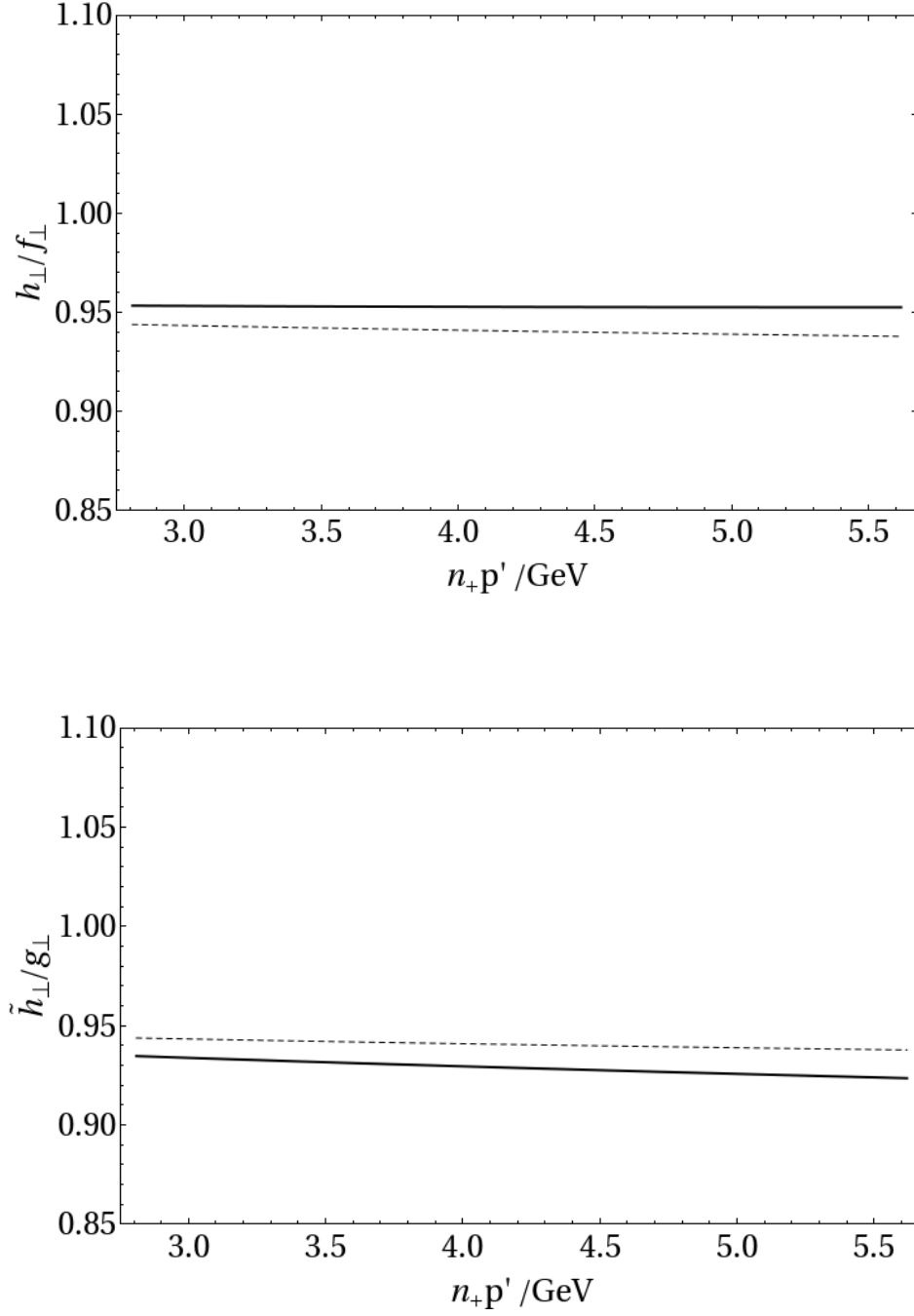


Figure 5.12: Energy dependence of two form-factor ratios, including  $\mathcal{O}(\alpha_s)$  corrections from hard (dashed line) and hard plus hard-collinear (solid line) gluon exchange.

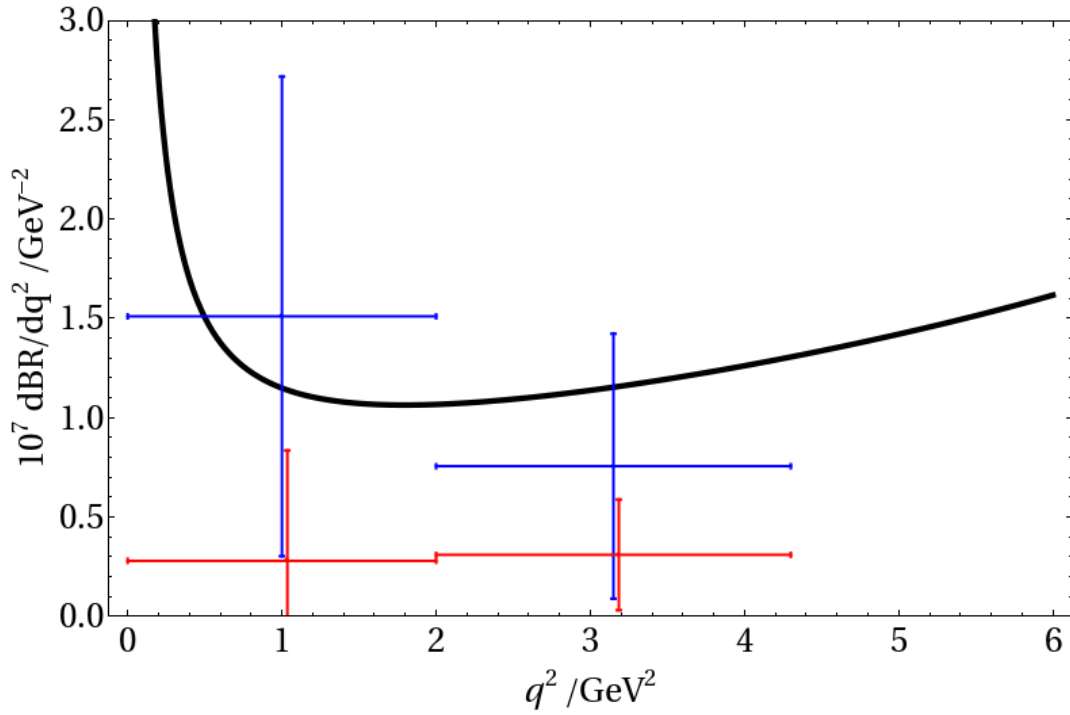


Figure 5.13: Differential branching ratio for  $\Lambda_b \rightarrow \Lambda \mu^+ \mu^-$  as a function of  $q^2$  in the large-recoil region. The theoretical estimate is valid in the SCET limit; data points are taken from CDF [74] (blue) and LHCb [75] (red). (Large) theoretical uncertainties in the theoretical result are omitted. The red vertical error bars are shifted slightly sideways to improve clarity.

form-factor uncertainties. For instance, we have

$$\frac{H_L(q^2)}{H_T(q^2)} \simeq \frac{q^2}{2M_{\Lambda_b}^2} \frac{|M_{\Lambda_b}^2 C_9^{\text{eff}}(q^2) + 2m_b M_{\Lambda_b} C_7^{\text{eff}}|^2 + |M_{\Lambda_b}^2 C_{10}|^2}{|q^2 C_9^{\text{eff}}(q^2) + 2m_b M_{\Lambda_b} C_7^{\text{eff}}|^2 + |q^2 C_{10}|^2}, \quad (5.23)$$

and

$$\frac{H_A(q^2)}{H_T(q^2)} \simeq -\frac{2 \operatorname{Re} [(q^2 C_9^{\text{eff}}(q^2) + 2m_b M_{\Lambda_b} C_7^{\text{eff}})^* q^2 C_{10}]}{|q^2 C_9^{\text{eff}}(q^2) + 2m_b M_{\Lambda_b} C_7^{\text{eff}}|^2 + |q^2 C_{10}|^2}, \quad (5.24)$$

where  $C_7^{\text{eff}}$ ,  $C_9^{\text{eff}}$  and  $C_{10}$  are Wilson coefficients.  $C_7^{\text{eff}}$  and  $C_9^{\text{eff}}$  include effects of universal 1-loop contributions from hadronic 4-quark operators. The leading-order result for the forward-backward asymmetry zero,  $q_0^2$ , can be determined by the same relation between Wilson coefficients,

$$\operatorname{Re} [q^2 C_9^{\text{eff}}(q^2) + 2m_b M_{\Lambda_b} C_7^{\text{eff}}]_{q^2=q_0^2} \simeq 0, \quad (5.25)$$

which is known from the inclusive  $b \rightarrow s \ell^+ \ell^-$  or exclusive  $B \rightarrow K^* \ell^+ \ell^-$  decays (see [112] and references within).

Our numerical estimates for the decay-rate ratios  $H_L/H_T$  and  $H_A/H_T$  as a function of  $q^2$  are shown in Figure 5.14 along with error estimates, and we also compare the SCET limit (5.23,5.24) with the more general result given in (A.4) in Appendix A. Again, we emphasise that information on potentially sizable non-factorisable corrections are not yet available. In the numerical analysis, the Wilson coefficients  $C_{1-7}$  are included to leading-logarithmic accuracy, and  $C_{9,10}$  to next-to-leading logarithmic accuracy, with the numerical values taken from the analysis in [32].

It is apparent from Figure 5.14 that the inclusion of kinematic corrections of order  $m_\Lambda/M_{\Lambda_b}$  together with perturbative corrections to the form-factor relations begets a significant change in the value of  $H_L/H_T$  above  $q^2 \simeq 2 \text{ GeV}^2$ , whereas  $H_A/H_T$  is affected to a much lesser degree. Meanwhile, the shift in the forward-backward asymmetry zero is rather small:

$$q_0^2 = \begin{cases} 3.6 \text{ GeV}^2 & (\text{SCET limit}), \\ 3.4 \text{ GeV}^2 & (\text{incl. corrections}). \end{cases} \quad (5.26)$$

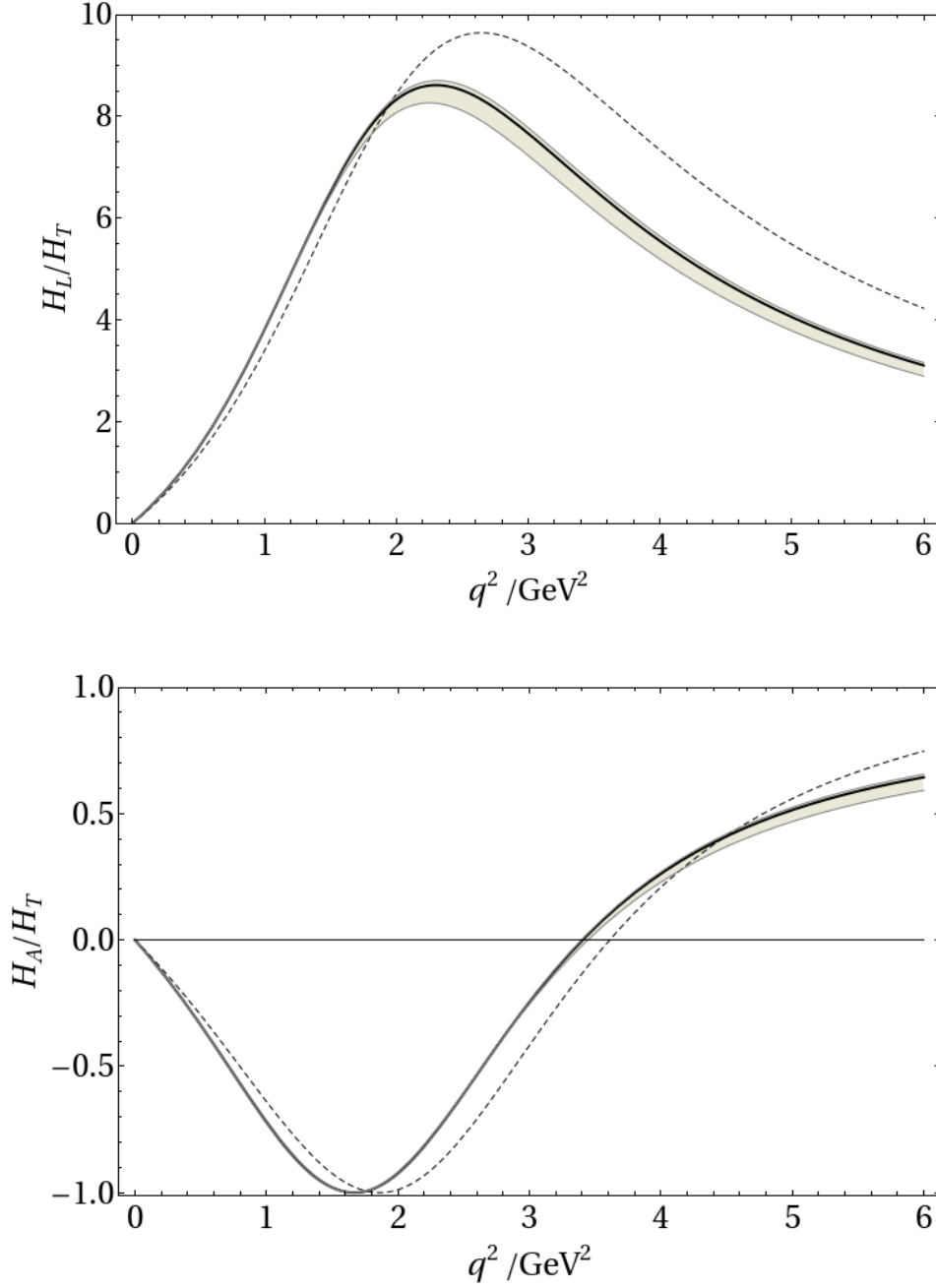


Figure 5.14: Ratios of observables  $H_L/H_T$  and  $H_A/H_T$  as a function of  $q^2$ . Dashed lines indicate the SCET limit (5.23,5.24). Solid lines include the default estimates for the form-factor corrections from hard gluons,  $C_{f_i}$  and hard-collinear gluons,  $\Delta\xi_\Lambda$ , as well as kinematic corrections of order  $m_\Lambda/M_{\Lambda_b}$ . In order to illustrate the (tiny) uncertainty from the variation of  $\Delta\xi_\Lambda/\xi_\Lambda$ , the error has been blown up to an interval of [25%, 400%] of its default value (shaded error band).

Because of the smallness of the imaginary part of the term  $(q^2 C_9^{\text{eff}}(q^2) + 2m_b M_{\Lambda_b} C_7^{\text{eff}})$  in the large-recoil region, the function  $H_A/H_T$  sports a pronounced minimum where  $H_A \simeq -H_T$ . Again, its position is only slightly shifted from  $q^2 \simeq 1.9 \text{ GeV}^2$  to  $1.7 \text{ GeV}^2$  when corrections are added to the SCET limit.

We point out that the function  $\Delta\xi_\Lambda$ , responsible for spectator corrections to the form factors, enters these observables with an additional suppression factor of  $2m_\Lambda/M_{\Lambda_b} \sim 40\%$ , so even if we assign a large uncertainty to the  $\Delta\xi_\Lambda/\xi_\Lambda$ , the ratio observables do not change significantly. Thus we conclude the hard-vertex corrections from the SCET matching coefficients  $C_{f_i}$  and the purely kinematic corrections are responsible for the dominant numerical effects, together with the unspecified uncertainties from non-factorizable and power corrections.

# Chapter 6

## Outlook and Conclusions

### 6.1 “Non-Factorisable” Corrections to $\Lambda_b \rightarrow \Lambda \ell^+ \ell^-$

In the previous chapter, the leading soft form factor  $\xi_\Lambda$  entering symmetry relations at the heavy-quark limit and large-recoil limit of the decay  $\Lambda_b \rightarrow \Lambda \ell^+ \ell^-$  has been calculated. Using just this information at leading order the ratios of individual helicity form factors reduce to unity; this is broken after including the factorisable contribution involving hard-collinear gluon scattering with a spectator quark, and the correction from hard-vertex renormalisation. The effects of these two  $\mathcal{O}(\alpha_s)$  corrections on the 10 form factors are listed in Appendix C.3.

However there are more corrections still at the same order neglected in this work. These are the “non-factorisable” corrections, by which we mean those which involve in an essential way long-distance virtual photons (which then decay into  $\ell^+ \ell^-$ ) with the purely hadronic effective operators, such that the whole non-local matrix element  $\langle \gamma^*(q) \Lambda(p') | \cdots | \Lambda_b(p) \rangle$  cannot be factorised, and the results are not expressible in terms of the usual form factors of the form  $\langle \Lambda | \bar{s} \Gamma b | \Lambda_b \rangle$ . These “non-factorisable” contributions might as well be called “non-form-factor”, and the label should not be confused with that in the QCD factorisation sense.

Specifically these corrections come up in diagrams with insertions of the chro-

momagnetic dipole operators  $O_{8g}$  and the 4-quark operators  $O_{1-6}$ , where one now has to carefully include the photon field with large momentum in the  $n_+$  direction,  $n_- q \sim \mathcal{O}(m_b)$  in the SCET sum-rule calculations. First, there are those vertex corrections which, like the hard-vertex corrections in Appendix C.3, only concern the active-quark line, independent of the spectator quark system and are thus universal to all exclusive  $b \rightarrow s$  transitions. Hence these corrections, in the form of QCD/SCET matching coefficients, can be readily lifted from mesonic calculations like [51, 113, 114]. Figure 6.1 shows the relevant diagrams.

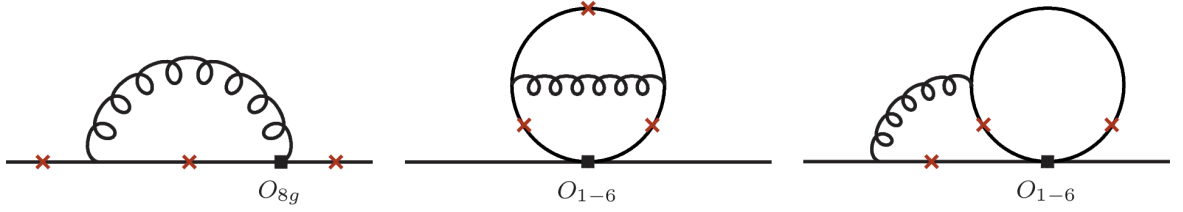


Figure 6.1: Vertex corrections for  $O_8$  and  $O_{1-6}$ . Possible locations of radiative vertices are marked by crosses. The light-quark lines irrelevant to these corrections are omitted. Diagrams related by symmetry are not shown.

These contributions enter as additional terms to the helicity form factors in expressions of observables like those in equations (A.4), and can be subsumed into a modified coefficient function  $C_{9,a}^{\text{eff}}(q^2) \rightarrow C_{9,a}^{\text{eff}}(q^2) + \Delta C_{9,a}^{\text{ver}}(q^2)$ , where  $a = +, \perp$  refers to those functions which appear with the longitudinal and transverse form factors; for form factors defined with  $\gamma_5$ ,  $C_{9,a}^{\text{eff}}(q^2) \rightarrow C_{9,a}^{\text{eff}}(q^2) + \Delta \tilde{C}_{9,a}^{\text{ver}}(q^2)$ , with

$$\Delta \tilde{C}_{9,a}^{\text{ver}}(q^2) = \Delta C_{9,a}^{\text{ver}}(q^2) \Big|_{m_\Lambda \rightarrow -m_\Lambda}.$$

As an example, corrections due to the gluonic penguin  $O_{8g}$  read:

$$\Delta C_{9,+}^{\text{ver}, O_8}(q^2) = -\frac{\alpha_s}{4\pi} C_8^{\text{eff}}(\mu) \left( F_8^{(9)}(\mu, q^2, m_b) + \frac{2m_b}{M_{\Lambda_b} + m_\Lambda} F_8^{(7)}(\mu, q^2, m_b) \right), \quad (6.1)$$

$$\Delta C_{9,\perp}^{\text{ver}, O_8}(q^2) = -\frac{\alpha_s}{4\pi} C_8^{\text{eff}}(\mu) \left( F_8^{(9)}(\mu, q^2, m_b) + \frac{2m_b(M_{\Lambda_b} + m_\Lambda)}{q^2} F_8^{(7)}(\mu, q^2, m_b) \right). \quad (6.2)$$



The leading  $\mathcal{O}(\alpha_s)$  contributions to the functions  $F_8^{(7)}$  and  $F_8^{(9)}$  have been calculated in [114], and the unexpanded analytical form can be found in [32],

$$F_8^{(7)} = -\frac{32}{9} \ln \frac{\mu}{m_b} - \frac{8}{9} \frac{\hat{s}}{1-\hat{s}} \ln \hat{s} - \frac{8}{9} i\pi - \frac{4}{9} \frac{11-16\hat{s}+8\hat{s}^2}{(1-\hat{s})^2} + \frac{4}{9} \frac{1}{(1-\hat{s})^3} \left( (9\hat{s}-5\hat{s}^2+2\hat{s}^3) B_0(\hat{s}) - (4+2\hat{s}) C_0(\hat{s}) \right), \quad (6.3)$$

$$F_8^{(9)} = \frac{16}{9} \frac{1}{1-\hat{s}} \ln \hat{s} + \frac{8}{9} \frac{5-2\hat{s}}{(1-\hat{s})^2} - \frac{8}{9} \frac{4-\hat{s}}{(1-\hat{s})^3} \left( (1+\hat{s}) B_0(\hat{s}) - 2 C_0(\hat{s}) \right), \quad (6.4)$$

where  $\hat{s} = q^2/m_b^2$  and the integral functions are defined as

$$B_0(\hat{s}) = -2\sqrt{4/\hat{s}-1} \arctan \frac{1}{\sqrt{4/\hat{s}-1}},$$

$$C_0(\hat{s}) = \int_0^1 dx \frac{1}{x(1-\hat{s})+1} \ln \frac{x^2}{1-x(1-x)\hat{s}}. \quad (6.5)$$

Analogously the 4-quark operators would contribute  $\Delta\mathcal{C}_{9,+}^{\text{ver}, O_{1-6}}(q^2)$  terms to  $C_{9,a}^{\text{eff}}(q^2)$ .

For completeness we also write down the vertex corrections to form-factor ratios:

$$\Delta\mathcal{C}_{9,+}^{\text{ver,FF}}(q^2) = \frac{\alpha_s C_F}{4\pi} C_7^{\text{eff}}(\mu) \frac{2m_b}{M_{\Lambda_b} + m_\Lambda} \left( \ln \frac{m_b^2}{\mu^2} - 2(1-L) \right), \quad (6.6)$$

$$\Delta\mathcal{C}_{9,\perp}^{\text{ver,FF}}(q^2) = \frac{\alpha_s C_F}{4\pi} C_7^{\text{eff}}(\mu) \frac{2m_b(M_{\Lambda_b} + m_\Lambda)}{q^2} \left( \ln \frac{m_b^2}{\mu^2} - 2 \right), \quad (6.7)$$

where  $L = -\frac{m_b^2 - q^2}{q^2} \ln \left( 1 - \frac{q^2}{m_b^2} \right)$ .

Second, the additional operators lead to contributions arising from hard scattering with one of the spectator quarks (Figure 6.2). The photon vertex can be placed on the active-quark line or the spectator-quark line in the initial or final state. The emission of a hard-collinear photon causes certain internal propagators to go off-shell and be integrated out. A careful power-counting should identify which polarisation of the radiation in which diagram would give the leading effects in this type of correction; analogous calculations like those in [113] already done for the  $B \rightarrow V \ell^+ \ell^-$  case should be a guiding light – whether the baryonic results fall in line with or defy expectations from the older case will be of great interest.

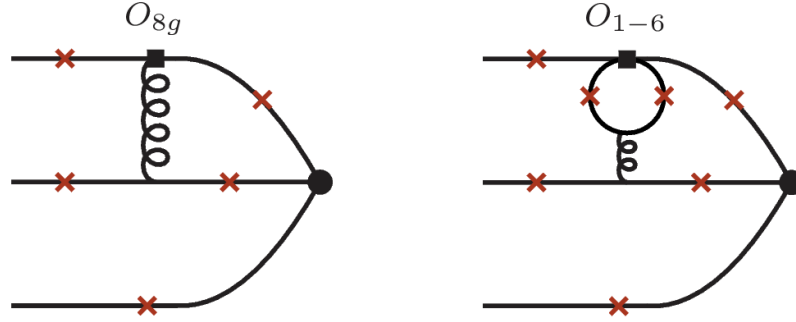


Figure 6.2: Emissions are possible from the heavy-quark line, the strange-quark line, or the light quark before or after hard scattering – and even from the other light quark. For the 4-quark operators, also from the quark loop.

However, there comes a major difference with the mesonic case, considering an energetic photon can be emitted from the light quark not involved in hard-scattering. This scenario is tricky in our current calculational framework as this would leave a diagram with a hard quark entering the final state which is represented by an interpolating current, which exists beyond the usual definitions within SCET sum rules; possibly this can be calculated in QCD factorisation where it can be formally considered factorisable, or other methods.

\* \* \*

In this work we have also overlooked diagrams with annihilation topologies (Figure 6.3). It actually enters the calculations at  $\mathcal{O}(\alpha_s^0)$ , but [113] has shown that for the simpler mesonic case, it is suppressed as only QCD penguin operators with numerically small coefficients are involved, and/or it is Cabibbo-suppressed. The  $\mathcal{O}(\alpha_s)$  corrections are understandably even more negligible. We suspect not dissimilar conclusions for the baryonic case but only an explicit calculation can verify that. Along with this we look forward to future work completing the calculations of non-factorisable corrections, to achieve a more confident set of predictions of observables for  $\Lambda_b \rightarrow \Lambda \ell^+ \ell^-$  (and the related  $\Lambda_b \rightarrow \Lambda \gamma$ ) for comparison with experimental data.

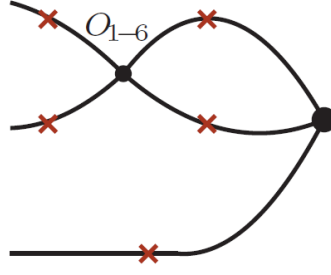


Figure 6.3: The leading annihilation diagram.

## 6.2 Other Calculations on $\Lambda_b \rightarrow \Lambda \ell^+ \ell^-$

Among the more recent results regarding  $\Lambda_b \rightarrow \Lambda \ell^+ \ell^-$  form factors and observables, one that is particularly exciting is the first and so far only calculation [115, 116] of the form factors using Lattice QCD. Lattice QCD [117] has long been a powerful player in providing important non-perturbative phenomenological information, and various collaborations have produced work on flavour physics encompassing mass spectra, decay constants, mixing parameters, decay form factors and more (see e.g. [118] for some recent reviews).

Heavy-to-light decays have been a relatively recent development, requiring a finer lattice due to  $1/m_b$  discretisation effects, while on the other hand it is costly to deal with fast light hadrons if they are involved. Technological advances in terms of theoretical experience and computing power have overcome certain problems to allow, say, semi-leptonic  $B \rightarrow \pi, K^{(*)}$  to be explored by a number of collaborations [119], but results are typically more reliable for the intermediate-recoil region in the calculation of hadronic transition form factors, and large extrapolations are needed to get an estimation of the values in the large-recoil region.

The results of [115] fit reasonably well with the intermediate-to-high  $q^2$  data from LHCb and CDF (though the highest bin falls short), and in the small  $q^2$  region a comparison is not especially meaningful as the lattice predictions have required a large

(model-dependent) extrapolation while the experimental data are quite insignificant in terms of yield. Despite the fact that the results of [115] and ours work in opposite regions of  $q^2$ , it is still useful to see whether the predictions match to ensure everyone is on the right track, speaking in general as well. Besides, in the current absence of any efficient method that can confidently preside over the entire kinematic  $q^2$  range for heavy-to-light decays, different methods could be treated as complementary in the attempt to achieve a combined global dataset, collated from each focussing on their own respective kinematic regions, where systematics are under the best control and usage of various symmetries and mathematical tricks are most reliable.

Elsewhere, lattice-based baryonic studies seem to be focussed on nucleons [120] and, for heavy baryons, mass spectroscopy (see [121] for a review and references within). There is also a very recent paper [122] on  $\Lambda_b \rightarrow p \ell^- \bar{\nu}_\ell$ , a non-FCNC decay good for determination of  $|V_{ub}|$ .

\* \* \*

Outside of the lattice arena, our SCET- and sum-rule-based calculations regarding  $\Lambda_b \rightarrow \Lambda \ell^+ \ell^-$  observables join a long line of investigations into semi-leptonic and radiative  $\Lambda_b \rightarrow \Lambda$  transitions, which began long before  $\Lambda_b \rightarrow \Lambda \mu^+ \mu^-$  was first experimentally observed. As mentioned in Chapter 5, we have found our results are compatible within uncertainty with [106] and [111]. Other sum-rule based approaches include [101, 123, 124].

Others have employed alternative approaches like quark models and Perturbative QCD [68, 69, 125–128] to make Standard-Model predictions of observables like cross sections, various asymmetries and angular observables, often designed to be efficiently sensitive to sources of New Physics, with some making use of polarised  $\Lambda$  and/or  $\Lambda_b$  baryons. But given the disappointing obedience of most new flavour data in sticking to SM predictions, it is not uncommon to contextualise the study of these decays within specific BSM scenarios, for example SM extensions with supersymmetry [129], extra dimensions [130] or four quark generations [131].

Let us end this section by saying we encourage and look forward to more, independent studies of related decays, as such are valuable and important for cross-checks; and we express our hope that our new helicity-based parametrisation scheme for baryonic transition form factors (4.3) will be found helpful in the near future by our experimental and lattice colleagues.

## 6.3 Conclusion

Heavy flavour physics is an indispensable part of the quest to solve the fundamental mysteries of our universe. Theory and Experiment have in the past few decades pushed each other to hone their techniques, on the way accumulating deep experience and expertise in unravelling the flavour jigsaw, decay by decay, observable by observable. The specific focus of this thesis is a theoretical study of the semi-leptonic baryonic  $\Lambda_b \rightarrow \Lambda \ell^+ \ell^-$  decay, a flavour-changing neutral-current process attuned to revealing potential New-Physics effects. The use of baryonic channels is well justified in an age where experimental technology has improved to a level where previously hard-to-detect effects are now measured well enough to provide statistically viable data and insights.

To investigate systematically the form factors entering the  $\Lambda_b \rightarrow \Lambda \ell^+ \ell^-$  transitions, we have used the framework of soft-collinear effective theory (SCET). But first as a starting point, we have proposed an alternative, helicity-based parametrisation of the relevant baryonic form factors, which yield relatively simple expressions for observables like decay widths and asymmetries, and simplify symmetry relations in the limit of heavy  $b$ -quark mass and/or large recoil energy, in the hope of bringing better clarity to calculations and physical understanding.

In the heavy-quark and large-recoil limits, the 10 physical form factors for  $\Lambda_b \rightarrow \Lambda$  transitions reduce to a single universal “soft” function  $\xi_\Lambda$ , which can be defined as

the matrix element of a universal decay current in SCET. In this work,  $\xi_\Lambda$  has been estimated using the technique of light-cone sum rules (LCSR), in which a SCET correlation function involving the decay current and an interpolating current for the light  $\Lambda$  baryon is calculated and analysed both perturbatively and hadronically. In this framework, the heavy  $\Lambda_b$  baryon is represented by its light-cone distribution amplitudes (LCDAs), the study of which is an important, intricate field in particle physics in its own right. Heavy baryonic LCDAs have received relatively little attention in the past, and this work includes a careful derivation and modelling of the momentum-space projection of the possible LCDA terms involved in the SCET sum-rule form-factor calculations. Hence this exercise also provides essential inputs required for other parts of this work.

The energy dependence of the soft form factor resulting from our sum-rule analysis is studied, as is its dependence on the various hadronic and sum-rule parameters entering the expression. These parameters include the characterisation of the shape of the  $\Lambda_b$  LCDAs – for which we have chosen a simple exponential model – and the hadronic spectrum of the  $\Lambda$  contributing to the sum-rule analysis. Our numerical result is consistent within experimental and theoretical uncertainties when compared to the 2011-12 measurement of the  $\Lambda_b \rightarrow \Lambda \mu^+ \mu^-$  rate by CDF at Tevatron. LHC has also very recently released their first data on the same channel with a larger data set (but a small significance in the lower  $q^2$  bins), and our predictions are too within order-of-magnitude consistency. However, our uncertainties are still large, especially with the known unknowns of “non-factorisable” effects – corrections to  $\xi_\Lambda$  that cannot be expressed in terms of hadronic  $\Lambda_b \rightarrow \Lambda$  form factors – and annihilation topologies, signifying the theoretical challenges ahead.

As a phenomenologist, constructing decay observables which are convenient from an experimental point of view is crucial, in order to facilitate precision tests of the Standard Model and searches of New Physics. To first approximation, we have found that the dependence on hadronic form factors drop out of decay asymmetries in the

large-recoil limit. In contrast to analogous mesonic decays, both  $H_L/H_T$  (the ratio of the longitudinal and transverse decay rates) and  $H_A/H_T$  (defining the forward-backward asymmetry zero) are independent of hadronic form factors in the SCET limit.

One of the sources of corrections to  $\xi_\Lambda$  arises from short-distance gluon exchange between the partonic  $b \rightarrow s$  transition and one of the light quarks in the  $\Lambda_b$ ; we have described the leading effect by defining a hadronic matrix element of a sub-leading SCET current. As only one light quark is involved in this hard-scattering process, the other light quark remains truly a spectator in the  $\Lambda_b \rightarrow \Lambda \ell^+ \ell^-$  decay and hence can still populate the kinematic end-point region, where the resulting convolution integrals are not well-defined. In this situation, the QCD factorisation framework cannot be straightforwardly applied, in contrast to analogous semi-leptonic mesonic  $B$  decays.

To calculate the correction term to the leading form factor relevant to this hard-collinear gluon-exchange contribution, we have once more used SCET sum rules to analyse a suitably defined correlation function; expressions for  $\Delta\xi_\Lambda$  are obtained, as are its contributions to individual transition form factors. It is shown that the correction  $\Delta\xi_\Lambda/\xi_\Lambda$  numerically only amounts to a few percent, and so does not affect in a significant way observables like decay asymmetries. We have also included hard-vertex corrections to Wilson coefficients appearing in the matching of QCD and leading SCET currents, and kinematic corrections of order  $m_\Lambda/M_{\Lambda_b}$ .

\* \* \*

As the Standard Model is evidently incomplete at the time of writing, with New Physics lurking somewhere waiting to be unearthed by our particle colliders, B-physics continues to occupy a central position at the leading experimental facilities. More and more previously unavailable channels are thrown open and observables teased out; the results LHCb announced in June 2013 on  $\Lambda_b \rightarrow \Lambda \mu^+ \mu^-$  have only used data

collected in 2011, so one can expect an update in the near future, as the LHC collected data until its scheduled shutdown for repair and upgrade in late 2012. LHCb has also released  $\Lambda_b$  lifetime measurements in July 2013 [132].

The LHC will restart in late 2014 at close to its full design energy, with 7 TeV per beam, and an LHCb upgrade is planned for 2018 during the second long shutdown [133]. All eyes will be on LHCb [134] for hadron-collider B-physics – CDF and D0 at Tevatron which produced so much important work in flavour physics were terminated in 2011 due to an unfortunate lack of funding. On the B-factory front, BaBar at PEP-II SLAC ended in 2008 while Belle at KEKB is still running. A major upgrade of KEKB, called SuperKEKB is already under way, for a new experimental collaboration Belle-II [135]. A brand new high-luminosity B-factory, the SuperB project to be located in Italy, was partially funded for years until hope was tragically squashed at an advanced stage of preparation in late 2012 due to financial constraints [136].<sup>1</sup>

\* \* \*

Clearly, much work is still left to be done in theoretical phenomenology, given the high-luminosity machines we have and hopefully shall have, whose deluge of high-statistics data will require considerable theoretical accuracy in Standard-Model (and BSM) predictions to judge against. (There is also much left to be done for experimentalists.) Despite the rather exasperating lack of unambiguous signs from beyond the Standard Model, there are hints here and there of the great excitements that physicists look forward to in flavour and beyond, and, maybe, a future theory of everything that generations have toiled hard to reach. We hope that this work represents a small step towards achieving that goal.

---

<sup>1</sup>For a discussion of future heavy-flavour-related experimental prospects, see Chapter 2 of [137].



# Appendix A

## Differential Decay Widths for

$$\Lambda_b \rightarrow \Lambda \mu^+ \mu^-$$

This appendix presents more general formulæ for the differential decay widths for radiative  $\Lambda_b \rightarrow \Lambda \mu^+ \mu^-$  transitions (Section 5.3), in terms of the 10 helicity-based form factors defined in Section 4.3. We consider the center-of-mass frame of the lepton pair, and define the angle  $\theta$  between the  $\Lambda_b$  baryon and the positively charged lepton. For simplicity, we consider massless leptons, such that  $q^2 = 2 k_{\ell^+} \cdot k_{\ell^-}$ . We then have

$$p_{\Lambda_b} \cdot k_{\ell^\pm} = \frac{M_{\Lambda_b}^2 - m_\Lambda^2 + q^2 \mp \lambda \cos \theta}{4} \quad \text{and} \quad p_\Lambda \cdot k_{\ell^\pm} = \frac{M_{\Lambda_b}^2 - m_\Lambda^2 - q^2 \mp \lambda \cos \theta}{4}, \quad (\text{A.1})$$

where

$$\lambda \equiv \sqrt{s_+ s_-} = \sqrt{\left((M_{\Lambda_b} + m_\Lambda)^2 - q^2\right) \left((M_{\Lambda_b} - m_\Lambda)^2 - q^2\right)} \quad (\text{A.2})$$

is the phase-space factor. We can define

$$\frac{d^2 \Gamma(\Lambda_b \rightarrow \Lambda \ell^+ \ell^-)}{dq^2 d \cos \theta} \equiv \frac{3}{8} \left\{ (1 + \cos^2 \theta) H_T(q^2) + 2 \cos \theta H_A(q^2) + 2(1 - \cos^2 \theta) H_L(q^2) \right\}, \quad (\text{A.3})$$

and if we neglect non-factorisable corrections, the differential decay rate can be written out in terms of the form factors in the helicity basis:

$$\begin{aligned}
 H_T(q^2) &= \frac{\lambda q^2 n}{96\pi^3 M_{\Lambda_b}^3} \left\{ s_- \left( \left| C_9^{\text{eff}}(q^2) f_\perp + \frac{2m_b (M_{\Lambda_b} + m_\Lambda) C_7^{\text{eff}}}{q^2} h_\perp \right|^2 + |C_{10} f_\perp|^2 \right) \right. \\
 &\quad \left. + s_+ \left( \left| C_9^{\text{eff}}(q^2) g_\perp + \frac{2m_b (M_{\Lambda_b} - m_\Lambda) C_7^{\text{eff}}}{q^2} \tilde{h}_\perp \right|^2 + |C_{10} g_\perp|^2 \right) \right\}, \\
 H_A(q^2) &= -\frac{\lambda^2 q^2 n}{48\pi^3 M_{\Lambda_b}^3} \text{Re} \left[ \left( C_9^{\text{eff}}(q^2) f_\perp + \frac{2m_b (M_{\Lambda_b} + m_\Lambda) C_7^{\text{eff}}}{q^2} h_\perp \right)^* (C_{10} g_\perp) \right. \\
 &\quad \left. + \left( C_9^{\text{eff}}(q^2) g_\perp + \frac{2m_b (M_{\Lambda_b} - m_\Lambda) C_7^{\text{eff}}}{q^2} \tilde{h}_\perp \right)^* (C_{10} f_\perp) \right], \\
 H_L(q^2) &= \frac{\lambda n}{192\pi^3 M_{\Lambda_b}^3} \left\{ s_- (M_{\Lambda_b} + m_\Lambda)^2 \left( \left| C_9^{\text{eff}}(q^2) f_+ + \frac{2m_b C_7^{\text{eff}}}{M_{\Lambda_b} + m_\Lambda} h_+ \right|^2 + |C_{10} f_+|^2 \right) \right. \\
 &\quad \left. + s_+ (M_{\Lambda_b} - m_\Lambda)^2 \left( \left| C_9^{\text{eff}}(q^2) g_+ + \frac{2m_b C_7^{\text{eff}}}{M_{\Lambda_b} - m_\Lambda} \tilde{h}_+ \right|^2 + |C_{10} g_+|^2 \right) \right\}, \tag{A.4}
 \end{aligned}$$

where

$$n = \frac{\alpha_s^2 G_F^2}{8\pi^2} |V_{ts} V_{tb}|^2. \tag{A.5}$$

These functions simplify considerably in the SCET limit  $q^2 \rightarrow 0$ , where

$$\begin{aligned}
 H_T(q^2) &\simeq \frac{\lambda^2 q^2 n}{48\pi^3 M_{\Lambda_b}^3} |\xi_\Lambda(n+p')|^2 \left\{ \left| C_9^{\text{eff}}(q^2) + \frac{2m_b M_{\Lambda_b} C_7^{\text{eff}}}{q^2} \right|^2 + |C_{10}|^2 \right\}, \\
 H_A(q^2) &\simeq -\frac{\lambda^2 q^2 n}{24\pi^3 M_{\Lambda_b}^3} |\xi_\Lambda(n+p')|^2 \text{Re} \left[ \left( C_9^{\text{eff}}(q^2) + \frac{2m_b M_{\Lambda_b} C_7^{\text{eff}}}{q^2} \right)^* C_{10} \right], \\
 H_L(q^2) &\simeq \frac{\lambda^2 n}{96\pi^3 M_{\Lambda_b}^3} |\xi_\Lambda(n+p')|^2 \left\{ \left| C_9^{\text{eff}}(q^2) + \frac{2m_b}{M_{\Lambda_b}} C_7^{\text{eff}} \right|^2 + |C_{10}|^2 \right\}. \tag{A.6}
 \end{aligned}$$

# Appendix B

## Form-Factor Parametrisations

### B.1 Connection to Convention by Chen and Geng

Here we state the relations between our helicity-based parametrisation of  $10 \Lambda_b \rightarrow \Lambda \ell^+ \ell^-$  form factors, and the basis commonly used in recent literature, defined in [106].

$$\begin{aligned} \text{Vector form factors:} \quad f_0 &= f_1 + \frac{q^2}{M_{\Lambda_b} - m_\Lambda} f_3, \\ f_+ &= f_1 - \frac{q^2}{M_{\Lambda_b} + m_\Lambda} f_2, \\ f_\perp &= f_1 - (M_{\Lambda_b} + m_\Lambda) f_2. \end{aligned} \tag{B.1}$$

$$\begin{aligned} \text{Axial-vector form factors:} \quad g_0 &= g_1 - \frac{q^2}{M_{\Lambda_b} + m_\Lambda} g_3, \\ g_+ &= g_1 + \frac{q^2}{M_{\Lambda_b} - m_\Lambda} g_2, \\ g_\perp &= g_1 + (M_{\Lambda_b} - m_\Lambda) g_2. \end{aligned} \tag{B.2}$$

$$\begin{aligned} \text{Tensor form factors:} \quad h_+ &= f_2^T - \frac{M_{\Lambda_b} + m_\Lambda}{q^2} f_1^T, \\ h_\perp &= f_2^T - \frac{1}{M_{\Lambda_b} + m_\Lambda} f_1^T. \end{aligned} \tag{B.3}$$

$$\begin{aligned} \text{Pseudo-tensor form factors:} \quad \tilde{h}_+ &= g_2^T + \frac{M_{\Lambda_b} - m_\Lambda}{q^2} g_1^T, \\ \tilde{h}_\perp &= g_2^T + \frac{1}{M_{\Lambda_b} - m_\Lambda} g_1^T. \end{aligned} \tag{B.4}$$

## B.2 Symmetry-based Form-Factor Parametrisation

Ways to parametrise decay form factors are not unique, and here we set up another alternative parametrisation which considers the different projections of the decay current in the heavy-quark limit ( $m_b \rightarrow 0$ ) and/or large-recoil-energy limit ( $E_\Lambda \rightarrow \infty$ ). On the heavy-quark side, we make use of the heavy-baryon velocity  $v^\mu = p^\mu/M_{\Lambda_b}$  such that  $\not{v} u_{\Lambda_b}(p) = u_{\Lambda_b}(p)$ . We also take into account the projections on the light-quark side (using parity invariance of strong interactions). In this system the general expression for the matrix element of the decay currents is:

$$\langle \Lambda(p', s') | \bar{q} \Gamma b | \Lambda_b(p, s) \rangle = \xi_{ij}^{(\pm)}(v, p') \bar{u}_\Lambda(p', s') \left\{ \Gamma_i \frac{\not{v}_\pm \not{v}_\mp}{4} \Gamma \Gamma_j \right\} u_{\Lambda_b}(p, s). \quad (\text{B.5})$$

Now the basis of Dirac matrices can be chosen as

$$\Gamma_i = \{1, \gamma_5, \gamma_\perp^\alpha\} \quad \text{and} \quad \Gamma_j = \{1, \gamma_5, \vec{\gamma}_\mu, \vec{\gamma}_\mu \gamma_5\}, \quad (\text{B.6})$$

where the standard definitions used are  $\gamma_\perp^\alpha = \gamma^\alpha - \frac{\not{v}_+}{2} n_-^\alpha - \frac{\not{v}_-}{2} n_+^\alpha$ , and  $\vec{\gamma}_\mu = \gamma_\mu - \not{v} v_\mu$ , etc. Here and in the following, we consider a frame where  $v^\mu = (n_-^\mu + n_+^\mu)/2$  and  $\not{v}'_\perp = 0$ . The non-vanishing form factors are:

$$\begin{aligned} \xi_{11}^{(\pm)}(v, p') &\equiv A^{(\pm)}(v \cdot p') \sim \mathcal{O}(1), & \xi_{13}^{(\pm)}(v, p') &\equiv \frac{p'^\mu}{v \cdot p'} B^{(\pm)}(v \cdot p') \sim \mathcal{O}(\epsilon), \\ \xi_{22}^{(\pm)}(v, p') &\equiv C^{(\pm)}(v \cdot p') \sim \mathcal{O}(\epsilon), & \xi_{24}^{(\pm)}(v, p') &\equiv \frac{p'^\mu}{v \cdot p'} D^{(\pm)}(v \cdot p') \sim \mathcal{O}(\epsilon), \\ \xi_{33}^{(\pm)}(v, p') &\equiv \delta_\alpha^\mu E^{(\pm)}(v \cdot p') \sim \mathcal{O}(\epsilon), \\ \xi_{34}^{(\pm)}(v, p') &\equiv i \epsilon_\alpha^{\mu\rho\sigma} \frac{v_\rho p'_\sigma}{v \cdot p'} F^{(\pm)}(v \cdot p') \sim \mathcal{O}(\epsilon). \end{aligned} \quad (\text{B.7})$$

After the equations-of-motion constraints have been taken into account, only 10 out of the 12 form factors above remain independent, as expected. The indicated suppression of the form factors in terms of  $\epsilon = \Lambda_{\text{QCD}}/M$  refers to the violation of the heavy-quark spin symmetry. In addition, in the large-recoil limit, the contributions from the form factors with index  $(-)$  are additionally suppressed. Therefore, we may neglect the 5 form factors  $B^{(-)}$  through  $F^{(-)}$ , which is a good approximation, because:

- In the HQET limit  $v \cdot p' \sim \mathcal{O}(m_\Lambda)$ , their contributions are suppressed by at least a factor of  $\Lambda_{\text{QCD}}/M$ .
- In the SCET limit  $n_+ p' \sim \mathcal{O}(M_{\Lambda_b})$ , their contributions are suppressed by at least a factor of  $(\Lambda_{\text{QCD}}/M)^2$  (for non-factorisable effects) or  $\alpha_s$  (for factorisable effects).

This gives a rather efficient description which simultaneously combines the symmetry constraints in both limits. It also allows one to take into account sub-leading corrections in the large-recoil limit systematically, which are partially calculable in the framework of QCD factorisation or light-cone sum rules. In this approximation, we find that the 10 physical helicity form factors are related by 5 equations (for vanishing light-quark masses,  $m_s \rightarrow 0$ ):

$$\begin{aligned}
f_0 &= \frac{M_{\Lambda_b} + m_\Lambda}{M_{\Lambda_b} - m_\Lambda} \frac{n_+ p' - m_\Lambda}{n_+ p' + m_\Lambda} f_+ + \frac{M_{\Lambda_b} - n_+ p'}{M_{\Lambda_b} - m_\Lambda} \left( g_\perp - \frac{n_+ p' - m_\Lambda}{n_+ p' + m_\Lambda} f_\perp \right), \\
g_0 &= \frac{M_{\Lambda_b} - m_\Lambda}{M_{\Lambda_b} + m_\Lambda} \frac{n_+ p' + m_\Lambda}{n_+ p' - m_\Lambda} g_+ + \frac{M_{\Lambda_b} - n_+ p'}{M_{\Lambda_b} + m_\Lambda} \left( f_\perp - \frac{n_+ p' + m_\Lambda}{n_+ p' - m_\Lambda} g_\perp \right), \\
\tilde{h}_\perp &= \frac{M_{\Lambda_b} + m_\Lambda}{M_{\Lambda_b} - m_\Lambda} \frac{n_+ p' - m_\Lambda}{n_+ p' + m_\Lambda} h_\perp + \frac{M_{\Lambda_b} - n_+ p'}{M_{\Lambda_b} - m_\Lambda} \left( g_\perp - \frac{n_+ p' - m_\Lambda}{n_+ p' + m_\Lambda} f_\perp \right), \quad (\text{B.8})
\end{aligned}$$

and

$$\begin{aligned}
h_+ &= \frac{M_{\Lambda_b} + m_\Lambda}{m_b} f_+ + \frac{n_+ p' - m_\Lambda}{m_b} \left( f_\perp - \frac{n_+ p' + m_\Lambda}{n_+ p' - m_\Lambda} g_\perp \right), \\
\tilde{h}_+ &= \frac{M_{\Lambda_b} - m_\Lambda}{m_b} g_+ + \frac{n_+ p' - m_\Lambda}{m_b} \left( g_\perp - \frac{n_+ p' - m_\Lambda}{n_+ p' + m_\Lambda} f_\perp \right). \quad (\text{B.9})
\end{aligned}$$

# Appendix C

## Corrections to Symmetry Relations

### C.1 HQET Symmetry Relations

Here we write down the relations linking the 10 helicity-based form factors to the 2 in the HQET limit, following from Section 4.3.1:

Vector form factors:

$$\begin{aligned} f_0(q^2) &= A(v \cdot p') + \frac{M_{\Lambda_b} + m_\Lambda - 2v \cdot p'}{M_{\Lambda_b} - m_\Lambda} B(v \cdot p') \approx A(v \cdot p') + B(v \cdot p'), \\ f_+(q^2) &= A(v \cdot p') - \frac{M_{\Lambda_b} - m_\Lambda - 2v \cdot p'}{M_{\Lambda_b} + m_\Lambda} B(v \cdot p') \approx A(v \cdot p') - B(v \cdot p'), \\ f_\perp(q^2) &= A(v \cdot p') - B(v \cdot p'). \end{aligned} \tag{C.1}$$

Axial-vector form factors:

$$\begin{aligned} g_0(q^2) &= A(v \cdot p') - \frac{M_{\Lambda_b} - m_\Lambda - 2v \cdot p'}{M_{\Lambda_b} + m_\Lambda} B(v \cdot p') \approx A(v \cdot p') - B(v \cdot p'), \\ g_+(q^2) &= A(v \cdot p') + \frac{M_{\Lambda_b} + m_\Lambda - 2v \cdot p'}{M_{\Lambda_b} - m_\Lambda} B(v \cdot p') \approx A(v \cdot p') + B(v \cdot p'), \\ g_\perp(q^2) &= A(v \cdot p') + B(v \cdot p'). \end{aligned} \tag{C.2}$$

Tensor form factors:

$$\begin{aligned} h_\perp(q^2) &= A(v \cdot p') - \frac{M_{\Lambda_b} - m_\Lambda - 2v \cdot p'}{M_{\Lambda_b} + m_\Lambda} B(v \cdot p') \approx A(v \cdot p') - B(v \cdot p'), \\ h_+(q^2) &= A(v \cdot p') - B(v \cdot p'). \end{aligned} \tag{C.3}$$

Pseudo-tensor form factors:

$$\begin{aligned}\tilde{h}_\perp(q^2) &= A(v \cdot p') + \frac{M_{\Lambda_b} + m_\Lambda - 2v \cdot p'}{M_{\Lambda_b} - m_\Lambda} B(v \cdot p') \approx A(v \cdot p') + B(v \cdot p'), \\ \tilde{h}_+(q^2) &= A(v \cdot p') + B(v \cdot p').\end{aligned}\tag{C.4}$$

## C.2 Hard-Vertex Corrections to SCET Symmetry Relations

The hard-vertex corrections to the individual QCD decay currents have been discussed before [37, 51]. Starting from the general 1-loop result in equation (28) of [51], we can deduce the  $\mathcal{O}(\alpha_s)$  corrections to the individual helicity form factors  $f_i = C_{f_i} \xi_\Lambda + \dots$  for  $\Lambda_b \rightarrow \Lambda \ell^+ \ell^-$ , as these corrections concern only the active-quark line, independent of the spectator system.

If we set

$$C_{f_+} = C_{g_+} \equiv 1,$$

(equivalent to choosing a renormalisation scheme), this leads to

$$\begin{aligned}C_{f_0} = C_{g_0} &= 1 + \frac{\alpha_s C_F}{4\pi} 2(1 - L), \\ C_{f_\perp} = C_{g_\perp} &= 1 + \frac{\alpha_s C_F}{4\pi} L, \\ C_{h_+} = C_{\tilde{h}_+} &= 1 + \frac{\alpha_s C_F}{4\pi} \left( \ln \frac{m_b^2}{\mu^2} - 2(1 - L) \right), \\ C_{h_\perp} = C_{\tilde{h}_\perp} &= 1 + \frac{\alpha_s C_F}{4\pi} \left( \ln \frac{m_b^2}{\mu^2} - 2 \right),\end{aligned}\tag{C.5}$$

where

$$L \equiv -\frac{m_b^2 - q^2}{q^2} \ln \left( 1 - \frac{q^2}{m_b^2} \right).$$

### C.3 Hard-Collinear Gluon Exchange

We consider the tree-level matching (in light-cone gauge), following [51]:

$$\bar{q} \Gamma Q_v \simeq \bar{\xi} \tilde{\Gamma} h_v - \frac{1}{n_+ p'} \bar{\xi} g_s \not{A}_\perp \frac{\not{p}_+}{2} \Gamma h_v - \frac{1}{m_b} \bar{\xi} \Gamma \frac{\not{p}_-}{2} g_s \not{A}_\perp h_v + \dots \quad (\text{C.6})$$

The hard-scattering contributions to the individual helicity-based form factors in the large-recoil limit can then be identified by means of (4.69) and setting  $m_\Lambda \rightarrow 0$  and  $M_{\Lambda_b} \rightarrow m_b \equiv M$ . This is equivalent to using

$$A^{(-)} \simeq -\frac{2M}{m_\Lambda} \Delta \xi_\Lambda \quad \text{and} \quad E^{(+)} = F^{(+)} = \frac{1}{2} \Delta \xi_\Lambda \quad (\text{C.7})$$

in (B.5). The final results including both hard-scattering and hard-vertex corrections read as follows, with  $C_i = C_i(\mu, n_+ p')$  denoting the hard-vertex coefficients:

Vector form factors:

$$\begin{aligned} f_0(q^2) &\simeq C_{f_0} \xi_\Lambda(n_+ p') - \frac{2M}{n_+ p'} \Delta \xi_\Lambda(n_+ p'), \\ f_+(q^2) &\simeq C_{f_+} \xi_\Lambda(n_+ p') - 2 \left( 2 - \frac{M}{n_+ p'} \right) \Delta \xi_\Lambda(n_+ p'), \\ f_\perp(q^2) &\simeq C_{f_\perp} \xi_\Lambda(n_+ p') + \frac{2M}{n_+ p'} \Delta \xi_\Lambda(n_+ p'). \end{aligned} \quad (\text{C.8})$$

Axial-vector form factors:

$$\begin{aligned} g_0(q^2) &\simeq C_{g_0} \xi_\Lambda(n_+ p') + \frac{2M}{n_+ p'} \Delta \xi_\Lambda(n_+ p'), \\ g_+(q^2) &\simeq C_{g_+} \xi_\Lambda(n_+ p') + 2 \left( 2 - \frac{M}{n_+ p'} \right) \Delta \xi_\Lambda(n_+ p'), \\ g_\perp(q^2) &\simeq C_{g_\perp} \xi_\Lambda(n_+ p') - \frac{2M}{n_+ p'} \Delta \xi_\Lambda(n_+ p'). \end{aligned} \quad (\text{C.9})$$

Tensor form factors:

$$\begin{aligned} h_+(q^2) &\simeq C_{h_+} \xi_\Lambda(n_+ p') + \frac{2M}{n_+ p'} \Delta \xi_\Lambda(n_+ p'), \\ h_\perp(q^2) &\simeq C_{h_\perp} \xi_\Lambda(n_+ p') - 2 \left( 1 - \frac{M}{n_+ p'} \right) \Delta \xi_\Lambda(n_+ p'). \end{aligned} \quad (\text{C.10})$$

Pseudo-tensor form factors:

$$\begin{aligned} \tilde{h}_+(q^2) &\simeq C_{\tilde{h}_+} \xi_\Lambda(n_+ p') - \frac{2M}{n_+ p'} \Delta \xi_\Lambda(n_+ p'), \\ \tilde{h}_\perp(q^2) &\simeq C_{\tilde{h}_\perp} \xi_\Lambda(n_+ p') + 2 \left( 1 - \frac{M}{n_+ p'} \right) \Delta \xi_\Lambda(n_+ p'). \end{aligned} \quad (\text{C.11})$$



# Bibliography

- [1] Th. Feldmann and M. W. Y. Yip, “Form Factors for  $\Lambda_b \rightarrow \Lambda$  Transitions in SCET” Phys. Rev. D **85**, 014035 (2012) [Erratum-ibid. D **86**, 079901 (2012)] [arXiv:hep-ph/1111.1844].
  
- [2] G. Bell, Th. Feldmann, Y.-M. Wang and M. W. Y. Yip, “Light-Cone Distribution Amplitudes for Heavy-Quark Hadrons,” (To be submitted to JHEP – 2013)
  
- [3] The author has during the course of his study benefitted from a range of useful textbooks and didactic materials, on topics from quantum field theory and flavour physics, to CP violation and more. Here is a non-exhaustive selection which do not feature elsewhere in this bibliography:
  - M. E. Peskin and D. V. Schroeder, “An Introduction to Quantum Field Theory,” Westview Press (1995).
  - D. Green, “Lectures in Particle Physics,” (World Scientific Lecture Notes in Physics Vol. 55), World Scientific Publishing (1994).
  - C. T. H. Davies and S. M. Playfer (ed.), “Heavy Flavour Physics” (Scottish Graduate Textbook Series), SUSSP Publications and Institute of Physics Publishing (2002).
  - H. R. Quinn, “Heavy flavor physics,” SLAC-PUB-9551.
  - M. Neubert, “Effective field theory and heavy quark physics,” [arXiv:hep-ph/0512222].
  - Lecture notes by Patricia Ball, Thorsten Feldmann, David Tong, etc.
  
- [4] G. Aad *et al.* [ATLAS Collaboration], “Observation of a new particle in the search for the Standard Model Higgs boson with the ATLAS detector at the LHC,” Phys. Lett. B **716**, 1 (2012) [arXiv:hep-ex/1207.7214].
  - S. Chatrchyan *et al.* [CMS Collaboration], “Observation of a new boson at a mass of 125 GeV with the CMS experiment at the LHC,” Phys. Lett. B **716**, 30 (2012) [arXiv:hep-ex/1207.7235].

- [5] N. Cabibbo, “Unitary Symmetry and Leptonic Decays,” *Phys. Rev. Lett.* **10**, 531 (1963).  
M. Kobayashi and T. Maskawa, “CP Violation in the Renormalizable Theory of Weak Interaction,” *Prog. Theor. Phys.* **49**, 652 (1973).
- [6] S. L. Glashow, J. Iliopoulos and L. Maiani, “Weak Interactions with Lepton-Hadron Symmetry,” *Phys. Rev. D* **2**, 1285 (1970).
- [7] G. C. Branco, L. Lavoura and J. P. Silva, “CP Violation”, (International Series of Monographs on Physics 103), Oxford University Press (1999).
- [8] CKMfitter Group (J. Charles *et al.*), *Eur. Phys. J. C* **41**, 1-131 (2005) [hep-ph/0406184], updated results and plots available at: <http://ckmfitter.in2p3.fr>
- [9] L. Wolfenstein, “Parametrization of the Kobayashi-Maskawa Matrix,” *Phys. Rev. Lett.* **51**, 1945 (1983).
- [10] J. H. Christenson, J. W. Cronin, V. L. Fitch and R. Turlay, “Evidence for the  $2\pi$  Decay of the  $K_2^0$  Meson,” *Phys. Rev. Lett.* **13**, 138 (1964).
- [11] A. D. Sakharov, “Violation of CP Invariance, C Asymmetry, and Baryon Asymmetry of the Universe,” *Pisma Zh. Eksp. Teor. Fiz.* **5**, 32 (1967) [*JETP Lett.* **5**, 24 (1967)] [*Sov. Phys. Usp.* **34**, 392 (1991)] [*Usp. Fiz. Nauk* **161**, 61 (1991)].
- [12] R. Kowalewski and T. Mannel, “Determination of  $V_{cb}$  and  $V_{ub}$ ” review, part of J. Beringer *et al.* (Particle Data Group), *Phys. Rev. D* **86**, 010001 (2012).
- [13] A. Abashian, K. Gotow, N. Morgan, L. Piilonen, S. Schrenk, K. Abe, I. Adachi and J. P. Alexander *et al.*, “The Belle Detector,” *Nucl. Instrum. Meth. A* **479**, 117 (2002).
- [14] B. Aubert *et al.* [BaBar Collaboration], “The BaBar detector,” *Nucl. Instrum. Meth. A* **479**, 1 (2002) [arXiv:hep-ex/0105044].
- [15] B. Aubert *et al.* [BaBar Collaboration], “Observation of CP violation in the  $B^0$  meson system,” *Phys. Rev. Lett.* **87**, 091801 (2001) [arXiv:hep-ex/0107013].  
K. Abe *et al.* [Belle Collaboration], “Observation of large CP violation in the neutral  $B$  meson system,” *Phys. Rev. Lett.* **87**, 091802 (2001) [arXiv:hep-ex/0107061].
- [16] A. A. Alves, Jr. *et al.* [LHCb Collaboration], “The LHCb Detector at the LHC,” *JINST* **3**, S08005 (2008).
- [17] R. Covarelli *et al.* [ATLAS Collaboration], “Measurement of Heavy-Flavor Properties at CMS and ATLAS,” [arXiv:hep-ex/1306.0790].

- C. Mironov [CMS Collaboration], “Overview of results on heavy flavour and quarkonia from the CMS Collaboration,” Nucl. Phys. A **904-905**, 194c (2013).
- C. Melachrinou [ATLAS Collaboration], “Production and spectroscopy of heavy flavor and quarkonia with the ATLAS detector,” PoS ConfinementX , 346 (2012).
- [18] V. M. Abazov *et al.* [D0 Collaboration], “Measurement of the anomalous like-sign dimuon charge asymmetry with  $9\text{ fb}^{-1}$  of  $p\bar{p}$  collisions,” Phys. Rev. D **84**, 052007 (2011) [arXiv:hep-ex/1106.6308].
- V. M. Abazov *et al.* [D0 Collaboration], “Evidence for an anomalous like-sign dimuon charge asymmetry,” Phys. Rev. Lett. **105**, 081801 (2010) [arXiv:hep-ex/1007.0395].
- [19] R. Aaij *et al.* [LHCb Collaboration], “Evidence for CP violation in time-integrated  $D^0 \rightarrow h^- h^+$  decay rates,” Phys. Rev. Lett. **108**, 111602 (2012) [arXiv:hep-ex/1112.0938].
- T. Aaltonen *et al.* [CDF Collaboration], “Measurement of the difference of CP-violating asymmetries in  $D^0 \rightarrow K^+ K^-$  and  $D^0 \rightarrow \pi^+ \pi^-$  decays at CDF,” Phys. Rev. Lett. **109**, 111801 (2012) [arXiv:hep-ex/1207.2158].
- B. R. Ko [Belle Collaboration], “Direct CP violation in charm at Belle,” [arXiv:hep-ex/1212.1975].
- R. Aaij *et al.* [LHCb Collaboration], “Search for direct CP violation in  $D^0 \rightarrow h^- h^+$  modes using semileptonic  $B$  decays,” Phys. Lett. B **723**, 33 (2013) [arXiv:hep-ex/1303.2614].
- [20] W. Altmannshofer, P. Ball, A. Bharucha, A. J. Buras, D. M. Straub and M. Wick, “Symmetries and Asymmetries of  $B \rightarrow K^* \mu^+ \mu^-$  Decays in the Standard Model and Beyond,” JHEP **0901**, 019 (2009) [arXiv:hep-ph/0811.1214].
- [21] R. Aaij *et al.* [LHCb Collaboration], “Differential branching fraction and angular analysis of the decay  $B^0 \rightarrow K^{*0} \mu^+ \mu^-$ ,” Phys. Rev. Lett. **108**, 181806 (2012) [arXiv:hep-ex/1112.3515].
- J. -T. Wei *et al.* [BELLE Collaboration], “Measurement of the Differential Branching Fraction and Forward-Backward Asymmetry for  $B \rightarrow K^{(*)} \ell^+ \ell^-$ ,” Phys. Rev. Lett. **103**, 171801 (2009) [arXiv:hep-ex/0904.0770].
- J. P. Lees *et al.* [BaBar Collaboration], “Measurement of Branching Fractions and Rate Asymmetries in the Rare Decays  $B \rightarrow K^{(*)} \ell^+ \ell^-$ ,” Phys. Rev. D **86**, 032012 (2012) [arXiv:hep-ex/1204.3933].
- J. L. Ritchie [BaBar Collaboration], “Angular Analysis of  $B \rightarrow K^* \ell^+ \ell^-$  in BABAR,” [arXiv:hep-ex/1301.1700].
- T. Aaltonen *et al.* [CDF Collaboration], “Measurement of the Forward-Backward Asymmetry in the  $B \rightarrow K^{(*)} \mu^+ \mu^-$  Decay and First Observation of the  $B_s^0 \rightarrow \phi \mu^+ \mu^-$  Decay,” Phys. Rev. Lett. **106**, 161801 (2011) [arXiv:hep-ex/1101.1028].

- [22] Y. Amhis *et al.* [Heavy Flavor Averaging Group Collaboration], “Averages of B-Hadron, C-Hadron, and tau-lepton properties as of early 2012,” [arXiv:hep-ex/1207.1158].  
Updates available at <http://www.slac.stanford.edu/xorg/hfag>
- [23] R. Aaij *et al.* [LHCb Collaboration], “First Evidence for the Decay  $B_s^0 \rightarrow \mu^+ \mu^-$ ,” Phys. Rev. Lett. **110**, 021801 (2013) [arXiv:hep-ex/1211.2674].
- [24] F. Beaujean, C. Bobeth, D. van Dyk and C. Wacker, “Bayesian Fit of Exclusive  $b \rightarrow s \bar{\ell} \ell$  Decays: The Standard Model Operator Basis,” JHEP **1208**, 030 (2012) [arXiv:hep-ph/1205.1838].
- [25] S. P. Martin, “A Supersymmetry primer,” in Kane, G. L. (ed.): “Perspectives on supersymmetry II” 1-153 [arXiv:hep-ph/9709356].
- [26] G. D’Ambrosio, G. F. Giudice, G. Isidori and A. Strumia, “Minimal flavor violation: An Effective field theory approach,” Nucl. Phys. B **645**, 155 (2002) [arXiv:hep-ph/0207036].
- [27] A. J. Buras, “Weak Hamiltonian, CP violation and rare decays,” [arXiv:hep-ph/9806471].
- [28] G. Buchalla, A. J. Buras and M. E. Lautenbacher, “Weak decays beyond leading logarithms,” Rev. Mod. Phys. **68**, 1125 (1996) [arXiv:hep-ph/9512380].
- [29] K. G. Wilson, “Non-Lagrangian Models of Current Algebra,” Phys. Rev. **179**, 1499-1512 (1969).
- [30] J. C. Collins, “Renormalization,” (Cambridge Monographs on Mathematical Physics), Cambridge University Press (1984).
- [31] K. G. Chetyrkin, M. Misiak and M. Münz, “Weak radiative  $B$  meson decay beyond leading logarithms,” Phys. Lett. B **400**, 206 (1997) [Erratum-ibid. B **425**, 414 (1998)] [arXiv:hep-ph/9612313].
- [32] M. Beneke, Th. Feldmann, D. Seidel, “Exclusive radiative and electroweak  $b \rightarrow d$  and  $b \rightarrow s$  penguin decays at NLO,” Eur. Phys. J. **C41** (2005) 173-188. [arXiv:hep-ph/0412400].
- [33] M. Neubert, “Heavy quark symmetry,” Phys. Rept. **245**, 259 (1994) [arXiv:hep-ph/9306320].
- [34] H. Georgi, “An Effective Field Theory For Heavy Quarks At Low-energies,” Phys. Lett. B **240**, 447 (1990).
- [35] A. V. Manohar and M. B. Wise, “Heavy Quark Physics,” (Cambridge Monographs on Particle Physics, Nuclear Physics and Cosmology 10), Cambridge University Press (2000).

- [36] N. Isgur and M. B. Wise, “Weak Decays of Heavy Mesons in the Static Quark Approximation,” *Phys. Lett. B* **232**, 113 (1989).
- [37] C. W. Bauer, S. Fleming, D. Pirjol and I. W. Stewart, “An Effective field theory for collinear and soft gluons: Heavy to light decays,” *Phys. Rev. D* **63**, 114020 (2001) [arXiv:hep-ph/0011336].
- [38] C. W. Bauer, S. Fleming and M. E. Luke, “Summing Sudakov logarithms in  $B \rightarrow X(s\gamma)$  in effective field theory,” *Phys. Rev. D* **63**, 014006 (2000) [arXiv:hep-ph/0005275].  
C. W. Bauer, O. Catà and G. Ovanessian, “On different ways to quantize Soft-Collinear Effective Theory,” [arXiv:hep-ph/0809.1099].  
C. W. Bauer, D. Pirjol and I. W. Stewart, “Soft collinear factorization in effective field theory,” *Phys. Rev. D* **65**, 054022 (2002) [arXiv:hep-ph/0109045].
- [39] M. J. Dugan and B. Grinstein, “QCD basis for factorization in decays of heavy mesons,” *Phys. Lett. B* **255**, 583 (1991).
- [40] J. Charles, A. Le Yaouanc, L. Oliver, O. Pene and J. C. Raynal, “Heavy to light form-factors in the heavy mass to large energy limit of QCD,” *Phys. Rev. D* **60**, 014001 (1999) [arXiv:hep-ph/9812358].
- [41] M. Beneke, A. P. Chapovsky, M. Diehl and Th. Feldmann, “Soft collinear effective theory and heavy to light currents beyond leading power,” *Nucl. Phys. B* **643**, 431 (2002) [arXiv:hep-ph/0206152].
- [42] M. Beneke and Th. Feldmann, “Multipole expanded soft collinear effective theory with non-Abelian gauge symmetry,” *Phys. Lett. B* **553**, 267 (2003) [arXiv:hep-ph/0211358].
- [43] R. J. Hill and M. Neubert, “Spectator interactions in soft collinear effective theory,” *Nucl. Phys. B* **657**, 229 (2003) [arXiv:hep-ph/0211018].  
T. Becher, R. J. Hill and M. Neubert, “Soft collinear messengers: A New mode in soft collinear effective theory,” *Phys. Rev. D* **69**, 054017 (2004) [arXiv:hep-ph/0308122].
- [44] T. Becher, R. J. Hill, B. O. Lange and M. Neubert, “External operators and anomalous dimensions in soft collinear effective theory,” *Phys. Rev. D* **69**, 034013 (2004) [arXiv:hep-ph/0309227].
- [45] B. O. Lange and M. Neubert, “Factorization and the soft overlap contribution to heavy to light form-factors,” *Nucl. Phys. B* **690**, 249 (2004) [Erratum-ibid. *B* **723**, 201 (2005)] [arXiv:hep-ph/0311345].

- B. O. Lange, “Soft-collinear factorization and Sudakov resummation of heavy meson decay amplitudes with effective field theories,” [arXiv:hep-ph/0409277].
- [46] M. Beneke, G. Buchalla, M. Neubert and C. T. Sachrajda, “QCD factorization for  $B \rightarrow \pi\pi$  decays: Strong phases and CP violation in the heavy quark limit,” Phys. Rev. Lett. **83**, 1914 (1999) [arXiv:hep-ph/9905312].
- [47] M. Beneke, G. Buchalla, M. Neubert and C. T. Sachrajda, “QCD factorization for exclusive, nonleptonic  $B$  meson decays: General arguments and the case of heavy light final states,” Nucl. Phys. B **591**, 313 (2000) [arXiv:hep-ph/0006124].
- [48] M. Beneke, G. Buchalla, M. Neubert and C. T. Sachrajda, “QCD factorization in  $B \rightarrow \pi K, \pi\pi$  decays and extraction of Wolfenstein parameters,” Nucl. Phys. B **606**, 245 (2001) [arXiv:hep-ph/0104110].
- [49] S. Descotes-Genon and C. T. Sachrajda, “Sudakov effects in  $B \rightarrow \pi\ell\nu(\ell)$  form-factors,” Nucl. Phys. B **625**, 239 (2002) [arXiv:hep-ph/0109260].
- [50] N. Isgur and M. B. Wise, “Weak Transition Form-factors Between Heavy Mesons,” Phys. Lett. B **237**, 527 (1990).
- [51] M. Beneke and Th. Feldmann, “Symmetry breaking corrections to heavy to light  $B$  meson form-factors at large recoil,” Nucl. Phys. B **592**, 3 (2001) [arXiv:hep-ph/0008255].
- [52] M. Beneke and Th. Feldmann, “Factorization of heavy to light form-factors in soft collinear effective theory,” Nucl. Phys. B **685**, 249 (2004) [arXiv:hep-ph/0311335].
- [53] P. Colangelo and A. Khodjamirian, “QCD sum rules, a modern perspective,” [arXiv:hep-ph/0010175].
- [54] M. A. Shifman, A. I. Vainshtein and V. I. Zakharov, “QCD and Resonance Physics. Sum Rules,” Nucl. Phys. B **147**, 385 (1979).  
M. A. Shifman, A. I. Vainshtein and V. I. Zakharov, “QCD and Resonance Physics: Applications,” Nucl. Phys. B **147**, 448 (1979).
- [55] V. L. Chernyak and I. R. Zhitnitsky, “ $B$  meson exclusive decays into baryons,” Nucl. Phys. B **345**, 137 (1990).
- [56] V. M. Braun and I. E. Filyanov, “QCD Sum Rules in Exclusive Kinematics and Pion Wave Function,” Z. Phys. C **44**, 157 (1989) [Sov. J. Nucl. Phys. **50**, 511 (1989)] [Yad. Fiz. **50**, 818 (1989)].

- [57] I. I. Balitsky, V. M. Braun and A. V. Kolesnichenko, “Radiative Decay  $\Sigma^+ \rightarrow p\gamma$  in Quantum Chromodynamics,” Nucl. Phys. B **312**, 509 (1989).
- [58] V. M. Belyaev, A. Khodjamirian and R. Rückl, “QCD calculation of the  $B \rightarrow \pi, K$  form-factors,” Z. Phys. C **60**, 349 (1993) [arXiv:hep-ph/9305348].
- [59] P. Ball and V. M. Braun, “Exclusive semileptonic and rare  $B$  meson decays in QCD,” Phys. Rev. D **58**, 094016 (1998) [arXiv:hep-ph/9805422].
- [60] P. Ball and R. Zwicky, “ $B(D, S) \rightarrow \rho, \omega, K^*, \phi$  decay form-factors from light-cone sum rules revisited,” Phys. Rev. D **71**, 014029 (2005) [arXiv:hep-ph/0412079].
- [61] A. Khodjamirian, T. Mannel, N. Offen, “Form-factors from light-cone sum rules with  $B$ -meson distribution amplitudes,” Phys. Rev. D **75** (2007) 054013. [arXiv:hep-ph/0611193];
- [62] S. Faller, A. Khodjamirian, C. Klein, T. Mannel, “ $B \rightarrow D^{(*)}$  Form Factors from QCD Light-Cone Sum Rules,” Eur. Phys. J. C **60** (2009) 603-615. [arXiv:hep-ph/0809.0222].
- [63] A. Bharucha, “Two-loop Corrections to the  $B \rightarrow \pi$  Form Factor from QCD Sum Rules on the Light-Cone and  $|V_{ub}|$ ,” JHEP **1205**, 092 (2012) [arXiv:hep-ph/1203.1359].
- [64] P. Ball, “QCD sum rules on the light cone, factorization and SCET,” [arXiv:hep-ph/0308249].
- [65] F. De Fazio, Th. Feldmann, T. Hurth, “Light-cone sum rules in soft-collinear effective theory,” Nucl. Phys. B **733** (2006) 1-30. [arXiv:hep-ph/0504088].
- [66] J. Beringer *et al.* (Particle Data Group), Phys. Rev. D **86**, 010001 (2012). <http://pdg.lbl.gov/>
- [67] T. Mannel, W. Roberts and Z. Ryzak, “Baryons in the heavy quark effective theory,” Nucl. Phys. B **355**, 38 (1991).
- [68] G. Hiller, M. Knecht, F. Legger and T. Schietinger, “Photon polarization from helicity suppression in radiative decays of polarized  $\Lambda_b$  to spin-3/2 baryons,” Phys. Lett. B **649** (2007) 152 [arXiv:hep-ph/0702191].
- [69] G. Hiller and A. Kagan, “Probing for new physics in polarized  $\Lambda_b$  decays at the  $Z$ ,” Phys. Rev. D **65** (2002) 074038 [arXiv:hep-ph/0108074].
- [70] D. Asner *et al.* [Heavy Flavor Averaging Group Collaboration], “Averages of  $b$ -hadron,  $c$ -hadron, and  $\tau$ -lepton Properties,” [arXiv:hep-ex/1010.1589].

- [71] B. Aubert *et al.* [BaBar Collaboration], “Direct CP, Lepton Flavor and Isospin Asymmetries in the Decays  $B \rightarrow K^{(*)}\ell^+\ell^-$ ,” Phys. Rev. Lett. **102**, 091803 (2009) [arXiv:hep-ex/0807.4119].
- [72] J.-T. Wei *et al.* [BELLE Collaboration], “Measurement of the Differential Branching Fraction and Forward-Backward Asymmetry for  $B \rightarrow K^{(*)}\ell^+\ell^-$ ,” Phys. Rev. Lett. **103**, 171801 (2009) [arXiv:hep-ex/0904.0770].
- [73] T. Aaltonen *et al.* [CDF Collaboration], “Observation of the Baryonic Flavor-Changing Neutral Current Decay  $\Lambda_b \rightarrow \Lambda\mu^+\mu^-$ ,” Phys. Rev. Lett. **107**, 201802 (2011) [arXiv:hep-ex/1107.3753];
- [74] S. Behari [CDF Collaboration], “CDF results on  $b \rightarrow s\mu\mu$  decays,” [arXiv:hep-ex/1301.2244].  
“Updated Branching Ratio Measurements of Exclusive  $b \rightarrow s\mu^+\mu^-$  Decays and Angular Analysis in  $B \rightarrow K^{(*)}\mu^+\mu^-$  Decays”, [http://www-cdf.fnal.gov/physics/new/bottom/120628.blessed-b2smumu\\_96/](http://www-cdf.fnal.gov/physics/new/bottom/120628.blessed-b2smumu_96/)
- [75] R. Aaij *et al.* [LHCb Collaboration], “Measurement of the differential branching fraction of the decay  $\Lambda_b^0 \rightarrow \Lambda\mu^+\mu^-$ ,” [arXiv:hep-ex/1306.2577].
- [76] G. P. Lepage and S. J. Brodsky, “Exclusive Processes in Perturbative Quantum Chromodynamics,” Phys. Rev. D **22**, 2157 (1980).  
G. P. Lepage and S. J. Brodsky, “Exclusive Processes in Quantum Chromodynamics: Evolution Equations for Hadronic Wave Functions and the Form-Factors of Mesons,” Phys. Lett. B **87**, 359 (1979).
- [77] V. L. Chernyak and A. R. Zhitnitsky, “Asymptotic Behavior of Hadron Form-Factors in Quark Model,” JETP Lett. **25**, 510 (1977) [Pisma Zh. Eksp. Teor. Fiz. **25**, 544 (1977)].
- [78] V. L. Chernyak and A. R. Zhitnitsky, “Asymptotics of Hadronic Form-Factors in the Quantum Chromodynamics,” Sov. J. Nucl. Phys. **31**, 544 (1980) [Yad. Fiz. **31**, 1053 (1980)].
- [79] V. M. Braun, G. P. Korchemsky and D. Müller, “The Uses of conformal symmetry in QCD,” Prog. Part. Nucl. Phys. **51**, 311 (2003) [arXiv:hep-ph/0306057].
- [80] P. Ball and V. M. Braun, “The  $\rho$  meson light cone distribution amplitudes of leading twist revisited,” Phys. Rev. D **54**, 2182 (1996) [arXiv:hep-ph/9602323].  
P. Ball, “Theoretical update of pseudoscalar meson distribution amplitudes of higher twist: The Nonsinglet case,” JHEP **9901**, 010 (1999) [arXiv:hep-ph/9812375].  
P. Ball, V. M. Braun and A. Lenz, “Higher-twist distribution amplitudes of the  $K$  meson in



- QCD,” JHEP **0605**, 004 (2006) [arXiv:hep-ph/0603063].
- P. Ball, V. M. Braun and A. Lenz, “Twist-4 distribution amplitudes of the  $K^*$  and  $\phi$  mesons in QCD,” JHEP **0708**, 090 (2007) [arXiv:hep-ph/0707.1201].
- [81] P. Ball, V. M. Braun, Y. Koike and K. Tanaka, “Higher twist distribution amplitudes of vector mesons in QCD: Formalism and twist – three distributions,” Nucl. Phys. B **529**, 323 (1998) [arXiv:hep-ph/9802299].
- [82] T. Zhong, X. -G. Wu, J. -W. Zhang, Y. -Q. Tang and Z. -Y. Fang, “New results on Pionic Twist-3 Distribution Amplitudes within the QCD Sum Rules,” Phys. Rev. D **83**, 036002 (2011) [arXiv:hep-ph/1101.3592].
- [83] K. -C. Yang, “Light-cone distribution amplitudes of axial-vector mesons,” Nucl. Phys. B **776**, 187 (2007) [arXiv:hep-ph/0705.0692].
- [84] V. M. Braun, M. Gockeler, R. Horsley, H. Perlt, D. Pleiter, P. E. L. Rakow, G. Schierholz and A. Schiller *et al.*, “Moments of pseudoscalar meson distribution amplitudes from the lattice,” Phys. Rev. D **74**, 074501 (2006) [arXiv:hep-lat/0606012].
- P. A. Boyle *et al.* [UKQCD Collaboration], “A Lattice Computation of the First Moment of the Kaon’s Distribution Amplitude,” Phys. Lett. B **641**, 67 (2006) [arXiv:hep-lat/0607018].
- I. C. Cloët, L. Chang, C. D. Roberts, S. M. Schmidt and P. C. Tandy, “Pion distribution amplitude from lattice-QCD,” [arXiv:nucl-th/1306.2645].
- [85] J. R. Forshaw and R. Sandapen, “Extracting the  $\rho$  meson wavefunction from HERA data,” JHEP **1011**, 037 (2010) [arXiv:hep-ph/1007.1990].
- H. -M. Choi and C. -R. Ji, “Distribution amplitudes and decay constants for  $(\pi, K, \rho, K^*)$  mesons in light-front quark model,” Phys. Rev. D **75**, 034019 (2007) [arXiv:hep-ph/0701177].
- E. Ruiz Arriola and W. Broniowski, “Pion light cone wave function and pion distribution amplitude in the Nambu-Jona-Lasinio model,” Phys. Rev. D **66**, 094016 (2002) [arXiv:hep-ph/0207266].
- [86] V. Braun, R. J. Fries, N. Mahnke and E. Stein, “Higher twist distribution amplitudes of the nucleon in QCD,” Nucl. Phys. B **589**, 381 (2000) [Erratum-ibid. B **607**, 433 (2001)] [arXiv:hep-ph/0007279].
- [87] V. M. Braun, T. Lautenschlager, A. N. Manashov and B. Pirnay, “Higher twist parton distributions from light-cone wave functions,” Phys. Rev. D **83**, 094023 (2011) [arXiv:hep-ph/1103.1269].
- V. L. Chernyak, A. A. Ogloblin and I. R. Zhitnitsky, “On The Nucleon Wave Function,” Sov. J. Nucl. Phys. **48**, 536 (1988) [Yad. Fiz. **48**, 841 (1988)]; “Wave Functions Of Octet

- Baryons,” Z. Phys. C **42**, 569 (1989) [Yad. Fiz. **48**, 1410 (1988)] [Sov. J. Nucl. Phys. **48**, 896 (1988)].
- [88] Y. -L. Liu, M. -Q. Huang, “Distribution amplitudes of  $\Sigma$  and  $\Lambda$  and their electromagnetic form factors,” Nucl. Phys. **A821** (2009) 80-105. [arXiv:hep-ph/0811.1812].
- [89] Y. -L. Liu and M. -Q. Huang, “Light-cone Distribution Amplitudes of  $\Xi$  and their Applications,” Phys. Rev. D **80**, 055015 (2009) [arXiv:hep-ph/0909.0372].
- [90] P. Ball, V. M. Braun and E. Gardi, “Distribution Amplitudes of the  $\Lambda_b$  Baryon in QCD,” Phys. Lett. B **665**, 197 (2008) [arXiv:hep-ph/0804.2424].
- [91] A. G. Grozin and M. Neubert, “Asymptotics of heavy meson form-factors,” Phys. Rev. D **55**, 272 (1997) [arXiv:hep-ph/9607366].
- [92] V. M. Braun, D. Y. Ivanov and G. P. Korchemsky, “The  $B$  meson distribution amplitude in QCD,” Phys. Rev. D **69**, 034014 (2004) [arXiv:hep-ph/0309330].  
H. -N. Li and H. -S. Liao, “ $B$  meson wave function in  $k(T)$  factorization,” Phys. Rev. D **70**, 074030 (2004) [arXiv:hep-ph/0404050].  
H. Kawamura, J. Kodaira, C. -F. Qiao and K. Tanaka, “ $B$  meson light cone distribution amplitudes in the heavy quark limit,” Phys. Lett. B **523**, 111 (2001) [Erratum-ibid. B **536**, 344 (2002)] [arXiv:hep-ph/0109181].
- [93] G. Bell, Th. Feldmann, “Modelling light-cone distribution amplitudes from non-relativistic bound states,” JHEP **0804** (2008) 061. [arXiv:hep-ph/0802.2221].
- [94] B. O. Lange, M. Neubert, “Renormalization group evolution of the  $B$ -meson light-cone distribution amplitude,” Phys. Rev. Lett. **91** (2003) 102001. [arXiv:hep-ph/0303082].
- [95] S. Descotes-Genon, N. Offen, “Three-particle contributions to the renormalisation of  $B$ -meson light-cone distribution amplitudes,” JHEP **0905** (2009) 091. [arXiv:hep-ph/0903.0790].
- [96] S. J. Lee and M. Neubert, “Model-independent properties of the  $B$ -meson distribution amplitude,” Phys. Rev. D **72**, 094028 (2005) [arXiv:hep-ph/0509350].
- [97] M. Knoedlseder, N. Offen, “Renormalisation of heavy-light light-ray operators,” [arXiv:hep-ph/1105.4569].
- [98] W. Loinaz and R. Akhoury, “Exclusive semileptonic decays of  $b$  baryons into protons,” Phys. Rev. D **53**, 1416 (1996) [arXiv:hep-ph/9505378].

- [99] F. Hussain, J. G. Körner, M. Krämer and G. Thompson, “On heavy baryon decay form-factors,” *Z. Phys. C* **51**, 321 (1991).
- [100] A. Ali, C. Hambrock, A. Y. Parkhomenko and W. Wang, “Light-Cone Distribution Amplitudes of the Ground State Bottom Baryons in HQET,” *Eur. Phys. J. C* **73** (2013) 2302 [arXiv:hep-ph/1212.3280].
- [101] Y.-M. Wang, Y. Li and C.-D. Lü, “Rare Decays of  $\Lambda_b \rightarrow \Lambda \gamma$  and  $\Lambda_b \rightarrow \Lambda \ell^+ \ell^-$  in the Light-cone Sum Rules,” *Eur. Phys. J. C* **59** (2009) 861 [arXiv:hep-ph/0804.0648].  
Y. -M. Wang, Y. -L. Shen, C.-D. Lü, “ $\Lambda_b \rightarrow p, \Lambda$  transition form factors from QCD light-cone sum rules,” *Phys. Rev. D* **80** (2009) 074012. [arXiv:hep-ph/0907.4008].
- [102] S. Wandzura and F. Wilczek, “Sum Rules for Spin Dependent Electroproduction: Test of Relativistic Constituent Quarks,” *Phys. Lett. B* **72**, 195 (1977).
- [103] H. Kawamura, J. Kodaira, C. -F. Qiao and K. Tanaka, “ $B$  meson light cone wavefunctions in the heavy quark limit,” *Nucl. Phys. Proc. Suppl.* **116**, 269 (2003) [arXiv:hep-ph/0211270].
- [104] A. Bharucha, Th. Feldmann, M. Wick, “Theoretical and Phenomenological Constraints on Form Factors for Radiative and Semi-Leptonic  $B$ -Meson Decays,” *JHEP* **1009** (2010) 090. [arXiv:hep-ph/1004.3249].
- [105] C. G. Boyd, M. J. Savage, “Analyticity, shapes of semileptonic form-factors, and  $\bar{B} \rightarrow \pi \ell \bar{\nu}$ ,” *Phys. Rev. D* **56** (1997) 303-311. [arXiv:hep-ph/9702300].
- [106] C. H. Chen and C. Q. Geng, “Baryonic rare decays of  $\Lambda_b \rightarrow \Lambda \ell^+ \ell^-$ ,” *Phys. Rev. D* **64** (2001) 074001 [arXiv:hep-ph/0106193].  
C. H. Chen and C. Q. Geng, “Rare  $\Lambda_b \rightarrow \Lambda \ell^+ \ell^+$  decays with polarized  $\Lambda$ ,” *Phys. Rev. D* **63** (2001) 114024 [arXiv:hep-ph/0101171].  
C. H. Chen and C. Q. Geng, “Lepton asymmetries in heavy baryon decays of  $\Lambda_b \rightarrow \Lambda \ell^+ \ell^-$ ,” *Phys. Lett. B* **516** (2001) 327 [arXiv:hep-ph/0101201].  
C. H. Chen, C. Q. Geng and J. N. Ng, “ $T$  violation in  $\Lambda_b \rightarrow \Lambda \ell^+ \ell^-$  decays with polarized  $\Lambda$ ,” *Phys. Rev. D* **65** (2002) 091502 [arXiv:hep-ph/0202103].
- [107] T. Mannel, S. Recksiegel, “Flavor changing neutral current decays of heavy baryons: The Case  $\Lambda_b \rightarrow \Lambda \gamma$ ,” *J. Phys. G* **24** (1998) 979-990. [arXiv:hep-ph/9701399].
- [108] F. De Fazio, Th. Feldmann, T. Hurth, “SCET sum rules for  $B \rightarrow P$  and  $B \rightarrow V$  transition form factors,” *JHEP* **0802** (2008) 031. [arXiv:hep-ph/0711.3999].

- [109] N. Kivel, M. Vanderhaeghen, “Soft spectator scattering in the nucleon form factors at large  $Q^2$  within the SCET approach,” *Phys. Rev.* **D83** (2011) 093005. [arXiv:hep-ph/1010.5314].
- [110] A. Khodjamirian, C. Klein, T. Mannel and Y. M. Wang, “Form Factors and Strong Couplings of Heavy Baryons from QCD Light-Cone Sum Rules,” [arXiv:hep-ph/1108.2971].
- [111] T. M. Aliev, K. Azizi, M. Savci, “Analysis of the  $\Lambda_b \rightarrow \Lambda \ell^+ \ell^-$  decay in QCD,” *Phys. Rev.* **D81** (2010) 056006. [arXiv:hep-ph/1001.0227].  
T. M. Aliev and M. Savci, “Polarization effects in exclusive semileptonic  $\Lambda_b \rightarrow \Lambda \ell^+ \ell^-$  decay,” *JHEP* **0605** (2006) 001 [arXiv:hep-ph/0507324].  
T. M. Aliev, M. Savci and B. B. Sirvanli, “Double-lepton polarization asymmetries in  $\Lambda_b \rightarrow \Lambda \ell^+ \ell^-$  decay in universal extra dimension model,” *Eur. Phys. J. C* **52** (2007) 375 [arXiv:hep-ph/0608143].
- [112] M. Antonelli *et al.*, “Flavor Physics in the Quark Sector,” *Phys. Rept.* **494** 197-414 (2010) [arXiv:hep-ph/0907.5386].
- [113] M. Beneke, Th. Feldmann, D. Seidel, “Systematic approach to exclusive  $B \rightarrow V \ell^+ \ell^-, V \gamma$  decays,” *Nucl. Phys.* **B612** (2001) 25-58. [arXiv:hep-ph/0106067].
- [114] H. H. Asatrian, H. M. Asatrian, C. Greub and M. Walker, “Two loop virtual corrections to  $B \rightarrow X_s \ell^+ \ell^-$  in the standard model,” *Phys. Lett. B* **507**, 162 (2001) [arXiv:hep-ph/0103087].
- [115] W. Detmold, C.-J. D. Lin, S. Meinel and M. Wingate, “ $\Lambda_b \rightarrow \Lambda l^+ l^-$  form factors and differential branching fraction from lattice QCD,” [arXiv:lep-hat/1212.4827].
- [116] W. Detmold, C. -J. D. Lin, S. Meinel and M. Wingate, “Form factors for  $\Lambda_b \rightarrow \Lambda$  transitions from lattice QCD,” *PoS LATTICE* **2012**, 123 (2012) [arXiv:lep-hat/1211.5127].
- [117] R. Gupta, “Introduction to lattice QCD: Course,” [arXiv:hep-lat/9807028].
- [118] E. Gámiz, “Flavour physics from lattice QCD,” *PoS ConfinementX*, 241 (2012) [arXiv:hep-ph/1303.3971].  
C. Tarantino, “Lattice flavor physics with an eye to SuperB,” *PoS LATTICE* **2012**, 012 (2012).  
N. Tantalo, “Lattice flavour physics,” *PoS EPS -HEP2011*, 179 (2011).  
M. Wingate, “Lattice QCD Calculations with  $b$  Quarks: Status and Prospects,” *PoS BEAUTY* **2011**, 057 (2011) [arXiv:hep-ph/1105.4498].
- [119] J. A. Bailey, C. Bernard, C. E. DeTar, M. Di Pierro, A. X. El-Khadra, R. T. Evans, E. D. Freeland and E. Gámiz *et al.*, “The  $B \rightarrow \pi \ell \nu$  semileptonic form factor from three-flavor lattice QCD: A Model-independent determination of  $|V_{ub}|$ ,” *Phys. Rev. D* **79**, 054507 (2009)

- [arXiv:hep-lat/0811.3640].
- Z. Liu, S. Meinel, A. Hart, R. R. Horgan, E. H. Muller and M. Wingate, “A Lattice calculation of  $B \rightarrow K^{(*)}$  form factors,” [arXiv:hep-ph/1101.2726].
- R. Zhou, S. Gottlieb, J. A. Bailey, D. Du, A. X. El-Khadra, R. D. Jain, A. S. Kronfeld and R. S. Van de Water *et al.*, “Form factors for semi-leptonic  $B$  decays,” PoS LATTICE **2012**, 120 (2012) [arXiv:hep-lat/1211.1390].
- C. Bouchard, G. P. Lepage, C. Monahan, H. Na and J. Shigemitsu, “The rare decay  $B \rightarrow K\ell\ell$  form factors from lattice QCD,” [arXiv:hep-lat/1306.2384].
- [120] A. Walker-Loud, “Baryons in/and Lattice QCD,” [arXiv:hep-lat/1304.6341].
- [121] R. Lewis, “Bottom and charmed hadron spectroscopy from lattice QCD,” AIP Conf. Proc. **1374**, 581 (2011) [arXiv:hep-lat/1010.0889].
- H.-W. Lin, “Review of Baryon Spectroscopy in Lattice QCD,” Chin. J. Phys. **49**, 827 (2011) [arXiv:hep-lat/1106.1608].
- [122] W. Detmold, C. -J. D. Lin, S. Meinel and M. Wingate, “ $\Lambda_b \rightarrow p \ell^- \bar{\nu}_\ell$  form factors from lattice QCD with static  $b$  quarks,” [arXiv:hep-lat/1306.0446].
- [123] T. Mannel and Y.-M. Wang, “Heavy-to-light baryonic form factors at large recoil,” JHEP **1112**, 067 (2011) [arXiv:hep-ph/1111.1849].
- [124] L.-F. Gan, Y.-L. Liu, W.-B. Chen and M.-Q. Huang, “Improved Light-cone QCD Sum Rule Analysis Of The Rare Decays  $\Lambda_b \rightarrow \Lambda\gamma$  And  $\Lambda_b \rightarrow \Lambda\ell^+\ell^-$ ,” Commun. Theor. Phys. **58**, 872 (2012) [arXiv:hep-ph/1212.4671].
- [125] L. Mott, W. Roberts, “Rare dileptonic decays of  $\Lambda_b$  in a quark model,” [arXiv:nucl-th/1108.6129].
- [126] T. Gutsche, M. A. Ivanov, J. G. Körner, V. E. Lyubovitskij and P. Santorelli, “Rare baryon decays  $\Lambda_b \rightarrow \Lambda\ell^+\ell^-$  ( $\ell = e, \mu, \tau$ ) and  $\Lambda_b \rightarrow \Lambda\gamma$ : differential and total rates, lepton- and hadron-side forward-backward asymmetries,” Phys. Rev. D **87**, 074031 (2013) [arXiv:hep-ph/1301.3737].
- [127] R. Mohanta, A. K. Giri, M. P. Khanna, M. Ishida and S. Ishida, “Weak radiative decay  $\Lambda_b \rightarrow \Lambda\gamma$  and quark confined effects in the covariant oscillator quark model,” Prog. Theor. Phys. **102**, 645 (1999) [arXiv:hep-ph/9908291].
- [128] X.-G. He, T. Li, X.-Q. Li and Y.-M. Wang, “PQCD calculation for  $\Lambda_b \rightarrow \Lambda\gamma$  in the standard model,” Phys. Rev. D **74**, 034026 (2006) [arXiv:hep-ph/0606025].

- [129] K. Azizi, S. Kartal, A. T. Olgun and Z. Tavukoglu, “Comparative analysis of the semileptonic  $\Lambda_b \rightarrow \Lambda \ell^+ \ell^-$  transition in SM and different SUSY scenarios using form factors from full QCD,” JHEP **1210**, 118 (2012) [arXiv:hep-ph/1208.2203].  
M. J. Aslam, Y.-M. Wang and C.-D. Lu, “Exclusive semileptonic decays of  $\Lambda_b \rightarrow \Lambda \ell^+ \ell^-$  in supersymmetric theories,” Phys. Rev. D **78**, 114032 (2008) [arXiv:hep-ph/0808.2113].
- [130] K. Azizi, S. Kartal, A. T. Olgun and Z. Tavukoglu, “Analysis of the radiative  $\Lambda_b \rightarrow \Lambda \gamma$  transition in SM and scenarios with one or two universal extra dimensions,” [arXiv:hep-ph/1303.2233].  
Y.-M. Wang, M. J. Aslam and C.-D. Lü, “Rare decays of  $\Lambda_b \rightarrow \Lambda \gamma$  and  $\Lambda_b \rightarrow \Lambda \ell^+ \ell^-$  in universal extra dimension model,” Eur. Phys. J. C **59**, 847 (2009) [arXiv:hep-ph/0810.0609].  
P. Colangelo, F. De Fazio, R. Ferrandes and T. N. Pham, “FCNC  $B_s$  and  $\Lambda_b$  transitions: Standard model versus a single universal extra dimension scenario,” Phys. Rev. D **77** (2008) 055019 [arXiv:hep-ph/0709.2817].
- [131] K. Azizi and N. Katirci, “Analysis of  $\Lambda_b \rightarrow \Lambda \ell^+ \ell^-$  Transition in SM4 using Form Factors from Full QCD,” Eur. Phys. J. A **48**, 73 (2012) [arXiv:hep-ph/1112.5242].  
F. Zolfagharpour and V. Bashiry, “Double Lepton Polarization in  $\Lambda_b \rightarrow \Lambda \ell^+ \ell^-$  Decay in the Standard Model with Fourth Generations Scenario,” Nucl. Phys. B **796**, 294 (2008) [arXiv:hep-ph/0707.4337].
- [132] R. Aaij *et al.* [LHCb Collaboration], “Precision measurement of the  $\Lambda_b$  baryon lifetime,” [arXiv:hep-ex/1307.2476].
- [133] T. Gershon, “Flavour physics in the LHC era,” [arXiv:hep-ex/1306.4588].
- [134] R. Aaij *et al.* [LHCb Collaboration], “Implications of LHCb measurements and future prospects,” Eur. Phys. J. C **73**, 2373 (2013) [arXiv:hep-ex/1208.3355].
- [135] T. Abe [Belle II Collaboration], “Belle II Technical Design Report,” [arXiv:physics.ins-det/1011.0352].
- [136] M. Bona *et al.* [SuperB Collaboration], “SuperB: A High-Luminosity Asymmetric  $e^+e^-$  Super Flavor Factory. Conceptual Design Report,” Pisa, Italy: INFN (2007) 453. <http://www.pi.infn.it/SuperB/?q=CDR> [arXiv:hep-ex/0709.0451].  
M. Baszczyk *et al.* [SuperB Collaboration], “SuperB Technical Design Report,” [arXiv:physics.ins-det/1306.5655].
- [137] J. L. Hewett, H. Weerts, R. Brock, J. N. Butler, B. C. K. Casey, J. Collar, A. de Gouvea and R. Essig *et al.*, “Fundamental Physics at the Intensity Frontier,” [arXiv:hep-ex/1205.2671].